

97701



National Library of Canada

Bibliothèque nationale du Canada

CANADIAN THESES ON MICROFICHE

THÈSES CANADIENNES SUR MICROFICHE

NAME OF AUTHOR / NOM DE L'AUTEUR \_\_\_\_\_

TITLE OF THESIS / TITRE DE LA THÈSE \_\_\_\_\_

\_\_\_\_\_

UNIVERSITY / UNIVERSITÉ \_\_\_\_\_

DEGREE FOR WHICH THESIS WAS PRESENTED / GRADE POUR LEQUEL CETTE THÈSE FUT PRÉSENTÉE \_\_\_\_\_

YEAR THIS DEGREE CONFERRED / ANNÉE D'OBTENTION DE CE GRADE \_\_\_\_\_

NAME OF SUPERVISOR / NOM DU DIRECTEUR DE THÈSE \_\_\_\_\_

Permission is hereby granted to the NATIONAL LIBRARY OF CANADA to microfilm this thesis and to lend or sell copies of the film.

*L'autorisation est, par la présente, accordée à la BIBLIOTHÈQUE NATIONALE DU CANADA de microfilmer cette thèse et de prêter ou de vendre des exemplaires du film.*

The author reserves other publication rights, and neither the thesis nor extensive extracts from it may be printed or otherwise reproduced without the author's written permission.

*L'auteur se réserve les autres droits de publication, ni la thèse, ni de longs extraits de celle-ci ne doivent être imprimés ou autrement reproduits sans l'autorisation écrite de l'auteur.*

DATED / DATE \_\_\_\_\_ SIGNED / SIGNÉ \_\_\_\_\_

PERMANENT ADDRESS / RÉSIDENCE FIXE \_\_\_\_\_

\_\_\_\_\_

\_\_\_\_\_

INFORMATION TO USERS

THIS DISSERTATION HAS BEEN  
MICROFILMED EXACTLY AS RECEIVED

This copy was produced from a microfiche copy of the original document. The quality of the copy is heavily dependent upon the quality of the original thesis submitted for microfilming. Every effort has been made to ensure the highest quality of reproduction possible.

PLEASE NOTE: Some pages may have indistinct print. Filmed as received.

Canadian Theses Division  
Cataloguing Branch  
National Library of Canada  
Ottawa, Canada K1A 0N4

AVIS AUX USAGERS

LA THESE A ÉTÉ MICROFILMÉE  
TELLE QUE NOUS L'AVONS RECUE

Cette copie a été faite à partir d'une microfiche du document original. La qualité de la copie dépend grandement de la qualité de la thèse soumise pour le microfilmage. Nous avons tout fait pour assurer une qualité supérieure de reproduction.

NOTA BENE: La qualité d'impression de certaines pages peut laisser à désirer. Microfilmée telle que nous l'avons reçue.

Division des thèses canadiennes  
Direction du catalogage  
Bibliothèque nationale du Canada  
Ottawa, Canada K1A 0N4

THE UNIVERSITY OF ALBERTA

PHAGE R17 RNA PENETRATION

by

KENNETH WONG



A THESIS

SUBMITTED TO THE FACULTY OF GRADUATE STUDIES AND RESEARCH  
IN PARTIAL FULFILMENT OF THE REQUIREMENTS FOR THE DEGREE  
OF DOCTOR OF PHILOSOPHY

DEPARTMENT OF BIOCHEMISTRY

EDMONTON, ALBERTA

SPRING

1976

THE UNIVERSITY OF ALBERTA

FACULTY OF GRADUATE STUDIES AND RESEARCH

The undersigned certify that they have read, and recommend  
to the Faculty of Graduate Studies and Research for acceptance, a  
thesis entitled PHAGE R17 RNA PENETRATION submitted by KENNETH WONG  
in partial fulfillment of the requirements for the degree of Doctor  
of Philosophy.

*Wm. Paranchych*

Supervisor

*David D. McElhenny*

*M. H. H. H.*

*Tack Tucker*

*W. H. H. H.*

External Examiner

Oct. 20, 1975

Date .....

To Kim

with love

## ABSTRACT

The RNA ejection and penetration steps of phage R17 infection has been investigated in greater detail.

It was found that viral RNA extensively degraded *in situ* by the indirect effects of  $^{32}\text{P}$  decay is able to penetrate into host bacteria as fragments. These fragments are quickly degraded by cellular nucleases and the nucleotides are reincorporated into cellular ribonucleotides.

The presence of a saturating concentration ( $> 1.0 \mu\text{g/ml}$ ) of RNase in an infection medium does not affect the penetration of phage A protein; however, the RNase does reduce the level of RNA penetrating to 3% and 23% of that injected into cells by phage in a minus RNase infection, carried out at MOI's of 100 and 1000 particles/cell, respectively. Subsequent studies showed that the RNA penetrating in the presence of RNase in intact and infectious. It was surmised that there exist positions on the F-pilus where phage RNA may eject and penetrate without being degraded by RNase.

Rapid inactivation of R17 phage occurs when particles are incubated at  $37^\circ$  in the presence of ascorbate and  $\text{Cu}^{2+}$ . The inactivation of phage is temperature dependent, requires  $\text{O}_2$ , and is suppressed or reduced by the inclusion of EDTA, catalase or  $\text{I}^-$ , a scavenger of hydroxyl free radicals ( $\cdot\text{OH}$ ), in incubation mixtures. These observations support a mechanism whereby  $\text{O}_2$  and  $\text{Cu}^{2+}$  act as catalysts in the generation of reactive  $\cdot\text{OH}$  species from ascorbate.  $\cdot\text{OH}$  appears to inactivate phage primarily through the cleavage of viral RNA and probable alteration of bases.

When host bacteria are infected with ascorbate-Cu<sup>2+</sup>-treated phage of decreasing infectivities, the amount of penetrated RNA decreases in a nonlinear fashion while the amount of penetrated A protein is unaffected. This observation suggests that RNA fragments of decreasing average lengths are being transported into cells; perhaps as A protein-RNA complexes. A partial or fractional RNA ejection mode is also supported by the detection, in the supernatant of infected cultures, of partially empty capsids containing fragments of the original genome. The average size of the RNA fragment in such partially empty capsids was shown to increase with decreasing infectivities (or increasing average number of scissions per RNA molecule).

Hidden breaks in penetrated RNA were further demonstrated by comparing the radioactive profile of <sup>32</sup>P-labeled phage RNA (isolated from infected cells) separated under benign conditions to that separated under denaturing conditions in polyacrylamide gels. A shift toward lower molecular weight fragments was observed when the RNA was separated in 8M urea gels at 60°. It thus appears that RNA fragments held together by complementary base pairing were melted apart under denaturing conditions.

Analysis of the coat protein mass/RNA mass ratios of particles recovered in the supernatant yielded results which indicate that coat monomers may detach from the capsid and become cell-associated during phage infection. A substantial amount of <sup>35</sup>S-radioactivity was found to be associated with infected cells which were exhaustively washed; most of this radioactive material was shown to migrate as coat protein in SDS-polyacrylamide gels. It was tentatively concluded that phage

eclipse probably involves the dissociation from the capsid of some coat monomers which may be transported into the cell.

Partially empty capsids were prepared and isolated on a large scale from  $^3\text{H}$  adenosine or  $^3\text{H}$  guanosine labeled phage. The pppGp/Gp ratio of the RNA fragments remaining in partially empty capsids was found to increase following fractional RNA ejection, while the  $A_{\text{Gpp}}/A_p$  ratio was found to be markedly lower than the ratio obtained for intact phage RNA. These findings suggest that the 3' end of the phage genome (probably in association with A protein) acts as the pilot end during the RNA penetration process.



#### ACKNOWLEDGEMENTS

First and foremost I would like to thank Dr. Paranchych for his expert guidance and expert criticism and assessment of this research program. I also thank Dr. Morgan for his consultation and collaboration at one stage of this work.

I would like to extend my gratitude to Miss Cathy Hicks for the photographic reproduction of some figures, to Mr. Paul Barros for his aid in computer programming, to Mrs. Marg Bangen for her excellent plate preparations, and to Mrs. Jean Wynn for her typing of this thesis.

The encouragement and support of past and present members of Dr. Paranchych's research group are very much appreciated. Their collective good spirits have made life very enjoyable in the laboratory.

Finally, I am grateful to the Department of Biochemistry for providing financial support in the form of teaching assistantships.

TABLE OF CONTENT

	Page
Abstract	v
Acknowledgments	viii
Table of contents	ix
List of Figures	xiv
List of Tables	xvi
List of Abbreviations	xvii
CHAPTER I. INTRODUCTION	1
A. Phage Structure	2
B. Phage Adsorption and the A Protein	6
C. Phage DNA Ejection	11
D. The DNA Penetration Process	15
CHAPTER II. MATERIALS AND METHODS	19
A. Materials	
1. Bacteria and Bacteriophage	
(a) Bacteriophage	19
(b) Bacteria	19
2. Bacterial Culture Media	
(a) Tris (hydroxymethyl) amino methane maleic acid minimal salts (TMM) medium	20
(b) Various IMM-based media	20
(c) Trypticase soy broth (TSB)	21
(d) Hard agar	21
(e) Top agar	21
3. Bacteria and Phage Diluent	21
4. Chemicals, Enzymes and Reagents	21
5. Radioactive Materials	22

D. Growth of Bacteria . . . . . 24

C. Preparation and Purification of Phage R17

1. Cell Lysis and the Partial Purification of the Released Phage by a Two Phase Polymer . . . . . 25

2.  $\text{CaCl}_2$  Dropcentrifugation of Phage . . . . . 25

3. Assay for Phage Density . . . . . 25

B. Radioisotope Labeling of Phage R17

1.  $^{32}\text{P}$  Labeling of R17 Phage RNA . . . . . 26

2.  $^3\text{H}$  Adenosine and  $^3\text{H}$  Guanosine Labeling of R17 Phage RNA . . . . . 26

3.  $^{35}\text{S}$  Labeling of R17 Phage Proteins . . . . . 26

4. Labeling of R17 Phage A protein with  $^3\text{H}$  L-Glutamic Acid . . . . . 27

E. Boron and Gold TCA Radioassay

1. Boron TCA-Insoluble Products . . . . . 28

2. Gold TCA-Insoluble Products . . . . . 29

F. Radioisotope Counting . . . . . 29

G. Plaque Assay for Infectious Phage . . . . . 29

H. Phage Attachment Assay . . . . . 30

1. Penetration Assay . . . . . 30

J. Anion Ultrafiltration . . . . . 32

K. Sucrose Gradient Techniques . . . . . 32

L. Ascorbic Acid -  $\text{Cu}^{2+}$  Inactivation of R17 Phage . . . . . 32

M. Ethidium Bromide Binding Assay . . . . . 33

N. Isolation of RNA . . . . . 34

O. Alkaline Hydrolysis of RNA . . . . . 35

P. SDS-Polyacrylamide Gel Electrophoresis of Proteins . . . . . 35

1. Polyaniline Gel Electrophoresis of PNA . . . . . 36

    a. Experimental Conditions . . . . . 36

    b. Polyaniline Gel Electrophoresis of PNA Under Denaturing Conditions . . . . . 40

    c. High Voltage Gel Electrophoresis . . . . . 40

CHAPTER III. THE EFFECT OF PHASE AND STYDAD SECTIONS ON PENETRATION OF R17 PNA . . . . . 43

    A. Introduction . . . . . 43

    B. Results and Discussion . . . . . 44

        1. Penetration of R17 in the PNA Penetration . . . . . 44

        2. Penetration of R17 in the PNA . . . . . 46

        3. Penetration of R17 in the PNA Penetration . . . . . 47

    C. The Penetration of R17 in the PNA by ASCORBATE- $\text{Cu}^{2+}$  . . . . . 47

        A. Introduction . . . . . 47

        B. Results . . . . . 47

            1. Parameters of R17 Penetration by Ascorbate-Cu<sup>2+</sup> . . . . . 47

            2. Physical and Chemical Properties of Ascorbate-Cu<sup>2+</sup> Treated R17 PNA . . . . . 50

            3. Characterization of the PNA Isolated from Ascorbate-Cu<sup>2+</sup> Treated Phase . . . . . 85

        C. Discussion . . . . . 89

            1. The Mode of Action of Ascorbate-Cu<sup>2+</sup> . . . . . 89

            2. Free Radical Attack on Nucleic Acids . . . . . 94

CHAPTER V. PENETRATION STUDIES WITH ASCORBATE- $\text{Cu}^{2+}$  INACTIVATED R17 PHAGE . . . . . 97

    A. Introduction . . . . . 97

B. Results	
1. RNA Penetration of $^{32}$ P-Phage DNA into Goat Erythrocytes	90
(a) Radiochemical Assays for Identification of Penetrated DNA	90
(b) The Relationship between Inoculum Concentration and the Amount of Penetrated DNA	100
(c) Evidence for the Penetration of $^{32}$ P-Labelled Phage DNA into the Nucleus of the Host Cell	109
(d) Determination of the Molecular Weight of Penetrated DNA	111
2. Characterization of Partially Empty Capsids	111
(a) Polyacrylamide Gel Electrophoretic Analysis of DNA Released from Partially Empty Capsids	123
(b) Evidence for the Presence of Coat Protein in Partially Empty Capsids	127
(c) Polyacrylamide Gel Electrophoretic Analysis of Proteins Released from Cells Infected with $^{35}$ S-Labeled P17	129
3. The Formation of Partially Empty Capsids in Infections Carried out in the Absence of $^{32}$ P	131
C. Discussion	
1. Implications of the Possible Existence of Coat Protein in Partially Empty Capsids During RNA Replication	137
2. The Implications of the Separation of Coat Protein from RNA	139
CONCLUDE VI. DIRECTION OF PENETRATION OF P17 RNA	142
A. Introduction	142
B. Results	
1. Isolation of Partially Empty Capsids on a Preparative Scale	144
2. Paper Electrophoresis of Alkaline Hydrolysates of $^{35}$ S-Methionine and $^{35}$ S-Methionine Labeled P17 RNA	145

	Page
3. 5'-end Group Analysis . . . . .	151
3'-end Group Analysis . . . . .	152
C. Discussion . . . . .	155
CHAPTER VII. SUMMARY . . . . .	160
BIBLIOGRAPHY . . . . .	168
APPENDIX . . . . .	176

LIST OF FIGURES

Figure		Page
2.1	Schematic diagram of an exponential gradient gel-making apparatus . . . . .	37
3.1	The effect of bacterial strain and rifampicin on the kinetics of phage RNA penetration . . . . .	47
3.2	The effect of the multiplicity of infection on the amount of RNA penetrated at 5 minutes post infection . . . . .	49
3.3	Fate of penetrated $^{32}\text{P}$ -labeled R17 DNA . . . . .	53
3.4	A comparison of the fate of penetrated phage RNA in RNase I and wild type host bacteria . . . . .	57
3.5	The effect of rifampicin on penetrated R17 RNA . . . . .	59
3.6	The effect of RNase concentration on the penetration of phage RNA and A protein . . . . .	62
3.7	Polyacrylamide gel analysis of phage RNA isolated from <i>E. coli</i> infected with phage in the presence of RNase . . . . .	67
4.1	Kinetics of phage R17 inactivation by ascorbic acid, $\text{Cu}^{2+}$ incubation . . . . .	73
4.2	The effect of catalase on the inactivation of phage R17 by ascorbate- $\text{Cu}^{2+}$ . . . . .	77
4.3	The effect of the presence of free radical scavengers in ascorbate- $\text{Cu}^{2+}$ -phage incubation mixtures . . . . .	79
4.4	A comparison of the sedimentation property and buoyant density of R17 phage extensively inactivated with ascorbate- $\text{Cu}^{2+}$ . . . . .	82
4.5	The formation of extraneous 3'-A <sup>OH</sup> ends in R17 cleaved <u>in situ</u> as a result of ascorbate- $\text{Cu}^{2+}$ treatment . . . . .	86
5.1	Polyacrylamide gel electrophoresis of $^{32}\text{P}$ -RNA isolated from ascorbate- $\text{Cu}^{2+}$ -inactivated R17 phage and from <i>E. coli</i> (Hfr) cells infected with the same preparation . . . . .	100

Figure		Page
5.2	A comparison of the mass distribution of the total fragments produced in a system simulating a first-piece-injected process . . . . .	105
5.3	The kinetics of RNA penetration of ascorbate-Cu <sup>2+</sup> -inactivated R17 phage . . . . .	107
5.4	The relationship between the amount of RNA or A protein penetration, and the infectivity of ascorbate-Cu <sup>2+</sup> -treated R17 phage . . . . .	108
5.5	Analysis of penetrated phage RNA by polyacrylamide gel electrophoresis under non-denaturing and denaturing conditions . . . . .	114
5.6	Sucrose gradient analysis of ascorbate-Cu <sup>2+</sup> -treated R17 phage particles following incubation with host bacteria . . . . .	117
5.7	CsCl isopycnic analysis of ascorbate-Cu <sup>2+</sup> -treated R17 phage particles following incubation with host bacteria . . . . .	120
5.8	Polyacrylamide gel electrophoresis of RNA isolated from particles banding in heavy and intermediate regions of a CsCl gradient . . . . .	125
5.9	Polyacrylamide gel electrophoresis of total proteins extracted from <i>E. coli</i> W156 infected with <sup>35</sup> S-labeled R17 phage . . . . .	130
5.10	Sucrose gradient analysis of phage R17 particles exposed to sensitive host bacteria in the absence of free Mg <sup>2+</sup> . . . . .	134
5.11	CsCl gradient analysis of R17 phage exposed to host cells in the absence of Mg <sup>2+</sup> . . . . .	136
6.1	High voltage paper electrophoresis of alkaline hydrolysates of R17 RNA . . . . .	147
6.2	Enzymatic digestion of pppGp . . . . .	150
7.1	Schematic representation of a revised working model depicting the mechanism of R17 phage infection of <i>E. coli</i> . . . . .	162



LIST OF TABLES

Table		Page
2.1	Preparation of Paper Discs for Hot-TCA Insoluble Products . . . . .	28
3.1	Effect of Culture Medium and Multiplicity of Infection (MOI) on Phage R17 RNA Penetration. . . . .	45
3.2	Plaque Assay of <u>E. coli</u> (Hfr) Cells Infected with R17 Phage in the Presence of RNase . . . . .	69
4.1	Effect of Phage Concentration and Temperature on the Rate of Ascorbate-Cu <sup>2+</sup> -Inactivation of R17 Phage . . . . .	74
4.2	Estimation of the Proportion of RNA Strand Scissions to Overall Total Lesions Produced in R17 Phage Inactivated by Ascorbate-Cu <sup>2+</sup> . . . . .	90
5.1	A comparison of the <sup>35</sup> S-cpm/ <sup>3</sup> H-cpm Ratios of Cell-Exposed R17 Particles to Their Calculated Values . . . . .	128
6.1	End-Group Analysis of the RNA Isolated from Partially Empty Capsids of R17 . . . . .	153

LIST OF ABBREVIATIONS

DNA	deoxyribonucleate
RNA	ribonucleate
A <sub>OH</sub> or A	adenosine
G	guanosine
C	cytidine
U	uridine
Cp	cytidine 2',3'-monophosphate
Up	uridine 2',3'-monophosphate
Ap	adenosine 2',3'-monophosphate
Gp	guanosine 2',3'-monophosphate
GDP	guanosine 5'-diphosphate
pGp	guanosine 5'-mono, 2',3' monophosphate
GTP	guanosine 5'-triphosphate
ppppG	guanosine 5'-tetraphosphate
pppGp	guanosine 5'-tri, 2',3'-monophosphate
MOI	multiplicity of infection
PFU	plaque forming units
Ci	Curie; $2.22 \times 10^{12}$ disintegrations per minute
cpm	radioactive counts per minute
g	centrifugal force relative to gravity
rpm	revolutions per minute
MW	molecular weight
SDS	sodium dodecyl sulfate
EDTA	ethylenediaminetetraacetic acid

TCA	trichloroacetic acid
Tris	Tris (hydroxymethyl) aminomethane
NaDS	sodium dextran sulfate
PEG	polyethylene glycol
RNase	ribonuclease
pRNase	pancreatic ribonuclease
DNase	deoxyribonuclease
SVP	snake venom phosphodiesterase
TMM	Tris (hydroxymethyl) aminomethane maleic acid- minimal salts medium
TSB	trypticase soy broth
SSC	standard saline citrate 0.15M NaCl, 0.015M sodium citrate
TMED	N,N,N',N'-tetramethylethylenediamine
A <sub>650</sub> (A <sub>260</sub> )	light absorbancy of a solution in a 1 cm light path at 650 nm (260 nm)
S (following a number)	sedimentation constant in Svedberg units (10 <sup>-13</sup> sec)

All temperatures are expressed in degrees centigrade.

The terms 'penetrated RNA' or 'penetrated RNA fragments' in this thesis are defined as R17 RNA molecules, or fragments of molecules, which have penetrated into E. coli host cells. Similarly, 'penetrated A protein' refers to A protein or fragments of A protein which have penetrated into E. coli cells.

## CHAPTER 1

### INTRODUCTION

Since the discovery of the prototype of the male-specific RNA bacteriophages,  $\phi 2$ , in 1961 (Loeb and Zinder, 1961), a great wealth of scientific information has been garnered from in vivo studies of phage RNA as a model mRNA in protein synthesis and as a template in RNA replication. One notable highlight has been the elucidation of the strategy by which the phage utilizes the secondary structure of the RNA and various protein-RNA complexes to regulate translational and transcriptional processes. Extensive treatment of this aspect of the RNA phage infectious cycle can be found in reviews by Valentine et al. (1969), Sugiyama et al. (1972), Kozak and Nathans (1972), Hindley (1973) and Weissman (1974).

Despite the amount of effort expended in investigating the RNA phage system, one area of the phage life cycle remains poorly understood, namely that which concerns the early events occurring just before the RNA is injected into the host cell. This stage of the phage cycle can be further subdivided into three distinct sequential steps: (a) the attachment or adsorption of phage particles to receptor sites on sex pili; (b) a cell-mediated, structural change in the phage particle leading to the sensitization of the RNA to ribonuclease and/or the uncoating of the viral RNA; and (c) the transport of the RNA to and across the cell membrane. The following will be a brief survey of all aspects of the RNA phage system

that touches upon these early events.

A. Phage Structure

One of the most attractive points about the f2 class of RNA phages (members include R17, R23, MS2, fr, M12) and other related groups (Sakurai et al., 1968; Miyake et al., 1969) has been their simplicity of structure. Within a group such as the f2, members differ to the extent of only a few amino acid replacements in their coat proteins (Enger and Kaesberg, 1965; Weber, 1967) or base substitutions in their RNA sequences (Thirion and Kaesberg, 1968, 1970) and findings from one system can usually be applied to the others. In general, the f2 type phages have a molecular mass of about  $3.6 \times 10^6$  daltons (Gesteland and Boedicker, 1964). The protein capsid consists of 180 coat protein subunits (MW = 13,750) arranged in icosahedral symmetry (Vasquez et al., 1966) and enclosing a single stranded RNA of about 3,300 nucleotides (MW  $\approx 1.1 \times 10^6$ ) (Sinha et al., 1965). In addition, each particle contains a single copy of a minor component (MW = 40,000) known as the "A" or maturation protein (Steitz, 1968a, b).

Genetic studies have identified the presence of three cistrons (Horiuchi et al., 1966; Gussin, 1966), two of which are accounted for by the coat and A proteins; the third cistron codes for the viral RNA synthetase made during the early stages of intracellular infection. The order of these three cistrons on the R17 genome was deduced to be "5' end - A protein - coat protein - synthetase - 3' end" on the basis of the distribution of the three phage protein initiation sites between two specific R17 fragments (Jeppeson et al.,

1970). This approach to the problem was made possible by the elegant series of experiments executed by Steitz (1969), who isolated RNA fragments protected by ribosome-RNA initiation complexes corresponding to each of the three cistrons. Using the RNA sequencing techniques developed by Sanger's group (Sanger et al., 1965, Brownlee and Sanger, 1967, 1969; Brownlee et al., 1968), she was able to show that each initiation sequence was unique. Calculations based on the chain length of the phage RNA and the molecular weights of the three proteins indicate that sequences exist which are not translated. One of these sequences was identified and sequenced by Nichols (1970) and shown to be an intercistronic region between the coat protein and synthetase genes. More recently, Fiers' group (Min Jou et al., 1972; Fiers et al., 1975) has sequenced the entire coat protein and A protein cistrons of MS2 phage and have proposed several "flower models" showing the extensive intrastrand hydrogen bonding of the RNA sequence in thermodynamically stable states. On the whole, a helical content of about 70% has been estimated for the isolated RNA (Mittra et al., 1963) and about 80% for the RNA as packed into its capsid (Boedtker, 1967).

The phage RNA in situ is a highly organized structure. Low angle X-ray scattering studies have indicated that the phage particle has a mean outer radius of 131.7 Å and consists of an outer protein shell of about 30 to 40 Å thickness, an inner core of RNA and a small hollow region of about 15 Å radius at the center. The inner core contains only about 80% of the RNA, the remaining 20% is considered to penetrate and interact with the protein shell. Furthermore, the phage particle is a highly hydrated entity with

1.0 to 0.9 g of water associated with a gram of virus (Fischbach et al., 1965; Zipper et al., 1971). Hohn (1969) previously proposed that the sugar-phosphate backbone of the RNA is essential as a site of attachment for the coat protein. This was supported by the work of Matthews and Cole (1972a, b), who showed that the interaction between positively charged arginine residues in the coat protein and the negatively charged phosphate groups of RNA is essential for maintaining the structural integrity of phage particle. It is generally believed that mutually opposing forces generated by the close juxtapositioning of the phosphodiester backbone in the folded RNA are balanced by electrostatic interactions between the phosphate groups and basic residues of the coat subunits, as well as by the presence of chelating counterions such as  $Mg^{2+}$  (Spirin, 1964). Additional stabilization of the highly folded RNA molecule may be provided by the presence of spermidine, an organic cation which was recently shown by Fukuma and Cohen (1975) to be an indigenous component of purified R17 bacteriophage. Up to 1000 molecules of spermidine were associated with the virion when it was isolated in 0.01 M KCl, while the phage RNA isolated with phenol plus sodium lauryl sulfate contained approximately 70 to 90 molecules of spermidine.

Much progress has recently been made towards a clearer understanding of the structural organization of the phage capsid. Mathews and Cole, (1972a,b), on the basis of chemical modification studies on the  $f_2$  phage coat monomer, have proposed a structural model of phage capsid in which: (a) the basic amino acids are on the interior of the

shell neutralizing the RNA phosphate groups or interacting with counterions; (b) the acidic amino acids are on the exterior surface of the phage capsid interacting with solvent; and (c) the apolar (hydrophobic) residues are between these two charged shells, holding the protein subunits in place (Matthews and Cole, 1972a,b). Calculations based on the diameter of the phage particle and the number and molecular weight of the coat protein subunits indicate that about 80% of the surface area is accounted for by the 180 subunits (Zipper et al., 1971; Hohn and Hohn, 1970). This implies that a certain amount of porosity exists in the phage capsid. Evidence in support of this concept has come from the study of electron micrographs of phage particles and the observation that the capsid structure of R17 is readily permeable to heavy metal salts. Careful characterization of the breakdown products of R17 phage treated with guanidine hydrochloride by O'Callaghan et al. (1973a) led to the proposal that the phage capsid is made up of 20 nonagons arranged in icosahedral symmetry. However, a weakness of this model is that it was derived with the nonphysical assumption that identical polypeptide chains are arranged in nonidentical bonding environments. This situation clearly violates the principle of quasiequivalence which serves as a guideline for model building of viral structures (Caspar and Klug, 1962; Dunker, 1974). More recently, Dunker and Paranchych (1975) have advanced a revised model of RNA phage capsid structure in which the protein subunits are arranged in a hexagonal net with quasiequivalent



dimer bonds and quasiequivalent hexamer bonds. Additionally, they proposed that the A protein is situated in, and protrudes through one of the openings produced by the coat protein subunits, which circumscribe the 3-fold axis.

#### B. Phage Adsorption and the A Protein

The first step in the infectious cycle of the male-specific RNA phages begins with their adsorption to the sides of filamentous appendages produced by Hfr and  $F^+$  cells, but not by  $F^-$  cells. Crawford and Gesteland (1964), who first observed this adsorption phenomenon, called these appendages "fimbriae". The more widely accepted term, F-pili, was suggested by Brinton et al. (1964), who had shown that the presence of these structures is a necessary condition for sexual conjugation in various gram-negative organisms. Maximal attachment of the phage particles takes place in 0.1M NaCl solutions or in solutions with a similar ionic strength (Danziger and Paranchych, 1970a). Divalent cations are not required for attachment although their presence is required for RNA penetration (Paranchych, 1966). Adsorption studies carried out at 0 to 40° or with cell-free pili indicated that the process is reversible and that the recovered phage particles retain full infectivity (Valentine and Strand, 1965; Brinton and Beer, 1967; Paranchych et al., 1970). Furthermore, Knolle (1967b) has reported that the attachment step is a diffusion-limited reaction which probably requires little or no energy of activation. The process was demonstrated by Brinton and Beer (1967) to exhibit only a slight temperature dependence.

The A protein constituent of the phage appears to play an important role in determining the infectivity of the phage. Studies on defective particles synthesized during the growth of A cistron mutants of T2, T4 and R17 in non permissive cells (Lodish et al., 1965; Argetsinger and Gurwin, 1966; Heisenberg, 1966), and phage reconstitution studies (Roberts and Steitz, 1967), have revealed that the A protein is in some way required for the assembly of infectious phage. For example, it was found that defective particles of amber mutants assembled in non-permissive hosts lack the A protein and do not attach to F-pili (Valentine and Strand, 1965; Lodish et al., 1965; Heisenberg and Blessing, 1965; Steitz, 1968a,b). Particles reconstituted from coat protein subunits and viral RNA were completely non-infectious, whereas infectious particles were assembled when A protein molecules were included in the mixtures. The low yields of such reconstitution studies have been explained by Kaerner's finding (1970) that proper assembly is contingent upon correct sequential combinations of phage components. In vivo, the binding of A protein to viral RNA is an early event in the phage assembly process possibly governing the correct aggregation of the coat protein subunits to give rise to infectious viral particles. Such early in vivo assembly complexes between the RNA and A protein have also been reported by Richelson and Nathans (1967), and Bonner (1974).

The foregoing results led to the postulation of two models that attempt to define the role of the A protein. The "core" model

predicts that the A protein is located in the interior of the phage particle and functions by providing the proper orientation of the folded RNA and the coat protein subunits for the attachment and penetration steps (Bohn and Bohn, 1960). The "tail" model predicts that the A protein is located on the surface of the phage particle where it facilitates the absorption to the bacterial pilus and the injection of viral RNA (Caversham and Gussin, 1966; Valentine et al., 1965). Recently, direct evidence has been submitted by Curtis and Erneger (1974) to show that the A protein is localized on the surface of the phage particle. They found that in situ, the amino group of some of the lysine residue in M<sub>1</sub> A protein can be covalently linked to fluorescein isothiocyanate (FITC). Further confirmation of the surface location of the A protein was shown by the ability of lactoperoxidase to iodinate the A protein in the particle (Curtis and Erneger, 1974). The latter results have been corroborated for R17 by Reynolds (personal communication) in this laboratory.

The study of the early stages of phage attachment and RNA ejection and penetration is complicated by the heterogeneous nature of phage populations. It appears that not only is the physical presence of the A protein required for proper attachment and RNA penetration, but that the orientation of the A protein with respect to the RNA and protein subunits of the capsid may also be important. Three types of particles can be distinguished in a normal burst of phage from infected cells (Paranchych et al., 1970; Krahn and Paranchych, 1971). About 10% of the phage population, labeled as

Class III particles, lack the A protein and do not attach to piliated cells; the RNA of these particles is completely resistant to the activity of RNases. About 10 - 20% (Class I particles) are infectious and adsorb relatively strongly to F-pili, the equilibrium ratio of attached/unattached infectious phage being approximately 9:1. The other 70 - 80% of the particles (Class II particles), although noninfectious, are able to attach weakly to F-pili. Moreover, the equilibrium ratio of attached/unattached phage at each successive stage of a multi-step adsorption experiment has shown that the relative affinity of infectious Class I particles for F-pili is approximately 3-fold greater than that of the non-infectious Class II particles.

The structure of the receptor site on the F-pilus is unknown. F-pili have been characterized as flexible, filamentous structures, which are 8.5 - 9.5 nm in diameter and about 1 - 2  $\mu$ m long (Brinton, 1965). Negatively stained pili show an apparent axial hole about 2.5 nm in diameter. Electron micrographs show that RNA phage particles adsorb in large numbers along the entire length of these pili, suggesting that every pilin subunit has equivalent capacity to attach phage.

Highly purified F-pili preparations, homogeneous by both chemical and physical criteria, were recently studied in detail by Brinton and co-workers (1971, 1973). They found that the F-pili are composed of polymerized phosphoglycoprotein subunits of molecular weight 11,800. The pilin subunit is unusual with respect to amino acid composition; four of the commonly occurring amino

acids - cysteine, proline, histidine and arginine - are missing. The amino acid sequence has not been determined. The pilin molecule also contains two phosphate molecules and one D-glucose molecule covalently linked to it. It is not known where the phosphate and D-glucose molecules are attached or whether they are exposed at the surface of the pilus.

Genetic studies on the F factor transfer system have indicated that F-pilus synthesis is a complex process involving several biosynthetic steps responsible for synthesis, modification and assembly of pilin subunits. These studies have identified 12 cistrons required for F transfer (Achtman et al., 1972; Willetts and Achtman, 1972; Ippen - Ihler et al., 1972; Sharp et al., 1972; Willetts, 1973) and of these, probably one (tra A) codes for the F-pilin protein subunit (Paranchych, 1975). Mutants have also been isolated which are unable to adsorb certain male-specific phages.

---

These mutants comprise strains that are resistant to all tested male-specific RNA phages but susceptible to DNA filamentous phages (Meynell and Datta, 1967; Silverman et al., 1968), and others which are resistant to one RNA phage, MS2, but susceptible to another, Q $\beta$  (and to DNA phages) (Meynell and Aufreiter, 1969). It appears that factors such as the primary structure of the pilin subunit and the state of glucosylation and phosphorylation probably determine the tightness of phage adsorption as well as the type of phage adsorbed. Biochemical and physical characterization of the pili isolated from the aforementioned mutants may well shed light on the subject of phage-pilin interaction at the molecular level.

### C. Phage RNA Ejection

When F-piliated cells are infected with RNA phages at 37°, the phage attachment step is followed almost immediately by an irreversible step which is analogous to the irreversible binding step of T<sub>1</sub> bacteriophage (Garen and Puck, 1951). As is the case with phage attachment, the phage ejection process exhibits no need for divalent cations, and proceeds normally when all divalent cations are chelated by EDTA (Paranchych, 1966). The completion of this step results in the loss of phage infectivity and the sensitization of the viral RNA to the degradative action of RNases (Valentine and Wedel, 1965; Danziger and Paranchych, 1970b). This phenomenon is generally attributed to a stage of the infectious process involving the transfer of phage RNA from the virion to the F-pilus, and has been described as the ribonuclease-sensitive step (Valentine and Wedel, 1965; Paranchych, 1966), the injection step (Valentine and Wedel, 1965; Silverman and Valentine, 1969), the invasion step (Knolle, 1967a,b) and the eclipse reaction (Paranchych, 1966; Danziger and Paranchych, 1970b). Recently Paranchych (1975) has recommended that the more precise term, the RNA ejection step, be adopted to describe this stage of phage infection.

The temperature-dependence of the RNA ejection step together with the inability of cell-free F-pili to elicit this reaction strongly indicates that some high energy compound or "state" of cellular origin are required for the activation of this step. Danziger and Paranchych (1970b), by studying the effect of temperature on the rate of the ejection reaction, calculated the energy of activation to be 10 kcal/mole.

The additional finding that the presence of metabolic inhibitors blocked the ejection process was regarded as being consistent with the cellular energy premise. However, subsequent findings, that the addition of metabolic poisons such as cyanide and arsenate to certain bacterial systems leads to the loss of F-pili from cells, introduced an element of doubt to the previous interpretation (Novotny *et al.*, 1972; O'Callaghan *et al.*, 1973c).

More direct proof of the linkage of the cellular energy state to phage RNA ejection was furnished by studies in which the cellular levels of the four common nucleoside triphosphates (ATP, GTP, UTP, and CTP) were monitored during the phage RNA ejection step (Paranchych *et al.*, 1970). It was found that the addition of R17 phage to F-piliated bacteria produced sudden losses in cellular nucleoside triphosphate (NTP) levels, a process which was essentially completed after 5 minutes.

---

There is also some indirect evidence that the energy-dependent RNA ejection step is not directly coupled to the dephosphorylation of NTP's, but rather to an as yet unknown high energy compound located in the cellular membrane. Yamazaki (1969), for example, has shown that the ejection reaction causes an abrupt inhibition of amino acid transport into the cell, suggesting that the RNA ejection process and the amino acid transport process may compete for a common membrane-associated energy source. Additionally, Danziger and Paranchych (1970b) found that piliated cells still retain their ability to promote the ejection reaction with high efficiency under conditions where the level of ATP (and presumably other arsenate-

sensitive high-energy phosphate compounds) in glucose-grown cells was reduced to less than 10% of control levels. It thus seems that the NTP losses engendered by the RNA ejection process may reflect the general energy state of the cell rather than a direct utilization of these compounds.

The tail model described earlier predicts that the A protein is attached to one end of the RNA genome and "pulls" the RNA out of the particle during the ejection process. The proposed existence of a specific RNA-A protein complex implies that there is a polarity to RNA penetration; that is, either the 3' or the 5'-end of the RNA will act as the leading end during the movement of the RNA across the cellular membrane. Support for this concept can be found in the different fates of the Class I and II particles during the ejection step. Krahn *et al.* (1972) have quantitated the amount of phage RNA and A protein penetrating infected cells and found that these two components enter the cell in about equimolar amounts; presumably these components originate from Class I particles. Class II particles, on the other hand, appear to undergo an abortive RNA ejection step. The A proteins from such particles readily dissociate from the capsids and either remain adsorbed to pili or desorb into the medium. Due to a postulated weak linkage between the A protein and the RNA, all or most of the RNA is left behind in the capsid in the RNase-sensitive state (Krahn and Paranchych, 1971). Further evidence alluding to the existence of an A protein-RNA complex is provided by Oriel's (1969) finding that the A protein is associated with RNA fragments released from



whole phage following treatment with alkali or heat. As was mentioned earlier, an A protein-RNA complex was detected in the early assembly stage of infectious particles (Kaerner, 1970; Bonner, 1974).

At present, the nature of the signal which triggers the onset of the irreversible ejection step is not completely understood. A revealing piece of evidence has been the discovery that the A protein is fragmented into two subunits of molecular weights 15,000 and 24,000 prior to penetration into the host cell (Krahn et al., 1972). This event has been interpreted as a possible triggering mechanism which sets into motion the subsequent steps of RNA ejection and penetration. At the moment, it is not known whether one or both of the 2 fragments remain complexed to one end of the RNA during RNA ejection and penetration (*vis-à-vis* the tail model), or whether the fragments and RNA become separate entities after A protein fragmentation. Furthermore, the cleavage of a peptide bond is a strong indication that an enzyme is involved. This putative enzyme can either be located on the F-pilus (thus far no enzymatic activity has been detected in F-pili) or on the membrane at the base of the pilus. If the latter possibility were true, then the prediction can be made that phage would be eclipsed at the base of F-pili, and that attached phage particles have to be transported to the base to enter into this reaction. The possible role of the F-pilus as a transport system for phage is discussed below.

#### D. The RNA Penetration Process

There is some uncertainty regarding the requirement of energy for the RNA penetration step. Paranchych (1975) has suggested that since the pattern of NTP decrease in infected cells is the same whether RNA penetrates or not, it is probably the RNA ejection step alone that requires an energy of activation. Krahn (1971), on the other hand, believed that energy is needed for RNA penetration. He cited the figure of 36 kcal/mole reported by Knolle (1967b) as representing the overall activation energy required for the RNA phage ejection and penetration steps. The difference of 26 kcal/mole between Knolle's figure and the value of 10 kcal/mole found for the energy of activation for the ejection step (Danziger and Paranchych, 1970b) was interpreted by Krahn to represent the activation energy of RNA transport into cells.

---

The controlled extrusion of RNA from the phage capsid and its penetration into the cell appear to be critical stages in RNA phage infection. Their success seemingly depends on the RNA being in a proper physical state. As described previously, the RNA is exposed to the surrounding medium during these steps and the presence of RNase precludes RNA penetration by degrading the RNA before it can penetrate (Zinder, 1963; Knolle and Kaudewitz, 1963; Valentine and Strand, 1965). The penetration of phage RNA was also found to be blocked in the absence of divalent cations such as  $Mg^{2+}$ ,  $Ca^{2+}$ ,  $Sr^{2+}$ , or  $Ba^{2+}$  (Paranchych, 1966) or in presence of antibiotics such as neomycin or streptomycin (Brock, 1962; Brock and Wooley, 1963;

Schindler, 1965). Since the adsorption and the RNA ejection steps were not affected by the preceding conditions; the focus of action appears to be centered on the exposed RNA. Although the mechanism of action of divalent cations has yet to be elucidated, they may conceivably help to stabilize the phage RNA as it unfolds and ejects from the capsid. On the other hand, the injection of RNA may somehow be blocked by the binding to RNA of neomycin or streptomycin, compounds which are known to be able to form complexes with nucleic acids. The formation of this complex is probably reversible as it was observed that sufficiently high concentrations of  $Mg^{2+}$  ions were able to cancel the inhibitive effect of the drugs on phage infection (Brock and Wooley, 1963; Schindler, 1965).

Besides its role as a phage receptor site, the F-pilus is also regarded as the conduit through or on which the phage RNA is transported into the host cell. Various models have been proposed to explain the mechanism of nucleic acid transport by pili. Brinton (1965) originally suggested that the F-pilus was a hollow tube through which the nucleic acid is transported. More recently he has proposed that F-pili may consist of two parallel protein filaments, each consisting of an assembly of F-pilin monomers (Brinton, 1971). The transfer of single stranded DNA from donor to recipient cells is thus envisaged by Brinton to occur either by a conduction mechanism (DNA strand moves between stationary F-pilus filaments), a conveyor mechanism (DNA strand is bound to one of the filaments and F-pilus filaments move with respect to each other as continuous conveyor belt), or a carrier

mechanism (DNA strand is bound to both filaments; assembly of the F-pilus at the membrane of the donor cell and depolymerization at the membrane of the recipient cell results in the movement of the F-pilus towards the recipient). In contrast, Marvin and Hohn (1969) and Curtiss (1969) have proposed a model in which the F-pilus retracts into the donor cell after receiving an appropriate stimulus. According to this model, the adsorption of RNA phage to the side, filamentous DNA phage to the tip, or an  $F^-$  cell to the tip of the pilus all trigger a retraction of the pilus through a process of sequential depolymerization of pili subunits within or at the cell membrane. The model proposes that such retraction results in RNA phage being pulled to the base of the pilus, where it injects its RNA, the  $F^-$  bacterium being pulled up close to the male bacterium, where a classical conjugation bridge is formed, and male-specific DNA phage being pulled to the cell membrane, where it

---

either injects its DNA or is pulled into the cell as an entire virion.

The evidence advanced thus far to support the pilus retraction hypothesis has been ambiguous. Jacobson (1972), in a study of the penetration of the male-specific filamentous phage,  $\phi_1$ , has shown that the average number of F-pili with phage attached decreases as phage DNA enters the cell, and that a short lag of 1 - 2 minutes separates the loss of F-pili and the penetration of the DNA. During this lag period, phage particles were seen to accumulate at the surface of the cell. Similar observations were reported by Bradley (1972b) on

the interaction between the RNA phage PP7 and Pseudomonas aeruginosa pili and interpreted on the basis of pili retraction. From parallel studies on the R17 and M13 (a DNA filamentous phage) phage systems, however, Paranchych et al., (1971), and O'Callaghan et al. (1973a) concluded that no pili retraction had occurred but that observed losses of pili from infected cells were due to pili fragmentation. In these studies, the number of pili fragments in the medium were shown to rise soon after phage infection. The possibility that different mechanisms exist for nucleic acid transport in different pili systems, or that DNA or RNA may be transported by different means, cannot be ruled out at this time.

The purpose of the foregoing discussion has been to delineate the present level of understanding of the early stages of RNA phage infection. More importantly, it has attempted to pinpoint the many gaps in this knowledge and the contradictory information that exists in some areas. This thesis describes studies focusing on the fate of the phage RNA during these early stages of infection and shortly after its penetration into cells. It will also describe studies on the effects of free radicals on the phage RNA in situ, and the exploitation of the resulting findings to determine the polarity of RNA penetration. It is hoped that these investigations have resulted in the clarification of certain aspects of the early stages of infection although, understandably, the story is still far from complete.

## CHAPTER 11

### MATERIALS AND METHODS

#### A. Materials

##### 1. Bacteria and Bacteriophage

###### (a) Bacteriophage

The RNA phage R17 originally isolated by Paranchych and Graham (1962) was used throughout the studies described in this thesis.

###### (b) Bacteria

The various strains of Escherichia coli used are:

Strain	Genotype
<u>E. coli</u> WP156	Hfr met <sup>-</sup> T <sub>1</sub> <sup>r</sup> Sm <sup>s</sup> derived from AB257 (Hfr met <sup>-</sup> T <sub>1</sub> <sup>s</sup> Sm <sup>s</sup> ).
<u>E. coli</u> ED2644	Flac <sup>+</sup> Sm <sup>s</sup> Spc <sup>r</sup> T <sub>6</sub> <sup>r</sup> derived from ED24 (F <sup>-</sup> lac <sup>-</sup> Sm <sup>s</sup> Spc <sup>r</sup> T <sub>6</sub> <sup>r</sup> ).
<u>E. coli</u> AB301	Hfr met <sup>-</sup>
<u>E. coli</u> A19	Hfr met <sup>-</sup> RNase I <sup>-</sup> derived from AB301
<u>E. coli</u> ED2602	Flac <sup>+</sup> in ED2601 (F <sup>-</sup> lac <sup>-</sup> his <sup>-</sup> trp <sup>-</sup> Sm <sup>R</sup> Spc <sup>S</sup> T <sub>6</sub> <sup>r</sup> gal <sup>-</sup> lys <sup>-</sup> )
<u>E. coli</u> B	wild type.

Except where specified, E. coli WP156 was used as host cell in penetration experiments and as seed culture in plaque assays.

All strains of E. coli were maintained on hard agar plates for routine use. Permanent stocks were stored on hard agar slants

in wax-sealed vials. Cell cultures were started by transferring a single colony on an agar plate to 10 ml of medium which was then shaken in a 37° water bath overnight (12 to 18 hr).

## 2. Bacterial Culture Media

### (a) Tris (hydroxymethyl) amino methane maleic acid minimal salts (TMM) medium

The basic TMM salts solution contained the following components in moles per liter; Tris, 0.05; maleic acid, 0.05; NaCl, 0.043; KCl, 0.027; NH<sub>4</sub>Cl, 0.019; Na<sub>2</sub>HPO<sub>4</sub>, 0.001; Na<sub>2</sub>SO<sub>4</sub>, 0.001.

After dissolving the above in distilled water, the pH was adjusted to 7.3 with concentrated NaOH and the solution autoclaved at 126° for 15 min under a steam pressure of 20 lbs/in<sup>2</sup>.

Complete TMM (CTMM) medium was prepared by combining the sterile components listed in the following proportions:

Basic TMM salts solution	910 ml
Eagles amino acid concentrate (100X)	10 ml
50% (w/v) glucose	10 ml
0.25% (w/v) L-methionine	10 ml
0.5 M MgCl <sub>2</sub>	10 ml
20 mg % d-biotin	50 ml

### (b) Various TMM-based media

(i) CTMM(-aa) medium. This medium contained all the regular components of CTMM medium with the omission of the Eagles amino acid concentrate.

(ii) CTMM (+ casamino acids). Casamino acids (Difco, 0.05%) replaced the Eagles amino acid mixture.

## (c) Trypticase soy broth (TSB9)

Trypticase soy broth (Baltimore Biological Laboratories) 15 g/l

NaCl 8 g/l

Autoclaved solutions had a final pH of 7.2 - 7.3

## (d) Hard agar

Trypticase soy broth 30 g/l

Bacto-Agar (Difco) 15 g/l

After dissolving, the solution was autoclaved and dispensed while warm into disposable Petri dishes.

(e) Top agar

Top agar was prepared as above except that the final agar concentration was 11 g/l. Sterile top agar was stored in 50 ml volumes at 4° until used. In preparation for plaque assays, the agar was melted in a boiling water bath, dispensed in 2 ml aliquots into sterile culture tubes and maintained in the liquid state until used by incubating in a 45 - 50° Temp-Blok (Lab-line Instruments, Inc.).

3. Bacteria and Phage Diluent

All dilutions of bacteria or phage were made with a sterile solution composed of 0.9% (w/v) NaCl, 5 mM MgCl<sub>2</sub>, and 5 mg % bovine serum albumin (Sigma Chemical Co.). Diluent was dispensed in 10 ml volumes into sterile dilution tubes (20 mm) and stored at 4°. These solutions were prewarmed to room temperature before use.

4. Chemicals, Enzymes and Reagents

Unlabeled ribonucleosides, ribonucleoside mono-, di- and triphosphates, guanosine 5'-tetrphosphate (ppppG), sodium dextran



sulfate 500 (NADS), lysozyme (egg white), pancreatic ribonuclease (5X recrystallized) and bovine serum albumin were purchased from Sigma Chemical Co. Polyethylene glycol 6000 (PEG) was supplied by J.T. Baker and Co. Urea (ultra pure) was purchased from Mann Research Laboratories. Sodium dodecyl sulfate (SDS) was obtained from Matheson, Coleman and Bell. The NCS reagent employed for solubilizing polyacrylamide gel slices was from Nuclear Chicago. DNase (RNase free), snake venom phosphodiesterase (SVP), alkaline phosphatase (*E. coli*), and catalase (beef liver) in a powder form were purchased from Worthington Biochemical Corp. The source of Rifampin B-grade (Rifampicin) was Calbiochem.

N,N,N',N'-tetramethylethylenediamine (TEMED), acrylamide and N,N'-bis-methyleng (bis) acrylamide was obtained from Eastman Chem. Co. The latter two were recrystallized before use according to the procedure published by Loening (1967).

pGp was isolated according to the procedure outlined by Roblin (1968). About 200 mg of yeast tRNA (Sigma) was hydrolyzed in 5 ml 0.3N KOH for 24 hr. The hydrolysate was passed through a 7 x 1.4 cm column of Dowex 2(Cl<sup>-</sup>). After elution of the mononucleotides with 0.005 N-HCl, pGp was eluted with 0.03 N-HCl. Fractions containing pGp were lyophilized and the solid residue taken up in distilled water. At pH 8, pGp was identified by the spectral ratios: 250 nm/260nm = 1.12, 280 nm/260nm = 0.68.

#### 5. Radioactive Materials

Radioactive precursors for the preparation of labeled phage R17 were obtained from the following sources: <sup>32</sup>P (inorganic

phosphate, carrier free) and  $^{35}\text{S}(\text{Na}_2^{35}\text{SO}_4 \text{ in } \text{H}_2\text{O}, 800 \text{ mCi/mmole})$ , New England Nuclear,  $^3\text{H}$ -8-guanosine (5Ci/mmole),  $^3\text{H}$ -2,8-adenosine (30Ci/mmole),  $^3\text{H}$ -5,6-uridine (40Ci/mmole) and  $^3\text{H}$ -2,5-histidine (45 Ci/mmole), Amersham/Searle.

### B. Growth of Bacteria

Experimental cultures were grown at  $37^\circ$  in a rotary-shaking water bath from a 1/100 dilution of an overnight E. coli culture. In order to achieve maximum aeration and avoid excessive breakage of F-pilus, shallow cultures (generally 20% of the flask volume) were shaken at a speed of 125 rpm in baffled culture flasks (Bellco Glass Co.). Under these conditions, cultures generally reached a cell density of  $4 \times 10^8$  cells/ml about four hours after inoculation if grown in a minimal salts medium, and about 2 hours for cells growing in TSB.

The density of viable E. coli cells in TMM media was determined from a standard curve constructed by plotting the absorbancy at 650 nm of a 1.0 ml volume of culture (in a cuvette with a light path of 1 cm) vs the viable cell counts. Viable cell counts were determined by plating an appropriate dilution of the culture on hard agar plates and incubating overnight at  $37^\circ$ .

### C. Preparation and Purification of Phage R17

#### I. Cell Lysis and the Partial Purification of the Released Phage by a Two-Phase Polymer System

Cultures of WP156 cells were grown at  $37^\circ$  in CTMM(-aa) to

a cell density of  $4 \times 10^8$  cells/ml, then infected by the addition of purified phage R17 at a multiplicity of 40 PFU's/cell. After allowing about 10 min for phage adsorption, incubation was continued with vigorous shaking (150 rpm) for 3-4 hrs. Cell lysis was discernible through the appearance of clumps of cell wall debris accompanied by a reduction in the optical density of the infected culture. Cell lysis was completed by adding lysozyme (66 mg/l) and chloroform (3.3 ml/l) followed by a further incubation at 37° for 30 min. Titer of crude lysates thus obtained varied from  $8 \times 10^{11}$  -  $1.2 \times 10^{12}$  PFU/ml.

\*The phage in the crude lysate was concentrated and partially purified by using a modification of the liquid two-phase polymer method described by Albertsson (1967): To a 100 ml lysate was added 0.21 g sodium dextran sulfate (NaDS), 7.15 g polyethylene glycol (PEG) and 1.8 g NaCl, and the mixture was shaken to homogeneity before it was stored at 4° for 18 - 24 hrs in a 250 ml polycarbonate centrifuge bottle to allow phase formation. The next day, the bottle was centrifuged at 3000g for 20 min before most of the top PEG phase (comprising 90 - 95% of the total volume) was removed by aspiration, care being taken not to disturb the interphase. The pellet of cell debris and the NaDS phase with the concentrated phage was then resuspended in 5 ml of 0.15 M NaCl buffered with 0.015 M sodium citrate, pH 7.0 (SSC), and centrifuged at 10,000 g for 10 min. The pellet was washed 4 more times with 5 ml SSC. To the combined washings (20 ml) was added 0.15 volume of saturated KCl solution to precipitate the residual NaDS over a period of 2 hrs

at 4°. After removal of the precipitated NaDS by centrifugation at 10,000 g<sub>0</sub> for 10 min, the phage suspension was dialyzed against SSC (4°) for at least 18 hrs. The phage was then pelleted by centrifugation at 50,000 rpm for 2 hrs in the Beckman 60 Ti rotor and finally resuspended in 4 ml SSC in preparation for banding in a CsCl density gradient.

### 2. CsCl Isopycnic Banding of Phage

Equilibrium CsCl density gradient centrifugation was carried out by adding 2.4 g CsCl to the resuspended phage (4 ml) and spinning the mixture at 35,000 rpm for at least 18 hrs in the Beckman SW50.1 rotor at 4°. About 25 - 30 fractions were collected by piercing the bottom of the nitrocellulose tube and dripping 11 - 12 drop fractions into a series of 13 mm tubes. The position of the phage peak was determined by ascertaining the relative absorbance at 260 nm or the radioactivity (if the phage is labeled with radioactive precursors) of each fraction. Usually the infectious phage banded as a sharp peak towards the middle of the gradient while a small amount of noninfectious particles formed a shoulder at lower densities. The fractions corresponding to the main peak were pooled and subsequently dialyzed against SSC at 4° overnight to remove the CsCl.

### 3. Assay for Phage Density

The number of phage particles in a phage solution was determined from optical density measurements with a Beckman (DBG) spectrophotometer, using an extinction coefficient at 260 nm of  $7.66 \text{ Mg}^{-1} \text{ ml cm}^{-1}$  (Gesteland and Boedtke, 1964). Assuming a molecular mass of  $3.6 \times 10^6$  daltons per phage particle, as reported

by the foregoing workers, one absorbancy unit was calculated to contain  $2.18 \times 10^{13}$  particles. A yield of about 0.5 ml of phage at a density of  $5 - 10 \times 10^{14}$  particles/ml was usually obtained from a 100 ml crude lysate.

#### D. Radioactive Labeling of Phage R17

##### 1. $^{32}\text{P}$ -Labeling of R17 phage RNA

Overnight cultures of E. coli WP156 were grown in CTMM(-aa) medium with the phosphate concentration lowered to 0.5 mM. A one ml aliquot of the overnight culture was transferred to 100 ml of fresh medium with a similar phosphate concentration and the cells grown up to  $4 \times 10^8$  cells/ml. R17 phage infection was carried out as described for the preparation of crude lysates. At 5 min post-infection, a neutralized solution of  $^{32}\text{P}$  inorganic phosphate (10 mCi) was added and incubation continued. Freshly purified phage obtained from such crude lysates normally had a specific radioactivity of  $2 \times 10^{-6}$  cpm/particle.

##### 2. $^3\text{H}$ -Adenosine and $^3\text{H}$ -Guanosine Labeling of R17 phage RNA

The procedure followed for the labeling of R17 phage with  $^3\text{H}$ -guanosine or  $^3\text{H}$ -adenosine was identical to that described for the preparation of unlabeled phage except that one of the 2 radioisotopes was added at 20 min post-infection to a final activity of 50  $\mu\text{Ci/ml}$ . The specific  $^3\text{H}$  radioactivity of phage thus prepared was similar to that obtained for freshly purified  $^{32}\text{P}$ -labeled phage.

##### 3. $^{35}\text{S}$ -Labeling of R17 Phage Proteins

$^{35}\text{S}$ -labeled R17 was prepared as follows: A culture of E. coli

ED2644 was grown to a density of  $4 \times 10^8$  bacteria/ml in CTMM(-aa) medium containing a concentration of  $\text{Na}_2\text{SO}_4$  of 0.021 g/l ( $1.5 \times 10^{-4}$  M). The culture was infected with R17 phage at a multiplicity of 40 PFU/cell, incubated for 10 min at  $37^\circ$ , and then  $\text{Na}_2^{35}\text{SO}_4$  (0.8 - 1.0 Ci/mM) was added to a final activity of 50  $\mu\text{Ci/ml}$ . Purification of the resultant lysate was carried out as described for unlabeled phage preparations. The recovery of radioactivity was about  $2 - 4 \times 10^{-7}$  cpm/particle. All the  $^{35}\text{S}$ -labeled phage components were insoluble in hot trichloroacetic acid and SDS polyacrylamide gel analysis of the protein components revealed that 99% of the radioactivity was incorporated into coat protein.

#### 4. Labeling of R17 Phage A Protein with Radioactive Histidine

The fate of the A protein during phage infection can be followed by labeling the phage with radioactive histidine. This procedure exploits the fact that the A protein is the only histidine-containing polypeptide associated with wild-type R17 (Steitz, 1968a). R17 phage was labeled with  $^3\text{H}$ -histidine according to the method originally developed by Krahn (1971). A culture of *E. coli* WP156 was grown to a density of  $4 \times 10^8$  bacteria/ml in TMM medium containing 10  $\mu\text{g/ml}$  of 19 amino acids (no histidine), and 10  $\mu\text{g/ml}$  each of urocanic acid, adenosine, guanosine, cytidine, and uridine. At 15-min after infection, 2,5- $^3\text{H}$ -histidine was added to a final activity of 37.5  $\mu\text{Ci/ml}$ , and 7 min later, the pulse was terminated by the addition of unlabeled histidine to a final concentration of 10  $\mu\text{g/ml}$ . Incubation of the culture was then continued until lysis occurred 3-4 hr later. Purified phage obtained from such crude lysates gener-

ally had a specific radioactivity of  $1 \times 10^{-8}$  cpm/physical particle, and contained about 65-70% of the radioactivity in the A protein. The remainder of the radioactivity was found to be in the phage RNA, equally distributed between adenine and guanine residues (Krahn, 1971).

#### E. Hot and Cold TCA Radioassay

Radioactively labeled phage suspensions or *E. coli* infected with such phage were assayed for TCA-insoluble material by applying 0.1 ml aliquots onto 3MM Whatman filter discs (2.1 cm diameter) pinned to a board. If required, several aliquots were added in succession with a drying step separating each addition. The paper discs were processed by a scheme modified from that published by Mans and Novelli (1960). For reasons of safety, ethanol was used in place of ether.

#### 1. Hot TCA-Insoluble Products

Table 2.1

Preparation of Paper Discs for Hot-TCA Insoluble Products

Step	Time	Wash medium	Temperature
1.	30 min	10% TCA	4°
2	5 min	5% TCA	4°
3	45 min	5% TCA	90°
4	15 min	5% TCA	4°
5	15 min	85% EtOH	20°
6	15 min	90% EtOH	20°

## 2. Cold TCA-Insoluble Products

Treatment was similar to that shown in the above scheme with the substitution of a 15 min 5% TCA (4°) wash for step 3.

## F. Radioisotope Counting

Dry samples such as radioactive material embedded in air dried filter discs after TCA treatment were counted in 5.0 ml toluene-based scintillation fluor (prepared by the addition of 4 g Omnifluor from New England Nuclear per liter of scintillation grade toluene) in a Beckman LS-250 liquid scintillation spectrometer.

Aqueous samples were assayed by combining 0.5 - 1.0 ml samples with 10 ml Scinti Verse (Fischer Scientific) in a scintillation vial and shaking the mixture to homogeneity. The efficiency of counting in Scinti Verse was >95%, 85% and 30% for  $^{32}\text{P}$ ,  $^{35}\text{S}$  and  $^3\text{H}$  isotopes, respectively.

Single isotope restricted channels were used for double-labeling experiments and counts were corrected for overlap.

External standardization was used to monitor the efficiency of counting in a series of similarly prepared vials.

Samples with low levels of radioactivity were counted for a sufficient length of time to reduce the error to less than 5%. All sample values were corrected for background radioactivity registered in controls containing no added sample.

## G. Plaque Assay for Infectious Phage

The number of infectious phage in a suspension was deter-



mined by serially diluting the sample and mixing 1.0 ml of a dilution with 0.2 ml of seed culture ( $4 \times 10^8$  cells/ml) and 2.0 ml of liquified top agar. After agitation, the mixture was poured onto hard agar in a Petri dish and allowed to harden before the plates were inverted and incubated at  $37^\circ$  overnight before scoring for plaques. A single dilution was usually plated out in triplicate.

#### H. Phage Attachment Assay

The filtration assay employed to measure phage-pili complex formation was essentially that described by Danziger and Paranchych (1970a). WP156 bacteria ( $4 \times 10^8$  cells/ml) in CTMM medium were incubated at a multiplicity of  $10^3$   $^{32}\text{P}$ -labeled particles/cell at  $4^\circ$  for 20 min. Aliquots of 2.0 ml were then passed through Gelman GA-6 triacetate filters under a vacuum of 6 in. of mercury. The filters were washed 3 times with 5 ml of cold TMM medium, dried and assayed for radioactivity.

#### I. Penetration Assay

The penetration assay as applied in the quantitation of the amount of a given phage component (RNA, A protein, coat protein) having penetrated cells is essentially the method described by Krahn (1971) and Krahn *et al.* (1972). Aliquots of infected bacteria at various times post-infection were poured onto 0.5 volumes of frozen TMM ( $-\text{Mg}^{2+}$ ) salts medium to stop further penetration of phage components, and the chilled cells were then pelleted at 10,000 g for 10 min. The cells, after being resuspended in 0.2

volumes of cold TMM ( $-Mg^{2+}$ ) by repeated trituration with a pasteur pipette, were forced through a syringe tipped with a #26 gauge needle. After the cells were pelleted again by centrifugation, the supernatant containing the extracellular phage was removed and fresh cold TMM ( $-Mg^{2+}$ ) added; the wash cycle was repeated a total of 6 times before the final cell pellet was resuspended in a predetermined volume of TMM ( $-Mg^{2+}$ ). Aliquots of this suspension were directly assayed for radioactivity in combination with Scinti Verse or dripped onto Whatman filter discs in preparation for hot TCA treatment.

The efficiency of the above washing procedure in removing all extracellular phage from infected cells was shown by control infections in which *E. coli* B ( $F^-$ ) at  $37^\circ$  or Hfg cells at  $4^\circ$  were infected at similar multiplicities for the same period of time. It was found that negligible radioactive counts were associated with these cells after they were washed 6X (Krahn, 1971). In the latter case, the result agreed with Brinton and Beer's (1967) finding that no RNA penetrates sensitive bacterial at  $4^\circ$ .

Furthermore, when a sonicated extract of 6X washed cells, infected with R17 radioactively labeled in the RNA or A protein, was analyzed by centrifugation in sucrose gradients, greater than 95% of the RNA or A protein radioactivity remained at the top of the gradient while little material was found migrating with 78S intact phage (Krahn, 1971; Krahn *et al.*, 1972). These results indicated that the A protein and RNA components had penetrated as free components and were not associated with extracellular phage particles.

#### J. Amicon Ultrafiltration

Phage particles in a large volume were concentrated by ultrafiltration through a 6.2 cm Diaflo, XM-100A membrane (exclusion limit = 100,000 daltons) housed in an Amicon Model 202 unit (capacity: 200 ml). The procedure was carried out at 4° with a moderate rate of stirring under a N<sub>2</sub> gas pressure of 10 - 15 lbs/in<sup>2</sup>. The flow rate was about 2 - 4 ml/min.

#### K. Sucrose Gradient Techniques

Linear (5 - 20%), 4.6 ml sucrose gradients were usually prepared using a two-chamber Buchler gradient maker. Before using, gradients were equilibrated by storing at 4° for at least 4 hrs.

Aqueous samples (0.2 - 0.5 ml) were layered carefully onto gradients without disturbing the meniscus. Centrifugation was carried out at an appropriate speed and temperature using a SW 50.1 rotor in a Beckman L2-65B ultracentrifuge.

Fractions from gradients were collected by piercing the bottom of the cellulose nitrate tube with a hollow needle.

#### L. Ascorbic Acid-Cu<sup>2+</sup> inactivation of R17 Phage

Phage particles were incubated in a buffer solution made up with deionized distilled water and containing 0.09 M NaCl and 0.05 M Tris (pH 7.3). Phage suspensions, CuCl<sub>2</sub> and L-ascorbic acid solutions were made up with the buffer at 10X the concentration to be used in a particular experiment. Freshly made ascorbate solutions were used in all cases. Incubations were initiated by the combination of prewarmed solutions and buffer to give a tenfold

dilution of the components; zero time of incubation corresponded to the addition of the phage suspension to a reaction mixture as the last component. Phage inactivation was "quenched" at any time by removing aliquots of incubation solution and combining immediately with 0.1 volume of  $10^{-2}$  M ethylenediaminetetraacetic acid (EDTA). Subsequently, the quenched solutions were kept on ice while awaiting further treatment. In anoxic incubations, all manipulations were carried out in a glove bag kept inflated by a steady stream of nitrogen gas. Before use, all solutions, which were maintained at 37° in a "Temp-Blok", had nitrogen bubbled through them for 20-30 seconds to displace dissolved oxygen with  $N_2$ .

Phage suspensions having different ratios of plaque forming units (PFU) to physical particles were obtained on a preparative scale by incubating phage-ascorbate- $Cu^{2+}$  mixtures in 2- to 3-ml volumes. Aliquots of 0.5 ml were taken out at appropriate time intervals and quenched with EDTA. Separation of chelated  $Cu^{2+}$ , ascorbate, and EDTA from treated phage particles was achieved by passing the mixture through a Sephadex G-50 column (1 x 12 cm) equilibrated with the Tris buffer. The phage fraction was followed visually by an added blue dextran marker, or by measurement of radioactivity in the case of labeled phage.

#### M. Ethidium Bromide Binding Assay

The binding of ethidium bromide to phage RNA in situ was measured in a 2.0 ml solution containing  $5 \times 10^{-3}$  M Tris (pH 8.0),

$5 \times 10^{-4}$  M EDTA, and 0.5  $\mu\text{g/ml}$  ethidium bromide. Phage was added to the reaction mixture to a final concentration of  $10^{11}$  physical particles/ml. Fluorescence readings were made in a Turner 430 spectrofluorometer in round borosilicate cuvettes with the excitation wavelength set at 525 nm and emission at 600 nm. All readings were performed at 25°.

#### N. Isolation of RNA

The initial stages of the isolation of RNA from 6X washed infected *E. coli* were similar to those described by Sagik et al., (1962). About  $2 - 3 \times 10^9$  cells were resuspended in 1 ml of buffer containing 0.01 M Tris (pH 7.3), 0.01 M KCl, 0.005 M  $\text{MgCl}_2$ , 300  $\mu\text{g/ml}$  lysozyme and 50  $\mu\text{g/ml}$  DNase. The suspension was frozen rapidly in an EtOH-dry ice bath, then thawed and incubated for 5 min at 14°. The mixture was brought to 1% in SDS and 0.2% in Macaloid (Union Carbide) and shaken for 5 min at 20°. Deproteinization was completed by adding an equal volume of buffer-saturated phenol and shaking for 15 min at 4°. The resulting emulsion was centrifuged at 10,000 g for 10 min, after which the aqueous layer was removed, and Macaloid and phenol added as before. The phenol extraction procedure was repeated three times. The final aqueous solution was three times extracted with ether and  $\text{N}_2$  gas was bubbled through the solution as a last step to remove residual ether. The RNA was then precipitated by the addition of 2 volumes of cold (-20°) MeOH and 0.1 volumes of 20% potassium acetate and stored overnight at -20°. The precipitated RNA was then collected by centrifugation, dried under  $\text{N}_2$  and stored in a

desiccator at -20° until used.

The same procedure was followed for the isolation of RNA from intact phage except that particles were suspended in the Tris buffer minus DNase and Lysozyme. The freeze-thawing step was also omitted.

O. Alkaline Hydrolysis of RNA

Isolated RNA samples were taken up in 0.5 ml of 0.3 N KOH and incubated at 37° for 24 hrs in covered tubes. The hydrolysates were carefully neutralized to pH 7.0 by adding small increments of a slurry of Dowex-50 (in the pyridinium form). Quantitative recovery of nucleotides and nucleosides (especially in the case of A<sub>3'</sub> and Ap) was achieved by washing the Dowex beads with five, 0.5-ml aliquots of 10% aqueous pyridine. Lastly, the products of the alkaline hydrolysis were obtained in a powder form by the removal of water and pyridine through lyophilization of the combined washings.

P. SDS-Polyacrylamide Gel Electrophoresis of Protein

Radioactively labeled R17 phage proteins were analyzed by the SDS-polyacrylamide gel electrophoretic system described by Laemmli (1970). Gels containing 12.5% acrylamide were prepared from a stock solution of 30% (w/v) of acrylamide and 0.8% (w/v) of bis-acrylamide. The final concentrations in the gel were as follows: 0.375 M Tris-HCl (pH 8.8) and 0.1% SDS. The gels were polymerized chemically by the addition of 0.025% (v/v) of TEMED and 0.025% (w/v) ammonium persulfate. Ten cm gels were prepared in glass tubes with

a total length of 13 cm and with an inside diameter of 2 mm. The 3% stacking gels described by Laemmli were not used in this application. The electrode buffer (pH 8.3) contained 0.025 M Tris, 0.19% M glycine and 0.1% SDS. The samples were suspended in a solution with the following composition: 0.0625 M Tris HCl (pH 6.8), 2% SDS, 10% glycerol, 5% 2-mercaptoethanol and 0.001% tetraiodoquinol blue as the dye. The proteins were completely dissociated by immersing the samples for 5 - 7 min in boiling water. After layering the sample on top of gels, electrophoresis was carried out at 3 - 5 mA per gel at room temperature until the dye marker reached the bottom of the gel. Gels were sliced into about fifty, 1.67 mm wide sections with a multi-blade "cheese-cutter" used in conjunction with a teflon block slotted at 1.67 mm intervals. The radioassay of the gel slices was accomplished using the same procedure described below for RNA gels.

## 0. Polyacrylamide Gel Electrophoresis of RNA

### 1. Exponential Gradient Gels

For routine analysis of RNA, the polyacrylamide exponential-gradient system of Mirault and Scherrer (1971) was utilized.

To produce the exponential gradient, an apparatus as schematically represented in Figure 2.1 was used. The mixing vessel consists of a 5 ml glass chamber fitted tightly with a straight-sided rubber stopper and equipped with a 1.3 cm magnetic bar for stirring. Passing through the stopper are three outlets - one leads to two peristaltic pumps which draw acrylamide solution to two glass tubes.

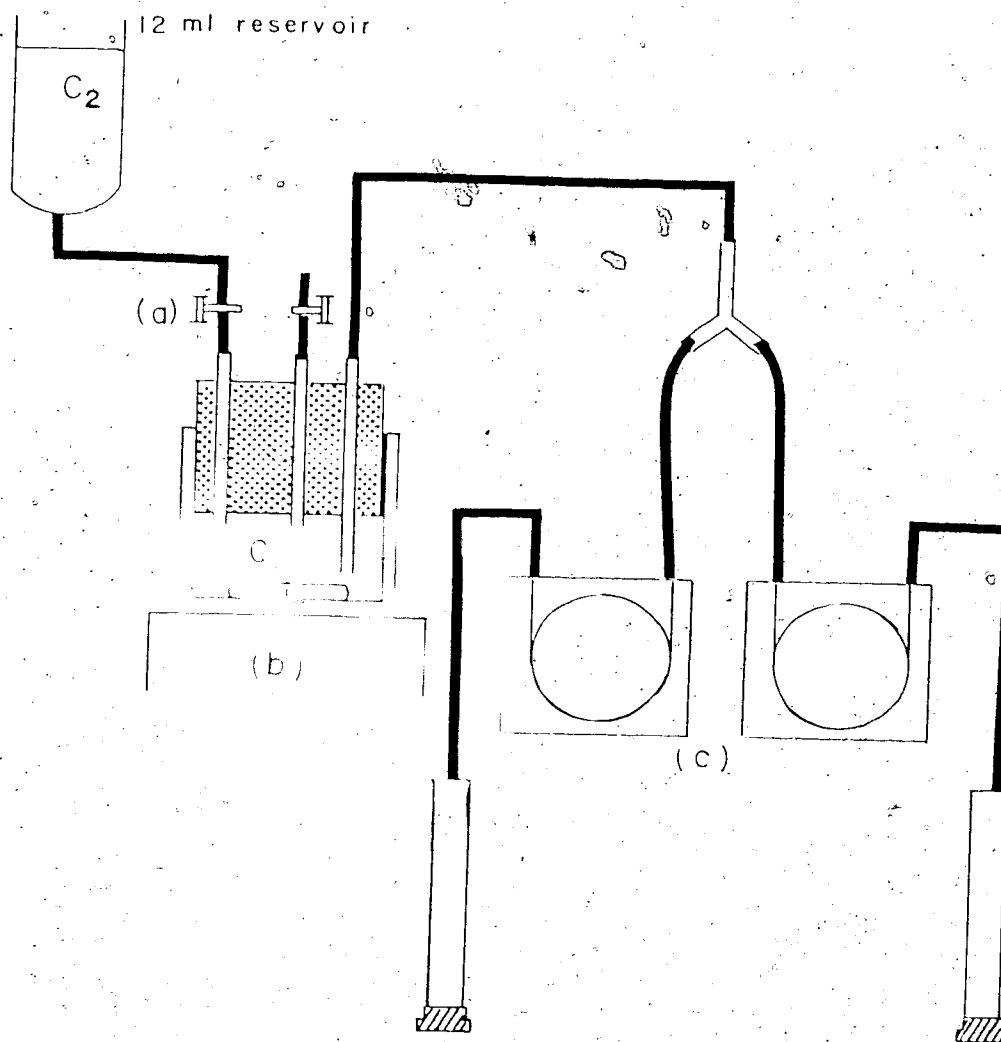


Figure 2.1 Schematic diagram of the exponential gradient gel making apparatus.

(a) clamps, (b) magnetic stirrer, (c) Perpex peristaltic pumps (LKB, instrument group 10200); gear box used: 1/25.  $C_1$  = acrylamide solution of higher concentration.  $C_2$  = acrylamide solution of lower concentration.



Another is the intake conduit through which a low concentration acrylamide solution ( $C_2$ ) passes at a rate equal to the rate of removal of solution from the chamber. The third opening serves as an air release valve.

The simultaneous preparation of two,  $0.7 \times 10$  cm, 2.5 - 15% exponential gradient gels began with the addition of 2.2 ml of a 15% acrylamide solution ( $C_1$ ) into the mixing chamber. The air release valve was opened and the stopper adjusted so that no air packet appeared in the chamber. The gel casting operation was initiated by switching on the magnetic stirrer and peristaltic pumps and releasing the intake tubing clamp.

According to Mirault and Scherrer (1971), the concentration of the acrylamide in the gels thus generated can be described by the equation:

$$C(V) = (C_1 - C_2)e^{V/V_1} + C_2 \quad (1)$$

where  $C(V)$  = acrylamide concentration in the mixing chamber after dilution by volume  $V$  of acrylamide solution ( $C_2$ );  $C_1$  = higher concentration acrylamide solution,  $C_2$  = lower concentration acrylamide solution,  $V_1$  = internal volume of the mixing chamber.

The composition of the  $C_1$  solution used is as follows: E-RNA buffer (0.04 M triethanolamine, 0.02 M sodium acetate, 0.002 M EDTA, pH 7.4); 20% glycerol; 15% acrylamide; 0.25% bis-acrylamide. Polymerization was initiated by the addition of 0.67  $\mu$ l of 10% TEMED and 10% ammonium persulfate to each ml of  $C_1$ .

$C_2$  consists of: E-RNA buffer; 2.5% glycerol; 2.5% acrylamide; and 0.042% bis-acrylamide. To each ml of  $C_2$  were added 4  $\mu$ l of 10%

TENED and 10% ammonium persulfate.

For filling, 0.7 (inside diameter) x 12 cm glass tubes coated with Canaleco "column coat" were inclined at about 45° when filled to a height of 10 cm, the acrylamide flow was interrupted and the tubes were carefully set upright and layered with buffer containing both catalysts at the same concentration as in the C<sub>0</sub> solution. The gels were polymerized at room temperature generally overnight before use.

Electrophoresis was carried out in an Ortec model 4200 apparatus modified to hold disc gels. A voltage gradient was supplied by an Ortec 4100 pulsed constant power pack with the discharge capacitance set at 1.0 microfarad and the pulsed rate set at 250 pulses per second.

Gels were prerun at 4° at 10 volts/cm for 30 to 60 min using an electrode buffer of the following composition: buffer, 2.5% glycerol, 0.2% SDS, 0.1% sodium deoxycholate. 0.5 ml samples containing 10% glycerol and 0.001% bromophenol blue was layered under the buffer and electrophoresis was carried out at 4° and under 10 volts/cm. Normal length of runs were 6 - 8 hrs.

After each run, gels were frozen in an ethanol-dry ice bath, thawed slightly and pushed out from the glass tubes. While still frozen, gels were sliced into discs with a cutting device fashioned from an array of razor blades spaced at 1.25 mm intervals. Each slice was then inserted into a scintillation vial, 1.0 ml of a mixture made up of concentrated NH<sub>4</sub>OH and NCS solubilizer in a 20:1 (v/v) ratio was added, and the vials capped and incubated at 40° for 12 hrs. The

vials were then uncapped, and the contents brought to dryness in a 60° oven. After thorough cooling, radioactivity in each sample was assayed with 5.0 ml of a toluene-based fluor.

## 2. Polyacrylamide Gel Electrophoresis of RNA Under Denaturing Conditions

The analysis of RNA under denaturing conditions was carried out using the 8 M urea and low salt buffer system of Reinders *et al.* (1973). Urea gels were prepared by combining 7 volumes of a solution containing 8 M urea (ultra-pure), 23 mM Tris-HCl, 2.3 mM EDTA (pH 7.5) with 1 volume of a solution containing 19% acrylamide, 1% bis-acrylamide and 8 M urea. After the addition of 0.004 volume of 10% TEMED and 10% ammonium persulfate, the solution was degassed under vacuum for 5 min before 0.7 x 10 cm gels were poured and allowed to set for at least 2 hrs.

The electrode buffer contains 8 M urea, 20 mM Tris-HCl and 2 mM EDTA. It was allowed to equilibrate overnight in a 60° oven before a run.

As was the case for gradient gels, urea gels were prerun at 10 volts/cm for 30 - 60 min at 60° before samples dissolved in the electrode buffer and containing 10% glycerol and 0.001% bromophenol blue were applied. Electrophoresis of samples were carried out under the same conditions for up to 6 hrs. The gels were sliced and the sections treated for radioassay according to the protocol described previously.

## R. High Voltage Paper Electrophoresis

Paper electrophoresis was performed in a Gilson High Voltage

Electrophorator (Model D) equipped with a large fiberglass tank as described by Dreyer and Bynum (1967). The reservoirs were filled with 0.04 M sodium citrate buffer at pH 3.5.

Whatman no. 3 MM paper was washed once with 0.01 N  $\text{NH}_4\text{OH}$  then rinsed with several changes of deionized water, and dried before sample application.

RNA alkaline hydrolysates redissolved in 50 - 100  $\mu\text{l}$  of deionized water together with added marker compounds were applied as 2 - 4 cm wide bands on the paper at a loading not greater than 1  $\mu\text{g}/\text{cm}$ . The paper was wetted with the sodium citrate buffer and electrophoresis carried out at 30 volts/cm for 105 min. After air drying, nonradioactive standards were located under short UV (254 nm) light.

Radioactive materials on an electropherogram were quantitated as follows: the electropherogram was cut up into 4 x 0.5 cm strips at right angles to the direction of migration of the samples. Then each strip was further cut into 4 sections and inserted into scintillation vials. Following the addition of 1.0 ml of 0.01 N  $\text{NH}_4\text{OH}$  to each fraction, the vials were capped and shaken in a reciprocating shaker overnight. Ten ml of Scinti Verse (Fischer) were then pipetted into each vial and the contents were shaken to homogeneity. The vials were periodically agitated over a period of 6 - 7 hrs to allow the water miscible fluor to completely elute and displace any aqueous material still associated with the paper fragments. The efficiency of recovery of tritium counts from the electropherogram was of the order of 97% or better.

Nucleotides to be further characterized were eluted from the appropriate section of an electropherogram with up to 5 ml of distilled water. Desalting of the elute was achieved by allowing nucleotides to adsorb onto a Norit (charcoal) column. The column was made by transferring 0.5 ml of a 1:1 (v/v) mixture of 20% packed volume Norit and 50% packed volume Celite on a sintered glass funnel (inside diameter of 2 cm, medium porosity). The Norit column was washed with 5 ml 0.01 N HCl, the sample (acidified to pH 3 - 4 with 1 N HCl) was filtered through, and the column was washed again with 5 ml 0.01 N HCl. The nucleotides were eluted from the Norit with three 5 ml portions of 0.5 ml concentrated  $\text{NH}_4\text{OH}/100$  ml of 50% ethanol. The ethanol eluates were evaporated to dryness under a stream of nitrogen at room temperature. More than 80% of the radioactivity was recovered in the ethanol eluates.

## CHAPTER III

### THE EFFECT OF RNASE AND STRAND SCISSIONS ON THE PENETRATION OF R17 RNA

#### A. Introduction

The inhibiting effects of RNase on phage RNA penetration are well known (Knolle and Kaudewitz, 1963; Zinder, 1963). However, the mechanism of action of the enzyme at the molecular level requires clarification. That RNase will degrade the RNA from phage particles having undergone the irreversible step of RNA ejection is clear enough, but it is not known whether the A protein is also prevented from entering the cell or whether RNA fragments could penetrate in the presence of RNase. It was surmised that if fragments of phage RNA can penetrate into the cell in the presence of RNase, then the polarity of RNA penetration (i.e. the pilot or leading end of the penetrating RNA) might be determined by isolating the penetrated fragments from infected cells and examining them for the presence or absence of the original 3'- or 5'-ends.

Engelberg and Artman (1970) had previously reported that non-infectious RNA can penetrate into *E. coli*. They showed that at a MOI of 25 particles/cell or 1 PFU/cell (their average <sup>3</sup>H-labeled MS2 phage stock had a PFU/particle ratio of 1/25), 30% of the input label was found to penetrate into cells during 60 min exposure of cells to phage. Since an average of only one out of 7 - 8 equivalents of penetrated RNA was infectious, most of the injected material appeared in some way to be defective. Furthermore, they found that the noninfectious RNA was degraded within 10 to 20 minutes into basic subunits which were incor-

porated into all nucleic acid components of the cell. Although the RNA isolated from their phage stocks appeared to be homogeneous on sucrose gradients, the authors did not rule out the possibility of hidden breaks being present in the folded RNA. It occurred to this writer that a logical extension of Engelberg and Artman's work would be the deliberate infection of cells with highly inactivated  $^{32}\text{P}$ -labeled RNA phage which had been obtained by long term storage. The penetrated  $^{32}\text{P}$ -labeled RNA could then be analyzed by polyacrylamide gel electrophoresis to determine its state of intactness. Such studies should provide information regarding the fate of any fragmented RNA following infection of sensitive cells.

The present chapter thus describes a series of studies relating the effect of limited fragmentation of the phage genome to the RNA penetration process. Also, the effect of the presence of RNase on phage infection was reexamined in greater detail. In brief, it was found that:

- (a) Phage RNA fragments can penetrate into E. coli; these fragments are quickly degraded by cellular nucleases.
- (b) A limited number of intact infectious viral RNA molecules is able to penetrate into cells in the presence of RNase. The number of molecules which are able to undergo successful penetration appears to increase with the multiplicity of infection.

## B. Results and Discussion

### 1. Conditions for Measuring RNA Penetration

The method employed to quantify the amount of phage RNA that has penetrated into E. coli cells is described in detail in Materials

and Methods. Briefly, infected cells were chilled and pelleted, resuspended in cold medium ( $-Mg^{2+}$ ) and forced through a #26 gauge syringe needle; complete removal of all extracellular phage was achieved after repeating the operations six times.

Using the above procedure, it was found that the amount of viral RNA penetrating male cells is dependent on the strain of bacteria, the medium, the duration of infection and the multiplicity of infection (MOI). As shown in Table 3.1 for example, it was found that the amount of RNA injected into ED2602 cells increased with the multiplicity of infection, and that culturing the cells in a rich medium such as Trypticase Soy Broth increased the relative amount of RNA penetrated approximately four-fold over that found for cells grown in a minimal medium.

Table 3.1

Effect of Culture Medium and Multiplicity of Infection (MOI) on Phage

## R17 RNA Penetration

a.	ED2602 cells in minimal medium	
	Phage Input	equivalents of phage RNA
	MOI (particles/cell)	penetrated/cell/20 min
	10	0.5
	100	3.0
	1000	4.6
b.	ED2602 cells in TSB	
	10	4.0
	100	13.0
	1000	17.6

ED2602 cells were infected at log phase ( $4 \times 10^8$  cells/ml) with  $^{32}P$ -labeled R17 phage (PFU/particle = 1/200) for 20 min. The assay procedure was as outlined in Materials and Methods.



In Figure 3.1, the kinetics of penetration of RNA into ED2602 (Flac) and WP156 (Hfr) cells are illustrated. When WP156 cells in log phase were challenged with R17, the RNA penetration process was found to be very rapid during the first 5 - 10 min of infection, then somewhat slower during the remainder of the experimental period. In the case of ED2602 cells, the RNA penetration was essentially completed in 10 min; thereafter little or no increase in RNA penetration was observed. A comparison of the phage equivalents of RNA penetrated per cell for the WP156 and ED2602 results showed that in minimal medium, 3 times as much RNA had entered the WP156 cells as compared to the ED2602 cells at 10 min post infection.

A two phase process of RNA penetration was originally reported by Brinton and Beer (1967). They suggested that the rapid initial phase of RNA penetration was apparently promoted by cell-associated F-pili which were present in the culture at zero time, while the second slower phase probably represented the promotion of RNA penetration by low levels of new F-pili which were asynchronously produced throughout the infectious period. This two-phase process was also evident in our hands when WP156 (Hfr) cells were used but not with ED2602 (Flac) cells.

To provide further support for the idea that the second phase of RNA penetration in Hfr cells was due to growth of new pili, phage infection was also carried out in the presence of rifampicin, an inhibitor of RNA polymerase. As can be seen in Figure 3.1, the inclusion of 50 µg/ml of rifampicin in the infection medium results in the curtailment of further RNA penetration after 10 min in the WP156 system. With

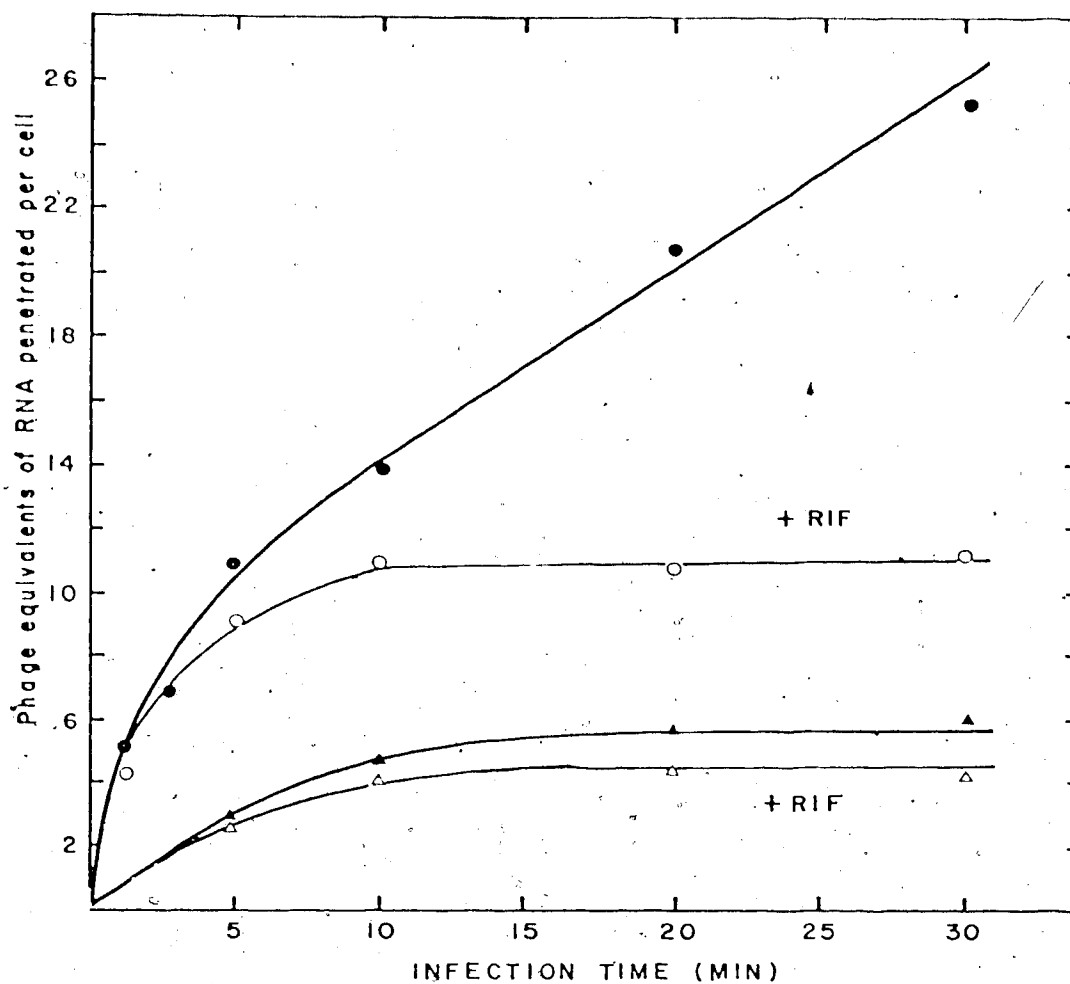


Figure 3.1 The effect of bacterial strain and rifampicin on the kinetics of phage RNA penetration.

*E. coli* WP156 cells (or ED2602) in 120 ml CTMM (+aa) at 37° were grown up to  $4 \times 10^8$  cells/ml and infected at a MOI of 1000 particles/cell with  $^{32}\text{P}$ -labeled RL7 phage (PFU/particle  $\approx 1/10$ ). Aliquots of 20 ml were taken out at appropriate time intervals and chilled by combining with 10 ml, frozen TMM ( $-\text{Mg}^{2+}$ ). The infected cells were washed 6X with TMM- $\text{Mg}^{2+}$  as described in Materials and Methods to remove extracellular phage particles. The washed cells were resuspended in TMM ( $\text{Mg}^{2+}$ ) to a density of  $8 \times 10^8$  cells/ml and three 1.0 ml aliquots were assayed for  $^{32}\text{P}$ -radioactivity with 10 ml Scinti Verse. In infections carried out with rifampicin, the drug was added to cultures (final concentration = 50  $\mu\text{g}/\text{ml}$ ) 5 min before phage addition. (●-●) WP156 cells; (○-○) WP156 + rifampicin; (▲-▲) ED2602; (△-△) ED2602 + rifampicin.

ED2602 cells, a 25% reduction in the amount of RNA penetration was also observed in the same concentration of the drug. Clearly, the second phase of RNA penetration into WP156 *E. coli* was totally suppressed by rifampicin. Although this observation is not conclusive, it is compatible with the hypothesis put forward before; i.e., the drug had probably inhibited the synthesis of new F-pili without affecting the biological function of pili existing at the time of its addition. This interpretation is supported by the findings that translation and transcription of mRNA in *E. coli* are coupled processes (Byrne et al., 1964; Miller et al., 1970), and that bacterial protein synthesis ceases within several minutes of inhibition of RNA transcription (Levinthal et al., 1962).

In subsequent experiments where the penetrated viral RNA was to be analysed by polyacrylamide gel electrophoresis, it was necessary for practical considerations to maximize the amount of RNA injected during the 5 min period to be used. An infection time of 5 min was chosen as a compromise between the need to recover as much labeled phage RNA as possible from infected cells for gel electrophoresis and the need to minimize the extent of degradation of penetrated phage RNA by cellular nucleascs. The results of a study correlating the amount of phage RNA penetrated per cell in 5 min to the MOI are illustrated in Figure 3.2. As is evident from the curve, the saturation of sites on the cell from which phage RNA could be injected appeared to be reached at a MOI of about 1000 particles/cell and the half maximal rate of RNA penetration was estimated to be at a phage concentration of about 85 particles/cell. A replotting of the data (Figure 3.2, inset) in a Lineweaver-Burke form indicated that the "Vmax" was equal to 110% of the amount of RNA penetrated at a MOI of 1000. At 5 min in minimal

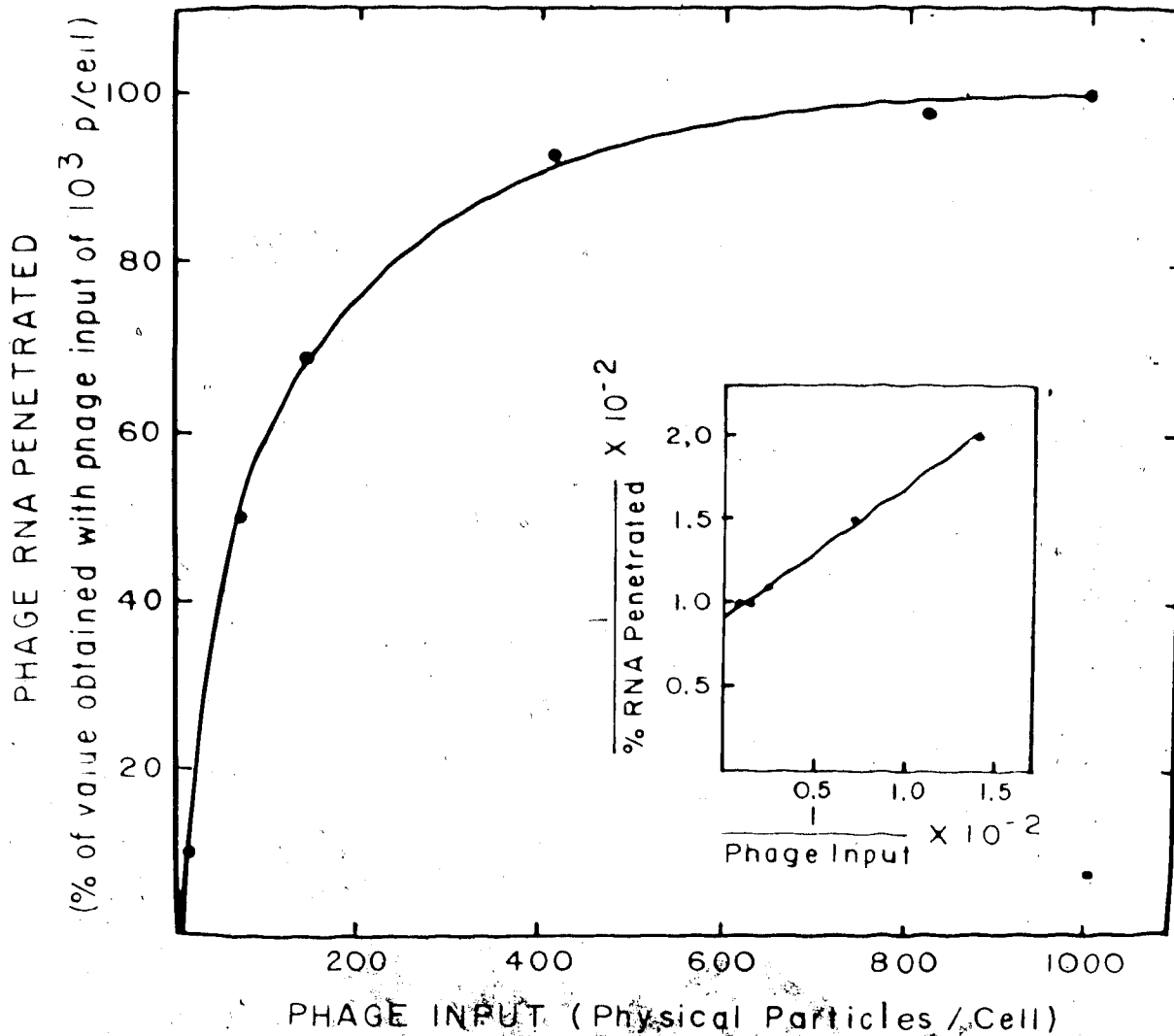


Figure 3.2 The effect of the multiplicity of infection on the amount of RNA penetrated at 5 minutes post infection.

*E. coli* WP156 in 120 ml CTMM(+aa) were grown up to  $4 \times 10^8$  cells/ml and then subdivided into six, 20 ml aliquots. Each culture was then infect at a different MOI with <sup>32</sup>P labeled R17 phage for 5 min, chilled and washed 6X as described in Figure 3.1. The washed cells were resuspended in TMM(-Mg<sup>++</sup>) to a density of  $4 \times 10^8$  cells/ml and three 1 ml aliquots from each sample were assayed for <sup>32</sup>P-radioactivity with Scinti Verse.

medium, this is equivalent to approximately 11 phage equivalents of RNA penetrated per cell. Note that the cells must be incubated for another 20 min to double the amount of penetrated RNA to about 22 phage equivalents RNA/cell (Figure 3.1).

### 2. Fate of Penetrated Phage RNA

A suspension of R17 phage particles labeled in the RNA with <sup>32</sup>P and stored at 4° in 1 x SSC gradually becomes inactivated as a result of strand scissions arising from the recoil energy released from dismutation of <sup>32</sup>P to <sup>32</sup>S. Strand breaks and base alterations also arise from attack by the radiolysis products of water (Singh and Nicolau, 1971; see also Chapter IV). Because of the resulting variability in the level of infectivity of <sup>32</sup>P-labeled phage, the infectivity of stock phage preparations in terms of the ratio of plaque forming units or infectious particles to the total number of physical particles (PFU/particle) was routinely assayed before cellular infections. Most of the inactivation of <sup>32</sup>P-labeled R17 stored at 4° can be attributed to the indirect effects of <sup>32</sup>P decay since it was observed that <sup>32</sup>P-labeled R17 preparations which were stored in a protective medium containing glycerol and bovine serum albumin at -80° (conditions under which secondary effects are minimized) experienced virtually no loss in infectivity over 30 days, while the infectivity decreased 10<sup>4</sup>-10<sup>6</sup> fold if the phage preparations were stored for the same period at 4° (see appendix). It was also found that the rate of inactivation of phage stored at 4° in SSC was highly unpredictable and a large variation was seen from preparation to preparation.

Repeated RNA penetration experiments using  $^{32}\text{P}$ -labeled R17 phage at MOI's of  $10^2$  to  $10^3$  particles/cell for periods up to 20 min led to the observation that highly inactivated phage stocks with PFU/particle ratios as low as  $10^{-5}$  to  $10^{-7}$  still resulted in the injection of 25 to 30% of the amount of RNA injected with freshly prepared  $^{32}\text{P}$ -labeled R17 stocks (i.e., about 5-8 phage equivalents of RNA per cell in the case of the highly inactivated particles). These results are not presented at this time because a more detailed study of this problem is given in Chapter V of this thesis. What is important here is the fact that none of the injected RNA was found to give rise to infectious centers when cells were infected with R17 phage of PFU/particle ratios as low as  $10^{-7}$ . This finding confirms the earlier conclusions reached by Engelberg and Artman that noninfectious RNA most probably does penetrate cells.

To gain more information on the nature of the RNA in cells infected with  $^{32}\text{P}$ -labeled R17 having varying PFU/particle ratios, the RNA was extracted from infected cells and analyzed by exponential gradient polyacrylamide gels. It was found that the phage RNA isolated from cells infected for 5 min displayed a heterogeneous population of fragment sizes if the phage preparations used had infectivities significantly lower than that of a freshly labeled preparation (PFU/particle  $\approx 1/5$  to  $1/10$ ). Not surprisingly, the extent of fragmentation appeared to increase with decreasing infectivities of the particles (Figure 3.3A,B).

The fate of the injected RNA fragments was followed in a time course study as illustrated in Figure 3.3. Aliquots from infected cells

Repeated RNA penetration experiments using  $^{32}\text{P}$ -labeled R17 phage at MOI's of  $10^2$  to  $10^3$  particles/cell for periods up to 20 min led to the observation that highly inactivated phage stocks with PFU/particle ratios as low as  $10^{-5}$  to  $10^{-7}$  still resulted in the injection of 25 to 30% of the amount of RNA injected with freshly prepared  $^{32}\text{P}$ -labeled R17 stocks (i.e., about 5-8 phage equivalents of RNA per cell in the case of the highly inactivated particles). These results are not presented at this time because a more detailed study of this problem is given in Chapter V of this thesis. What is important here is the fact that none of the injected RNA was found to give rise to infectious centers when cells were infected with R17 phage of PFU/particle ratios as low as  $10^{-7}$ . This finding confirms the earlier conclusions reached by Engelberg and Artman that noninfectious RNA most probably does penetrate cells.

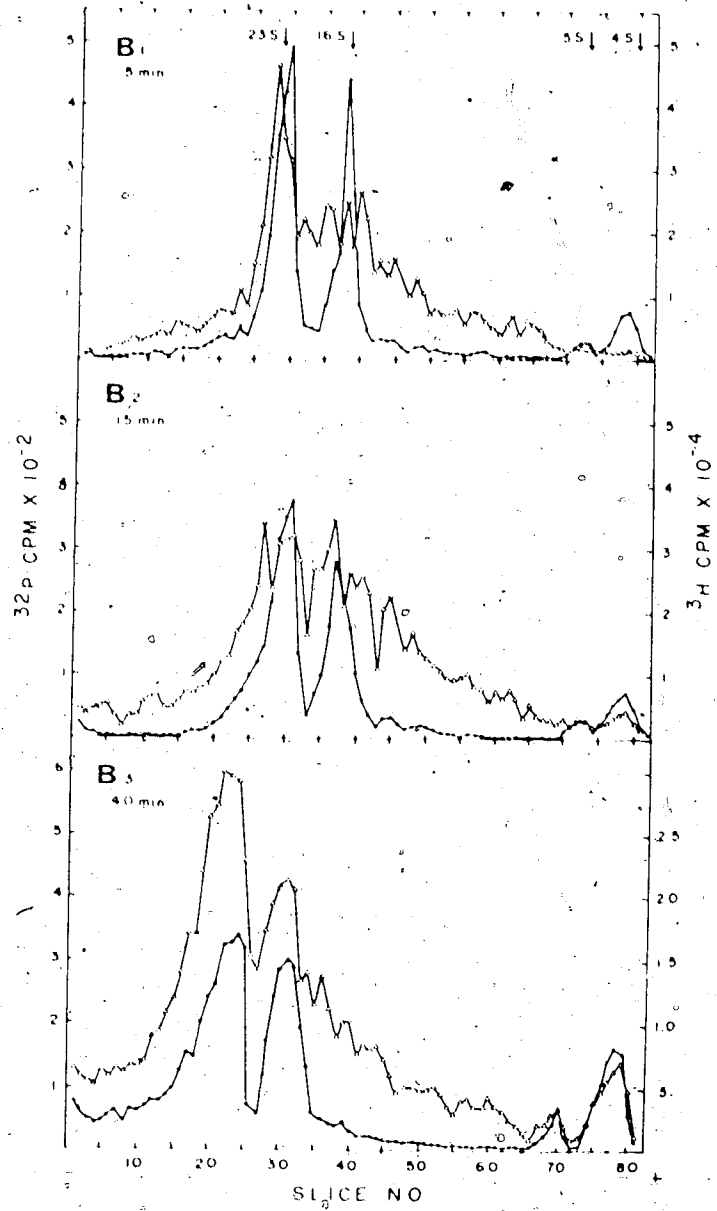
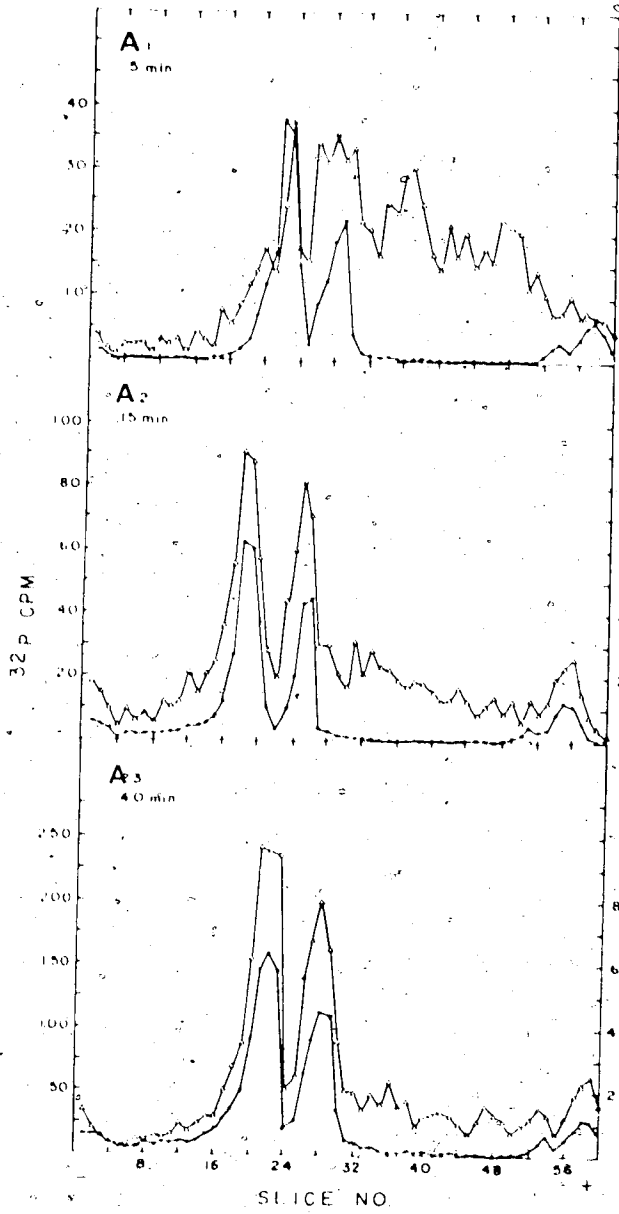
To gain more information on the nature of the RNA in cells infected with  $^{32}\text{P}$ -labeled R17 having varying PFU/particle ratios, the RNA was extracted from infected cells and analyzed by exponential gradient polyacrylamide gels. It was found that the phage RNA isolated from cells infected for 5 min displayed a heterogeneous population of fragment sizes if the phage preparations used had infectivities significantly lower than that of a freshly labeled preparation (PFU/particle  $\sim 1/5$  to  $1/10$ ). Not surprisingly, the extent of fragmentation appeared to increase with decreasing infectivities of the particles (Figure 3.3A,B).

The fate of the injected RNA fragments was followed in a time course study as illustrated in Figure 3.3. Aliquots from infected cells

Figure 3.3 Fate of penetrated  $^{32}\text{P}$ -labeled R17 RNA

50  $\mu\text{l}$  of  $^3\text{H}$ -5,6-uridine were added to 100 ml (CTMM + aa) of E. coli WP 156 cells. 30 min before cells were to reach a density of  $4 \times 10^8$  cells/ml. At this density, the cells were infected with  $^{32}\text{P}$ -labeled R17 phage at a MOI of  $10^3$  particles/cell. At 5, 15 and 40 min post infection, a 25 ml aliquot of the culture was removed and chilled by being swirled in a beaker with 10 ml frozen TMM(-Mg $^{2+}$ ) medium. The infected bacteria were then washed 6X to remove extra-cellular phage and then extracted for total RNA by SDS-phenol as described in Materials and Methods. The isolated RNA was then redissolved in E-RNA buffer containing 10% glycerol, 0.1% SDS and 0.001% bromophenol blue. Samples containing 300 to 500  $\mu\text{g}$  RNA in 0.3 ml were analyzed in exponential (2.5 - 15%) gradient gels at 10 volts/cm for 8 hours. The details of the electrophoretic system and the radioassay of polyacrylamide gels are given in Materials and Methods. (A) PFU/particle of phage =  $1 \times 10^{-7}$ ; (● ●)  $^3\text{H}$ -radioactivity in cellular RNA, (▲-▲)  $^{32}\text{P}$ -radioactivity in penetrated phage RNA. (B) PFU/particle of infecting phage =  $1 \times 10^{-4}$ .





were extracted for total RNA by the SDS-phenol procedure described in Materials and Methods. Internal markers were provided by  $^3\text{H}$ -uridine-labeled rRNA coextracted with the penetrated phage RNA. In the gel system, the mobility of intact 28S R17 RNA ( $\text{MW} = 1.1 \times 10^6$ ) is slightly lower than that of 23S rRNA ( $\text{MW} = 1.1 \times 10^6$ ). As can be seen in panels A<sub>1-3</sub>, the extensively fragmented RNA from a highly inactivated phage stock was rapidly degraded and converted to 23S, 16S, 4S and 5S components within 15 min after entry. The viral RNA fragments that were still present at 15 and 40 min can be attributed to degradation products of larger fragments and fragments of RNA which continued to be injected during the second phase of RNA penetration. A similar fate was found for the RNA injected from phage of a higher PFU/particle ratio (B<sub>1-3</sub>). However, the rate of degradation of the parental RNA material appeared to be slower in B than in A. This can be rationalized on the basis of a longer time required to degrade the larger average size fragments found in B.

In a variation of the above experiment, Hfr cells were infected at a MOI of  $10^3$  particles/cell for 5 min before they were chilled and washed six times to remove all extracellular particles. The washed cells were resuspended in fresh medium and incubated at 37° for up to 40 min. Polyacrylamide gel analysis showed that at the end of 40 min, all the original phage RNA label that was associated with the washed cells had been converted into rRNA. This was further evidence that the six times washing procedure had reduced the level of extracellular phage particles to insignificant levels since extracellular

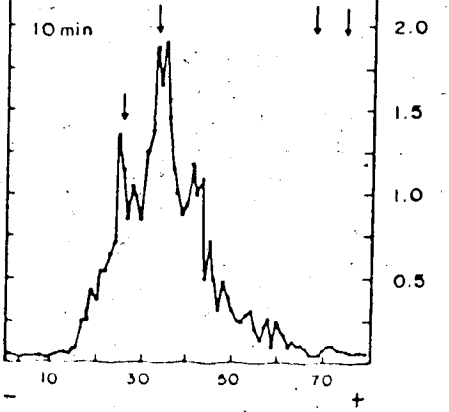
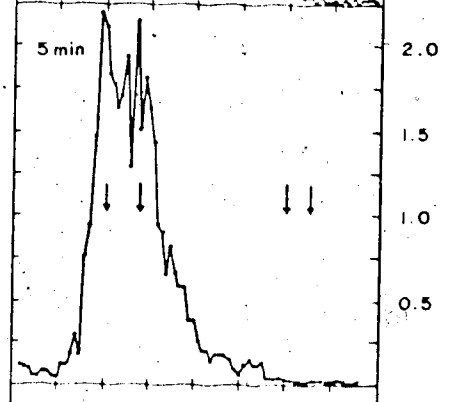
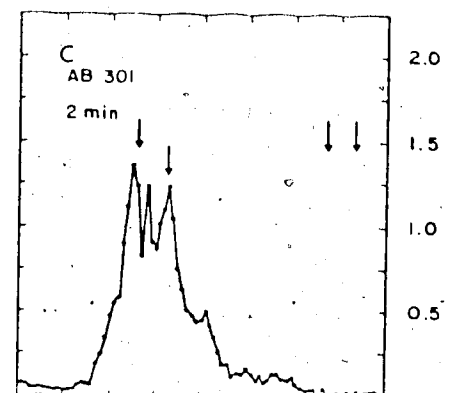
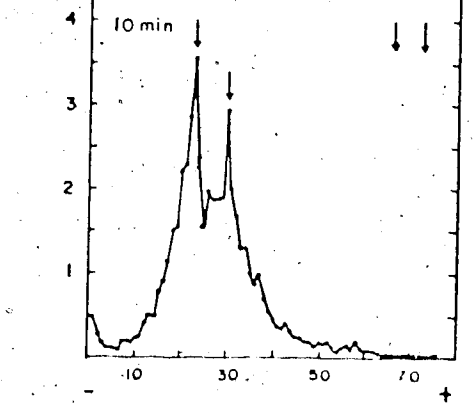
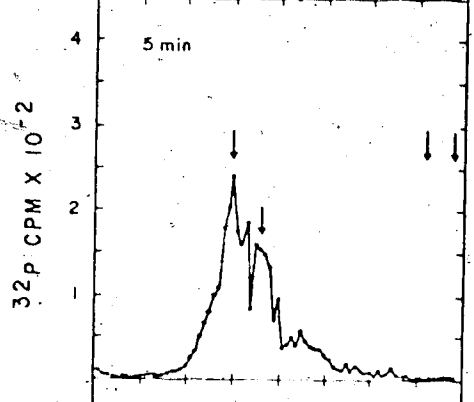
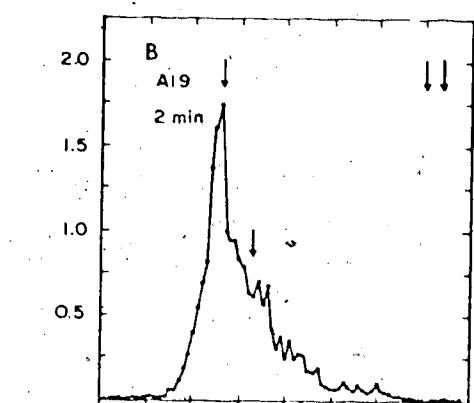
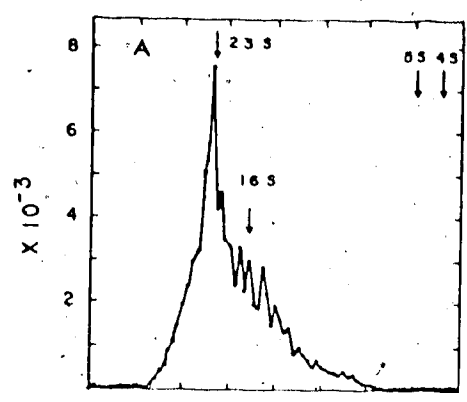
phage RNA enclosed in intact particles would not be expected to be catabolized and converted into cellular rRNA's.

An additional comparative study on the fate of penetrated RNA was carried out using the RNase I deficient *E. coli* strain A19, and a RNase I<sup>+</sup> control, AB301, as host cells. Figure 3.4 A shows the profile of the RNA isolated from <sup>32</sup>P-labeled R17 phage with PFU/particle =  $5.0 \times 10^{-3}$ . Figure 3.4 B and C show the profiles of the injected RNA at 2, 5 and 10 min post infection in A19 and AB301 cells, respectively. On comparing the distributions in A, B, and C, one sees that the amount of intact or near intact phage RNA was noticeably reduced at two min of infection in AB301 cells but not in A19 cells. At 5 and 10 min, the RNA in the AB301 host had been progressively degraded into smaller fragments, while in the A19 (RNase I<sup>-</sup>) host, the breakdown of the larger pieces of RNA into smaller fragments was less evident. In fact, the distribution of fragments at 10 minutes largely resembled that obtained at 2 min.

Although several types of nucleases must play a role in RNA catabolism, the above result indirectly implicates RNase I in such a role. Spahr and Hollingworth (1961) had originally isolated this "latent RNase" from the 30S ribosome subunit and had calculated that it was present in some but not all ribosomes of bacteria. Subsequent studies have shown that RNase I could be released into the medium when *E. coli* were osmotically shocked (Nossal and Heppel, 1966) or treated with EDTA - 1 enzyme (Neu and Heppel, 1964). This was interpreted to mean that some RNase I may be located on the outer cell membrane surface or that the bulk of the ribosomes containing RNase I

Figure 3.4 A comparison of the fate of penetrated phage in RNase I<sup>-</sup> and wild type host bacteria.

A19 (RNase I<sup>-</sup>) and AB301 *E. coli* in separate 100 ml (CTMM+aa) cultures were prelabeled with <sup>3</sup>H-uridine as described in Figure 3.3. At a density of  $4 \times 10^8$  cells/ml, each culture was infected with <sup>32</sup>P labeled phage at a MOI of  $10^3$  particles/cell; 25 ml aliquots were removed at 2, 5 and 10 min post infection, quickly chilled and all samples washed 6X as described in Materials and Methods. The radioactively labeled RNA from washed, infected cells was then isolated and subjected to exponential gradient polyacrylamide gel electrophoresis as described for Figure 3.3 and in appropriate sections in Materials and Methods. (A) Profile phage RNA isolated from intact phage (PFU/particle =  $5.0 \times 10^{-3}$ ), (B) RNA isolated from infected A19 (RNase I<sup>-</sup>) cells (C) RNA isolated from AB301 cells.



SLICE NO.

occurs near or at the cellular membrane. The data presented here are insufficient to tell whether phage RNA was being degraded while being transported across the membrane, or whether RNase I acts on the fragments after their entry.

Finally, it was observed that the DNA-dependent RNA polymerase inhibitor, rifampicin, has an apparent stabilizing effect on the foregoing degradation of phage RNA. As demonstrated earlier, the addition of 100 µg/ml rifampicin to cells at 0 - 10 min before the addition of phage precluded the penetration of viral RNA after 10 min infection. In Figure 3.5 the penetrated RNA from two different phage stocks has been isolated from WP156 cells infected for 5 and 40 min and analyzed by gel electrophoresis. Examination of the RNA profiles obtained at 5 and 40 minutes shows that the injected fragments had undergone little alteration, since no shift of the radioactive label toward smaller fragments could be discerned in either A or B at 40 min. Moreover, since the phage stock used in Figure 3.5 B had a PFU/particle ratio of  $10^{-7}$ , it would certainly have been degraded and the subunits reincorporated into rRNA had the rifampicin not been present.

The effect of rifampicin on phage replication has been investigated previously. In the presence of rifampicin, the later stages of RNA phage synthesis and replication are impaired (Rothwell and Yamazaki, 1972; Engelberg and Artman, 1972). More specifically, at 15 min post infection; the period of maximal inhibition, it has been found that RNA minus strands are synthesized on the parental template at a reduced rate, whereas the synthesis of progeny plus strands is completely

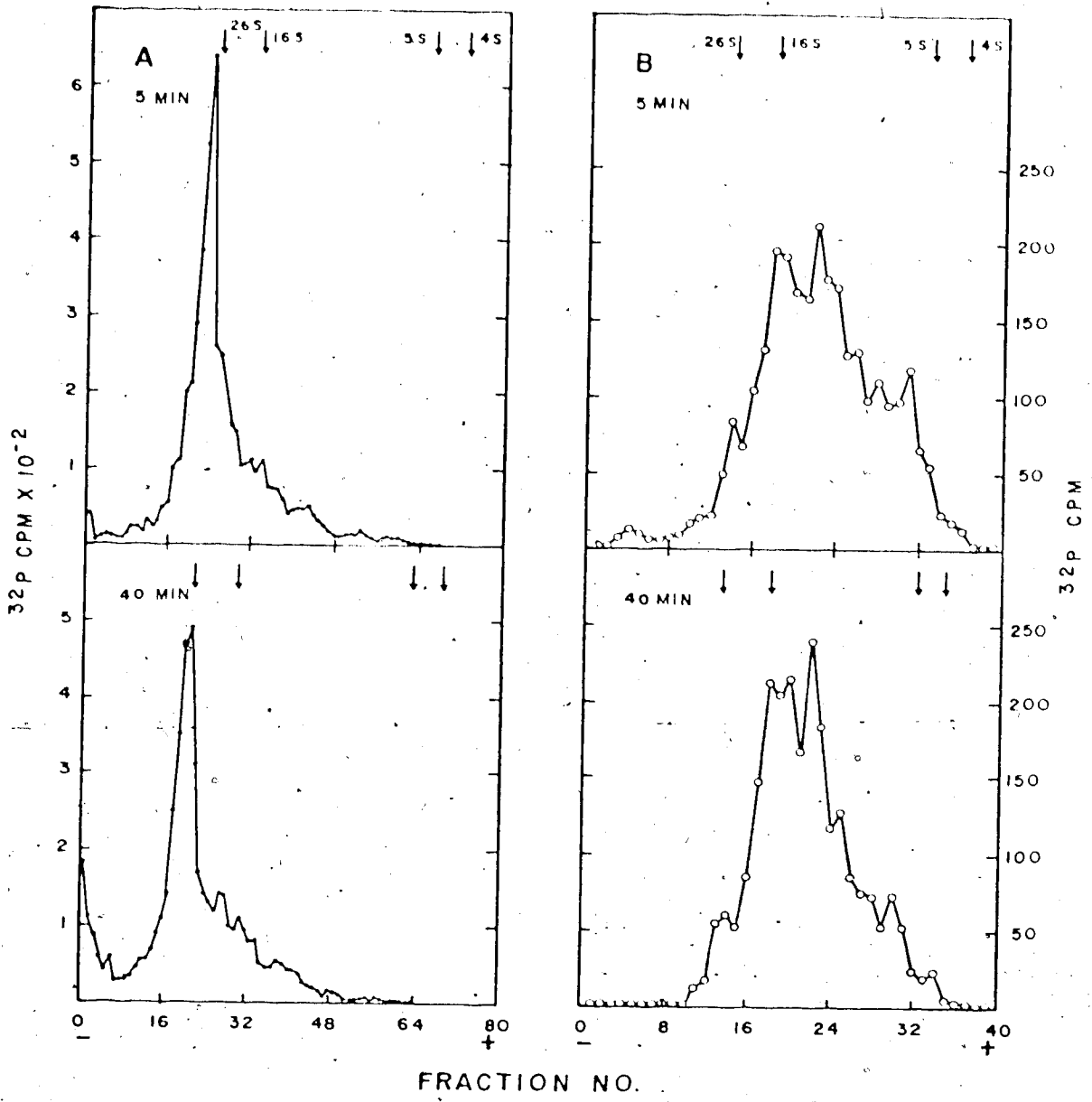


Figure 3.5 The effect of rifampicin on penetrated R17 RNA.

*E. coli* WP156 cells (in 50 ml CTMM + aa) pre-labeled with <sup>3</sup>H-uridine as described in Figure 3.3 were infected at log phase (4 x 10<sup>8</sup> cells/ml) with <sup>32</sup>P-labeled R17 phage in the presence of 100 µg/ml of rifampicin which was added 5 min before the phage; 25 ml aliquots of the infected cells were removed at 5 and 40 min post infection, quickly chilled and washed 6X to remove extracellular phage. The RNA from washed cells was then isolated by SDS-phenol and subjected to exponential gradient polyacrylamide gel electrophoresis as described for Figure 3.3 and in Materials and Methods. (A) PFU/particle of infecting phage 5 x 10<sup>-3</sup> (B) PFU/particle of infecting phage = 1 x 10<sup>-7</sup>. In both A and B, the MOI = 1000 part/cell.

inhibited. On the other hand, the initial processes of RNA penetration and protein synthesis are apparently not affected (Engelberg and Artman, 1972). Since rifampicin is known to inhibit bacterial RNA polymerase both in vivo and in vitro (Wehrli et al., 1971), it was anticipated that its presence would prevent the channeling of radioactive labels from the parental phage RNA to cellular RNA components, but that the breakdown of the phage RNA fragments would continue. The fact that rifampicin was found to inhibit phage RNA degradation as well as host RNA synthesis was thus unexpected, and the mechanism by which the protective effect is achieved is not clear. A direct protective effect exerted by rifampicin against messenger degradation seems unlikely, although this cannot be ruled out entirely. Possibly the breakdown of the RNA fragments might be coupled to bacterial RNA synthesis. In this context, it is interesting to note that Singer and Penman (1972) have observed that He La cell mRNA is stabilized in the presence of actinomycin, an inhibitor of RNA transcription. The basis for this protective effect was not explained.

From a biological standpoint, it is pertinent to ask whether any of the RNA fragments injected from highly degraded particles are active in directing viral protein synthesis. Since some of the larger than half size fragments should contain at least one complete viral cistron, there is no obvious reason why the formation of initiation complexes and the process of translation should not proceed on these fragments at early times after injection. A worthwhile investigation would be to infect cells in the presence or absence of rifampicin with highly inactivated <sup>32</sup>P-labeled phage, isolate the polyribosome fractions, and to analyze for any subnormal size viral RNA fragment that might be



associated with the polyribosome fractions.

### 3. The Effect of RNase on RNA Penetration

Previous studies have shown that the presence of RNase in the medium results in the complete suppression of plaque formation by cells infected at a MOI of 1 PFU/cell (Knolle and Kaudewitz, 1963; Zinder, 1963) and that a concomitant hydrolysis of the infecting RNA occurs (Valentine and Strand, 1965). It was observed in this laboratory, on the other hand, that a considerable amount of RNA is able to penetrate into cells infected with a high MOI in the presence of RNase (unpublished preliminary observations). This observation raised the possibility that at higher MOI's, fragments of phage RNA produced by RNase activity might be able to penetrate before they were totally hydrolyzed.

As mentioned in the introductory chapter, the tail model of phage RNA penetration envisages one end of the RNA being attached to the A protein (or to one or both A protein polypeptide fragments produced during the onset of the RNA ejection step) and being "pulled" into the cell by the A protein. If the A protein were to precede the RNA during its entry, then the above hypothesis would predict that the amount of A protein penetrating into the host cell should be unaffected while that of the RNA should decrease with increasing concentrations of RNase in the medium. That this is indeed the case is illustrated in Figure 3.6, which shows the relative amounts of RNA and A protein penetration in the presence of increasing concentrations of RNase in the medium. The penetration of A protein was determined in a separate experiment in which cells were infected with R17 phage labeled in the A pro-

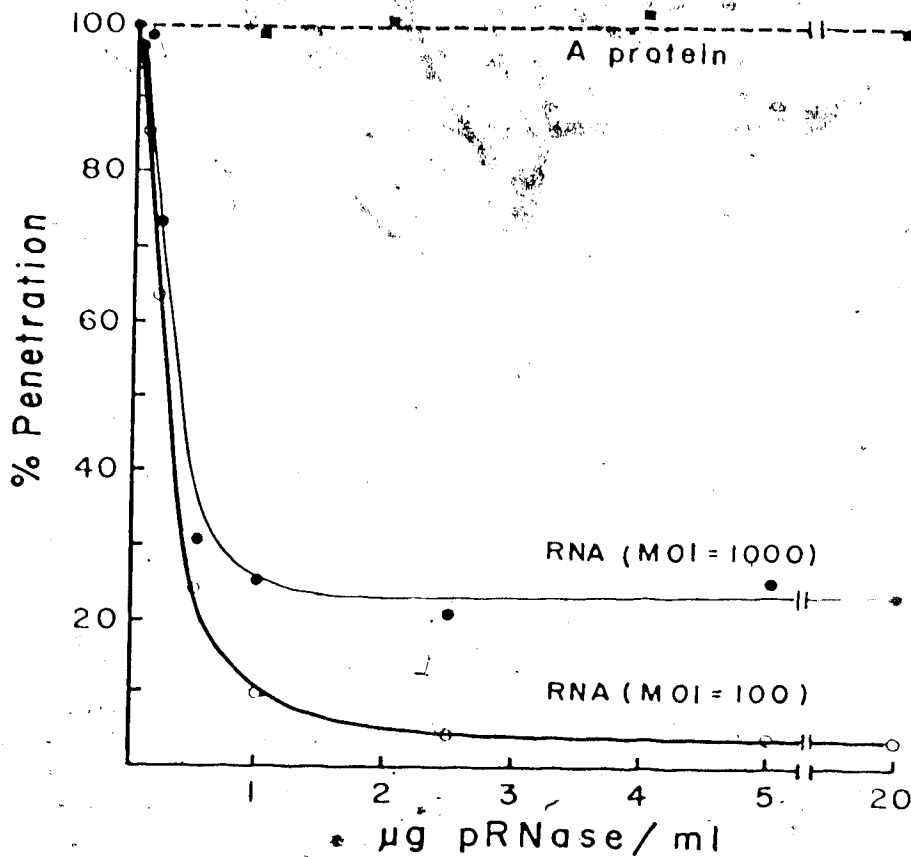


Figure 3.6 The effect of RNase concentration on the penetration of phage RNA and A protein.

*E. coli* WP156 (in CFMMta) at  $4 \times 10^8$  cells/ml were subdivided into eight, 25 ml cultures and 1 ml of an appropriately diluted solution of pRNase added to give final concentrations of 0.1, 0.2, 0.4, 1.0, 2.5, 5, and 20  $\mu\text{g/ml}$ . Each culture was then infected with  $^{32}\text{P}$ -labeled R17 phage at a MOI of  $10^3$  particles/cell for 20 min ( $37^\circ$ ) before it was quickly chilled and washed 6X to remove all extracellular particles. The washed cells were resuspended to a density of  $4 \times 10^8$  cells/ml, and three, 1.0 ml aliquots assayed for radioactivity with 10 ml ScintiVerse. The experiment was repeated using a MOI of 100 particles/cell. R17 A protein penetration in the presence of varying concentrations of RNase was similarly determined except that R17 phage labeled with  $^3\text{H}$ -histidine was used\*. The washed infected cells were dripped onto Whatman 3MM filter discs ( $10^9$  cells/disc), dried and treated with hot TCA according to the procedure outlined in Table 2.1. The dried discs were assayed for  $^3\text{H}$ -radioactivity with a toluene fluor as described in Materials and Methods.

\* In this case, cells were infected at a MOI of  $10^2$  particles/cell for 40 min.

tein with  $^3\text{H}$ -histidine.

It may be seen that the amount of phage RNA penetrated was sensitive to RNase concentrations as low as 0.1  $\mu\text{g}/\text{ml}$ , and that a rapid decrease in RNA penetration occurred between 0.1 and 1.0  $\mu\text{g}/\text{ml}$  of RNase. The reduction in the amount of RNA penetrated did not approach zero but reached a steady level at RNase concentrations in excess of 1.0  $\mu\text{g}/\text{ml}$ . At a MOI of 1000 particles/cell the plateau level corresponded to about 23% of the amount of RNA penetrated in the minus RNase control. At the lower MOI of 100 particles/cell the level reached was equal to about 3% of the control. The amount of A protein penetrating cells was not affected by the presence of RNase in the medium. Under the conditions of the experiment, about 15 phage equivalents of A protein material penetrated each cell regardless of the concentration of RNase.

A trivial explanation for the reduced but significant level of penetrated RNA at higher MOI's might be that the standard washing procedure failed to wash off all the extracellular phage particles and that the greater the MOI the greater would be the background levels of intact phage. This can be discounted, however, since various controls (see discussion in Materials and Methods) have shown that the washing procedure successfully reduces the number of such particles to insignificant levels. Moreover, the fact that the RNA which has penetrated at high MOI's can be catabolized and incorporated into rRNA provides further support for the contention that the cell-associated radioactivity was due to RNA which had been injected into cells.

Two possible models can be advanced to explain the observed

pattern of phage RNA penetration in the presence of RNase.

First states that the penetration process itself is unaffected, but that the decrease in the amount of RNA penetration results from the decreasing size of the RNA fragments which manage to penetrate before further degradation. A defined segment of RNA perhaps protected from RNase by association with A protein will always penetrate even at saturating ( $\sim 1.0$   $\mu\text{g/ml}$ ) concentrations of RNase.

The second possibility would be a process in which only those particles which undergo the ejection reaction at the base of the pilus succeed in injecting the phage RNA into the cell. Attachment and ejection by phage particles at a point on the F-pilus somewhat removed from the cell surface would result in the complete degradation of the RNA by the RNase. According to this scheme, the penetrated RNA originating from the particles at the cell surface would not be accessible to the RNase in the medium, and would therefore remain intact even in the presence of saturating concentrations of RNase.

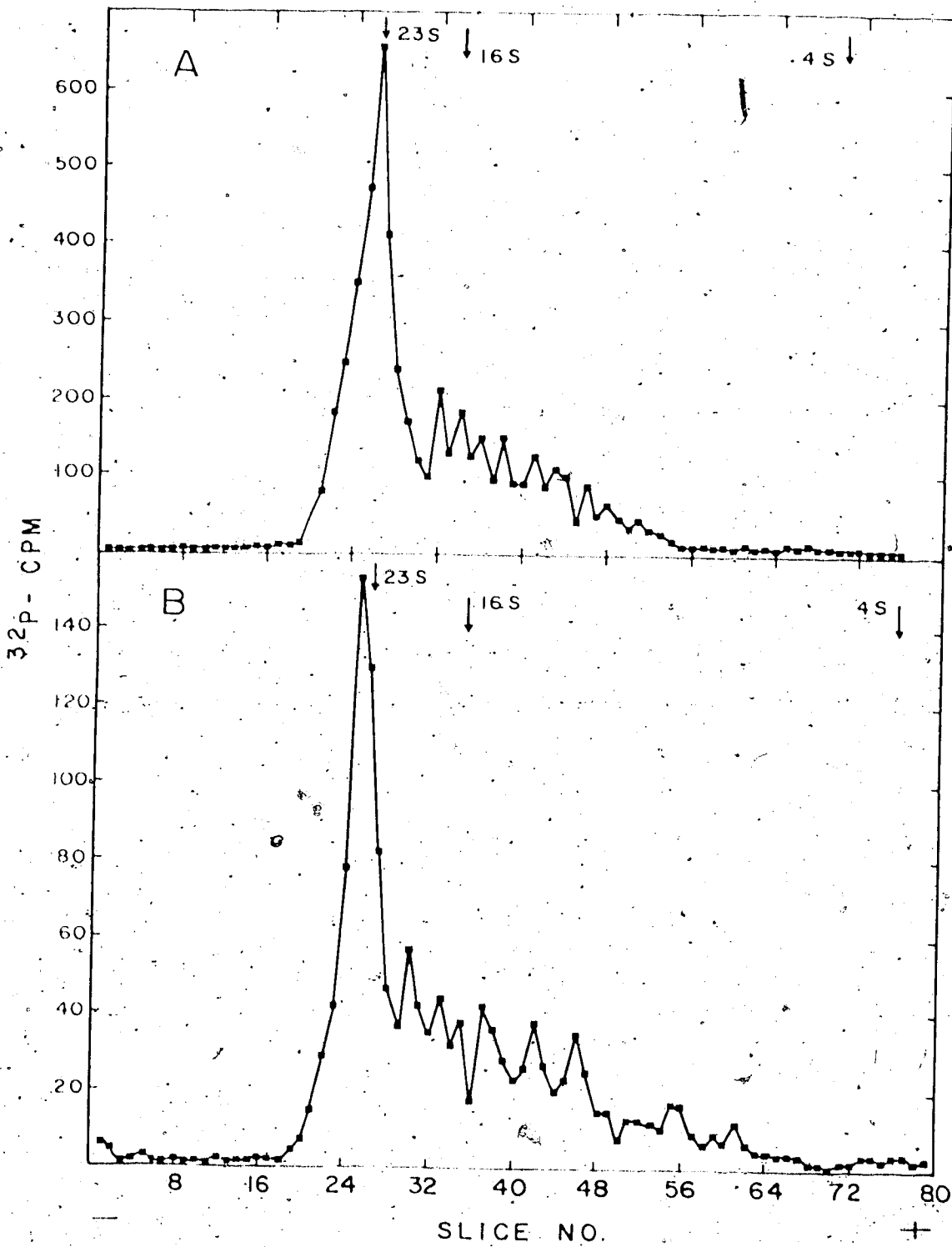
The experimental results (Figure 3.6) show that the amount of penetrated A protein is unaffected by the presence of RNase. This phenomenon can be rationalized in either model on the assumption that the A protein penetrates independently of viral RNA after the RNA ejection step. Alternatively, from the standpoint of the tail model, the A protein component of an A protein - RNA complex may continue to be transported into the cell under conditions where the RNA "tail" has been entirely removed or reduced to a small, protected fragment by RNase digestion.

The data presented in Figure 3.6 tend to rule out the first of the foregoing models. If a discrete RNA fragment on the penetrating end were indeed resistant to RNase, then one would expect the amount of RNase-resistant RNA injected in the presence of a saturating concentration of RNase to be a constant fraction of the amount injected in the absence of RNase regardless of the multiplicity of infection. As shown in Figure 3.6, this was not the case. On the other hand, the second of the foregoing schemes predicts that the greater the MOI, the greater will be the number of phage particles that will become attached to the "optimum" binding sites at or near the cell surface and be able to inject intact RNA. The data in Figure 3.6 are therefore consistent with this hypothesis.

Additional support for the latter hypothesis was also obtained from a polyacrylamide gel electrophoretic analysis of viral RNA isolated 5 min post infection from cells infected in the presence of saturating concentration of RNase. The latter model predicts that the penetrated R17 RNA would appear in polyacrylamide gels as intact RNA (provided that the viral RNA is not fragmented in situ), while the former model predicts that only RNA fragments (or a fragment) would be found. As may be seen in Figure 3.7, native intact R17 RNA predominates whether the RNA is extracted from the infecting phage (3.7A) or from cells (thoroughly washed) infected by the phage in the presence of 5 µg/ml RNase (3.7 B). Since A protein penetration is unaffected by RNase, it is still possible that penetrated A protein material originating from phage which had adsorbed to a RNase sensitive position on the F-pilus may have brought into the cell a segment of RNA protected from degradation by the

Figure 3.7 Polyacrylamide gel analysis of phage RNA isolated from *E. coli* infected with phage in the presence of RNase.

*E. coli* WPI50 at  $5 \times 10^8$  cells/ml (in 50 ml CFMM P<sub>1</sub> aa) were infected with  $^{32}\text{P}$ -labeled R17 phage at a MOI of  $10^3$  particles/cell in the presence of 2  $\mu\text{g}/\text{ml}$  RNase. At 5 min post infection, the culture was quickly chilled by being poured onto 20 ml frozen TMM ( $-\text{Mg}^{2+}$ ). The cells were then washed 6X and extracted for total RNA by the SDS-phenol procedure described in Materials and Methods. The  $^{32}\text{P}$ -labeled RNA was then analyzed by exponential gradient gel electrophoresis according to procedures described in Figure 3.5 and in Materials and Methods: (A) Profile of RNA isolated from intact phage used for the infection, (PFE/particle =  $1 \times 10^{-3}$ ) (B) Profile of  $^{32}\text{P}$ -labeled RNA isolated from infected, washed cells.



A protein. However, such fragments, if small, may not be discernible in a distribution such as that given in Figure 3.

Since the foregoing results indicate that intact phage RNA is able to penetrate into host bacteria in the presence of RNase, especially when relatively high MOI's are used, it seemed reasonable to expect that some of the infecting genomes might be infectious. An experiment was thus carried out to test this assumption. Host bacteria (WP156) in CTMM (Luo) medium were infected at log phase ( $4 \times 10^8$  cells/ml) with  $^{32}\text{P}$ -labeled phage (PFU/particle = 1/80) at a MOI of  $10^3$  particles/cell for 20 min. The cells were then washed as described in Materials and Methods to remove extracellular phage, then plated with a lawn of sensitive Hfr bacteria and assayed for plaque-forming units (infection centers). The results are shown in Table 3:2.

It was found that the number of plaque-forming centers corresponding to cells infected with infectious RNA was proportional to the average phage equivalents of infectious RNA penetrated per cell. It is relevant to note that if the experiment was carried out using phage of very low infectivity (e.g. PFU/particle =  $10^{-7}$ ), then the infected cells would not give rise to infectious centers although some noninfectious RNA would still be able to penetrate cells in the presence of RNase. Of interest are the results obtained with the F<sub>2</sub> control cells which showed that the washing procedure left an extracellular phage background of about 1 PFU/900 cells or 1 physical particle/30 cells. Such background levels are insignificant in terms of radioactive counts. It was concluded from these results that at high MOI's, infectious phage RNA can penetrate cells even in the presence of saturating concentrations of RNase.



Table 3.2

Plaque Assay of *E. coli* (H1r) Cells Infected with R17 Phage in  
the Presence of RNase

Condition of infection	equivalents of RNA penetrated/cell	equivalents of infectious RNA penetrated/cell	infectious centers (PFU/ $5 \times 10^8$ cells)
Normal infection (no RNase)	15.0	0.5	$1.5 \times 10^8$
RNase (5.0 $\mu\text{g}/\text{ml}$ )	3.1	0.1	$3.8 \times 10^7$
<i>E. coli</i> B (control)	0		$4.4 \times 10^5$

\* Since PFU/particle of the phage = 0.0125 and since up to 40% of the phage may inject RNA, the ratio of infectious RNA/RNA injected

$$\frac{0.0125}{0.4} = 0.3$$

Although it was originally hoped that the present studies might provide clues to the question of the polarity of RNA penetration, it soon became evident that the intracellular degradation of the penetrated RNA precluded a meaningful chemical analysis of the 5' and 3' termini. On the positive side, these studies have yielded information on the fate of the phage RNA soon after penetration; i.e., they have shown that fragments of phage RNA can and do penetrate into host bacteria. The gel profiles of the phage RNA isolated from cells infected for 5 min with phage in the presence of RNase showed that the bulk of the penetrated RNA appears to be intact 28S ribonucleate. This has suggested to us that the sensitivity of the infectious process towards RNase applies only to particles which adsorb to the F pilus at some distance from the cell surface. The RNA from these particles appears to be almost completely degraded en route to the cell surface. Particles which attach to the F pilus near the cell surface, on the other hand, appear to be resistant to RNase, and manage to inject intact, infectious RNA into the cell. It is believed that viral RNA is able to penetrate cells at all multiplicities of infection in the presence of RNase, but that the probability of a successful hit (attachment of the phage to F-pilus) would be very much reduced at lower MOI's (cf. the experimental results of the infections carried out at MOI's of 100 and 1000 in Figure 3.6). This may account for the earlier conclusions, reached on the basis of low multiplicity infections, that RNase prevents the penetration of phage RNA and plaque formation (Knolle and Kaudewitz, 1963; Zinder, 1963).

## CHAPTER IV

### THE INACTIVATION OF PHAGE R17 BY ASCORBATE AND COPPER(II)

#### (A RADIOIMETRIC SYSTEM)

##### A. Introduction

There are several methods which can be employed to cleave R17 RNA *in situ* without unduly affecting the protein constituents of the particle. By storing  $^{32}\text{P}$  labeled phage suspensions in a protective medium at  $-80^\circ$  over varying periods of time it is possible to obtain phage preparations with a known average number of breaks per chain from calculations based on the specific radioactivity of the labeled phage (Lupker et al., 1973). However, this procedure is impractical from the point of view of it being time consuming; a series of phage preparations with different degrees of RNA fragmentation would be obtained in a matter of months instead of minutes (see appendix). A more rapid method involves the irradiation of phage particles with high energy X-rays or  $\gamma$ -rays (Ginoza, 1963; Sharp and Freifelder, 1971; Coquerelle and Hagen 1972; Pao and Speyer, 1973).

The molecular degradation of biological targets irradiated by high energy X- and  $\gamma$ -rays can occur through the direct absorption of energy or indirectly through attack by the radiolysis products of water. The ionization and excitation processes triggered by the absorption of high energy photons by water give rise to products such as solvated electrons ( $e^-_{aq}$ ), hydroxyl radicals ( $\cdot\text{OH}$ ), hydrogen radical ( $\cdot\text{H}$ ), molecular hydrogen, and hydrogen peroxide (Singh and Nicolau, 1971). The first three are known to be highly reactive



species and the most important one, the  $\cdot\text{OH}$  radical, has been shown to be the causative agent of 50 to 95% of all lesions produced by X or  $\gamma$  irradiation of molecular targets in aqueous medium (Blol and co-workers, 1967 and 1968; Powers and Gumpel-Jobbagy, 1972; Auda and Emborg, 1973). Redox systems such as the Fenton reagent ( $\text{Fe}^{2+} + \text{H}_2\text{O}_2$ ) or the Dixon-Norman system ( $\text{Ti}^{3+} + \text{H}_2\text{O}_2$ ) have been labeled as radioimetic systems as they, through the production of  $\cdot\text{OH}$  radicals, give rise to molecular lesions similar to those found after X or  $\gamma$  irradiation (Singh and Nicolau, 1971).

Recently it has been observed that the incubation of DNA in the presence of ferric or cupric ions and ascorbic acid results in the formation of single stranded breaks in DNA (Fomenko et al., 1974; Morgan et al., 1975). It was decided that it would be of interest for practical and general scientific reasons to investigate the possibility of RNA strand cleavage in R17 particles incubated in the presence of ascorbate- $\text{Cu}^{2+}$ , and if possible to ascertain the parameters that are involved in this cleavage.

## B. Results

### 1. Parameters of R17 Phage Inactivation by Ascorbic Acid and $\text{Cu}^{2+}$

Figure 4.1 illustrates the effect of the incubation of R17 particles in the presence of  $10^{-5}\text{M}$   $\text{Cu}^{2+}$  and  $10^{-3}\text{M}$  ascorbic acid in a high ionic strength buffer. As can be seen, the inactivation of the phage particles follows first order kinetics; more than a 4 log drop in infectious particles was produced within two min at  $37^\circ$ . Control mixtures incubated with only  $\text{Cu}^{2+}$  or ascorbic acid showed little or

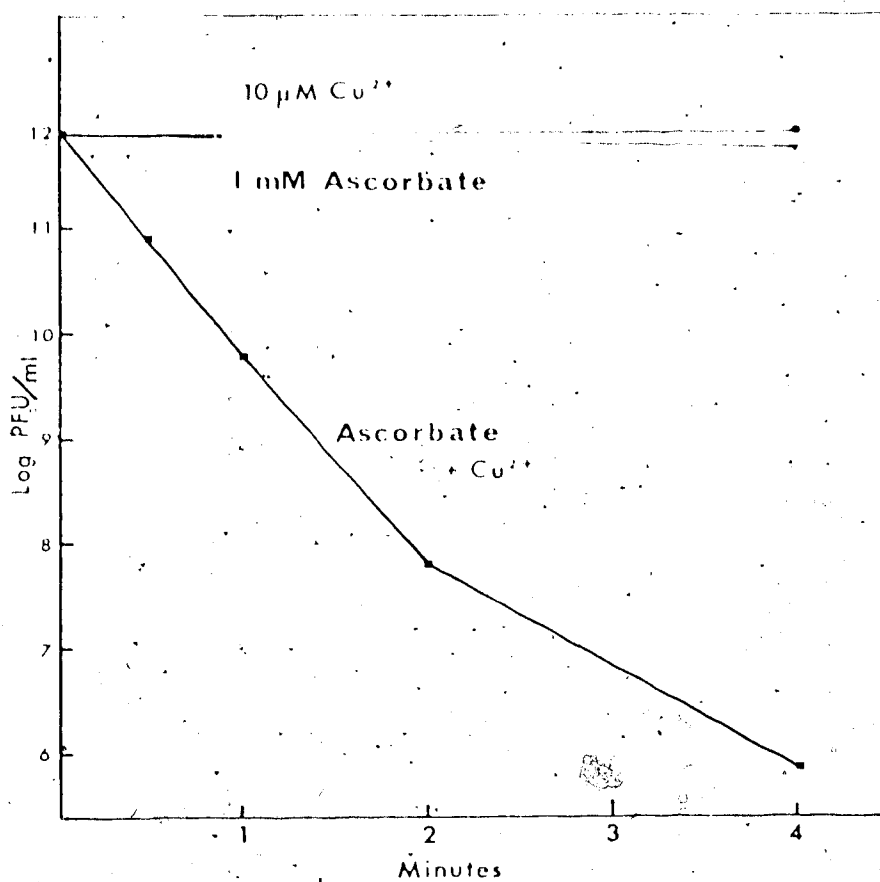


Figure 4.1 Kinetics of phage R17 inactivation by ascorbic acid,  $\text{Cu}^{2+}$  incubation.

Prewarmed solutions were combined to give a 0.5 ml mixture containing  $10^{-3}\text{M}$  L-ascorbic acid,  $10^{-5}\text{M}$   $\text{CuCl}_2$  and  $10^{13}$  R17 particles/ml in 0.05M Tris (pH 7.3) with 0.09M NaCl. After the addition of the last component (phage), the mixture was agitated in a vortex mixer for 1 sec and then incubated at  $37^\circ$ . 0.1 ml aliquots were taken out at appropriate time intervals and quenched with 0.01 ml  $10^{-2}\text{M}$  EDTA. Samples were serially diluted immediately and assayed for infectious centers (PFU) as described in Materials and Methods.

no phage inactivation in a period of four minutes. A  $\text{Cu}^{2+}$  concentration of  $10^{-4}$  M in the presence of  $10^{-3}$  ascorbate inactivated phage at a rate too fast to be measured; at  $10^{-6}$  M  $\text{Cu}^{2+}$ , about 90% of phage was inactivated in four minutes.

The foregoing standard concentrations of ascorbate ( $10^{-3}$  M) and  $\text{Cu}^{2+}$  ( $10^{-6}$  M) were chosen in order to have a saturating amount of ascorbate in the presence of a limiting amount of  $\text{Cu}^{2+}$ . Under these conditions, the inactivation of phage was found to be easily stopped through the addition of 0.1 volumes of  $10^{-2}$  M EDTA and subsequent maintenance of the related solutions at 0°.

The rate of inactivation of phage by ascorbate and  $\text{Cu}^{2+}$  was found to be temperature dependent and to a lesser extent dependent on the concentration of particles. Table 4.1 summarizes an experiment in which phage particles were incubated under standard conditions with varying particle concentrations and at different temperatures. After 25 seconds, EDTA was added and the mixtures were chilled and serially diluted for plaque assays.

Table 4.1

Effect of Phage Concentration and Temperature on the Amount of Ascorbate- $\text{Cu}^{2+}$  Inactivation of RLZ Phage\*

Phage Conc. (Part/ml)	Temp. °C	Surviving Fraction
$5.0 \times 10^{13}$	37	0.15
$5.0 \times 10^{12}$	37	0.014
$5.0 \times 10^{11}$	37	0.008
$5.0 \times 10^{10}$	37	0.004
$5.0 \times 10^{12}$	0	0.7
$5.0 \times 10^{12}$	25	0.2

\* Particles were incubated in  $10^{-3}$  M ascorbate and  $10^{-6}$  M  $\text{Cu}^{2+}$  for 25 sec PFU/particles of phage at 0 time = 1/10.

It was found that only 30% of the infectious particles were inactivated in 25 sec. at 0°, whereas at 37° the survivors were reduced by a factor of . . . . The magnitude of phage inactivation is similar at particle concentrations from  $5 \times 10^{10}$  to  $5 \times 10^{12}$  particles/ml, although the absolute rate of inactivation appears to be higher at lower phage concentrations. It is presently not clear why the rate of inactivation decreases at higher phage concentrations. In contrast, Orr (1967a) found that the rate of inactivation of catalase at low ionic strengths by ascorbate  $\text{Cu}^{2+}$  is independent of catalase concentrations.

Orr (1967a) has advanced the thesis that ascorbate probably acts through hydroxyl free radicals ( $\cdot\text{OH}$ ) formed from the reduction of oxygen. If this were the case, the partial or complete exclusion of oxygen from ascorbate- $\text{Cu}^{2+}$  incubation mixtures should bring about a sharp reduction in the loss of phage infectivity. Anoxic incubations were therefore carried out under  $\text{N}_2$  saturated conditions as described in Materials and Methods. It was found that under standard concentrations of ascorbic acid and  $\text{Cu}^{2+}$ , no loss of infectivity occurred when phage was incubated in the absence of  $\text{O}_2$ , whereas the control mixtures incubated under normal atmospheric conditions resulted in a 100-fold decrease in infectivity (in about 40 sec). It was concluded that  $\text{O}_2$  is a necessary component for the rapid inactivation of phage R17 by the ascorbate- $\text{Cu}^{2+}$  system.

The requirement for  $\text{O}_2$  in the incubation mixtures suggested to us that the superoxide ( $\text{O}_2^{\cdot-}$ ) radical (McCord and Fridovich 1968, 1969; Lavelle et al., 1973) might be the ultimate causative agent of

inactivation. Superoxide is formed by the donation of an electron to  $O_2$  and, since ascorbic acid forms a stable free radical with the loss of an electron, it could provide a source of electrons. If  $O_2^{\cdot -}$  were the active agent, then the inclusion of the enzyme superoxide dismutase in incubation mixtures should afford some protection as the enzyme would catalyze the destruction of superoxide radicals by dismutation to oxygen and hydrogen peroxide.



Such studies were carried out and it was found that the enzyme had no detectable effect on the inactivation of phage at enzyme concentrations as high as 470 units/ml (McCord and Fridovich units). Controls showed that this concentration is more than 10 times that required for the total suppression of the reduction of oxychromone C by  $O_2^{\cdot -}$  generated from a xanthine - xanthine oxidase system. It was concluded that  $O_2^{\cdot -}$  radicals are not the reactive species responsible for phage inactivation.

To determine whether  $H_2O_2$  might be functioning as an intermediate in the generation of reactive free radicals by ascorbate plus  $Cu^{2+}$ , an experiment was carried out to ascertain the effect of catalase on the inactivation of R17 phage. Standard reaction mixtures were set up as described in Figure 4.1, with catalase being present in one of the incubation mixtures at a concentration of 4  $\mu$ g/ml. The results are shown in Figure 4.2.

It may be seen that the catalase provided a significant protective effect against ascorbate- $Cu^{2+}$  inactivation. When the



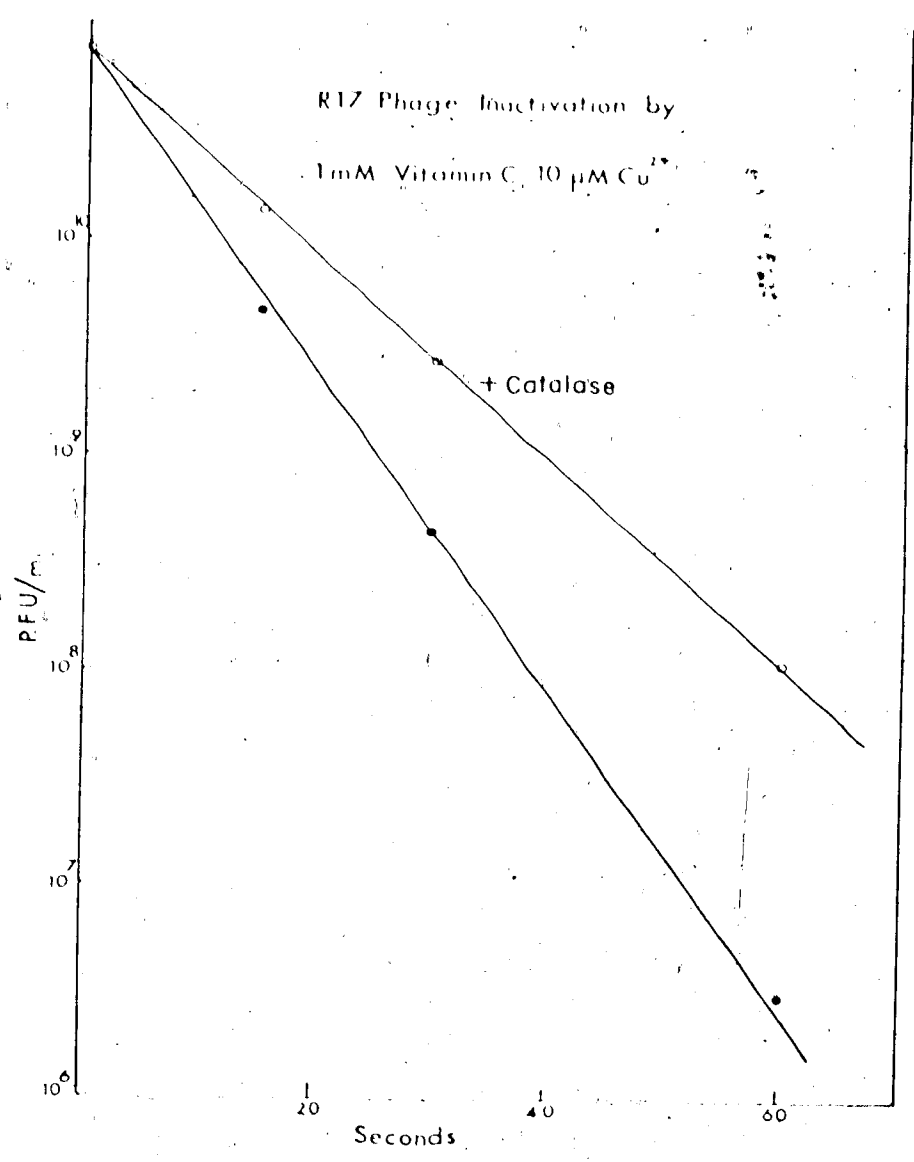


Figure 4.2. The effect of catalase on the inactivation of phage R17 by ascorbate- $Cu^{2+}$ .

Phage inactivation was carried out under the same conditions as described in Figure 4.1. In one incubation, beef liver catalase (Worthington, 6500 units/mg), was added to yield a final concentration of 4  $\mu$ g/ml. The phage concentration was  $6 \times 10^{11}$  PFU/ml (PFU/particle 1/10). Aliquots of the incubation mixture were treated with EDTA at appropriate time intervals and assayed for infectivity as described in Figure 4.1.

catalase was heated at 98° for 10 min prior to its addition to the reaction mixture, no protection was observed. Although the basis for this protective effect has yet to be clearly established, it seems unlikely that it arises from a simple competition for the reactive species between the phage particles and the catalase molecules. Orr (1967b) has shown that catalase can be inactivated by ascorbate and  $\text{Cu}^{2+}$ , presumably through degradative changes in the catalase molecule. However, this effect only occurred at low ionic strengths and was not found at all with the concentration of Tris buffer at 0.1M. It is thus possible that the present findings reflect the dismutation of  $\text{H}_2\text{O}_2$  by catalase and that  $\text{H}_2\text{O}_2$  may be an intermediate in the formation of reactive species. At present, the most likely candidate appears to be the hydroxyl free radical.

In Figure 4.3, the effect of increasing concentrations of the  $\cdot\text{OH}$  scavenger, potassium iodide, and that of the solvated electron scavenger, potassium nitrate, on the phage inactivating medium is shown. The bimolecular rate constants of  $\text{NO}_3^-$  with  $e^-_{\text{aq}}$  and  $\cdot\text{OH}$  as reported by Anbar and Neta (1967) are  $1.1 \times 10^{10}$  and  $< 5 \times 10^5 \text{ M}^{-1} \text{ sec}^{-1}$  respectively; the rate constant between  $\text{I}^-$  ions and  $\cdot\text{OH}$  is  $7 \times 10^9 \text{ M}^{-1} \text{ sec}^{-1}$ . The reaction between  $\text{I}^-$  and  $e^-_{\text{aq}}$  was too low to be measured. As can be seen in the figure, the phage infectivity was not protected by the presence of up to  $10^{-1} \text{ M}$  concentration of  $\text{KNO}_3$  under control conditions in which the phage was inactivated by a factor greater than  $10^4$ . On the other hand, the presence of  $10^{-1} \text{ M}$  KI conferred 100% protection. Protection of DNA from degradation by ascorbate- $\text{Cu}^{2+}$  was also observed when other  $\cdot\text{OH}$  trapping agents such as mannitol and benzoate were included in incubation mixtures (Morgan

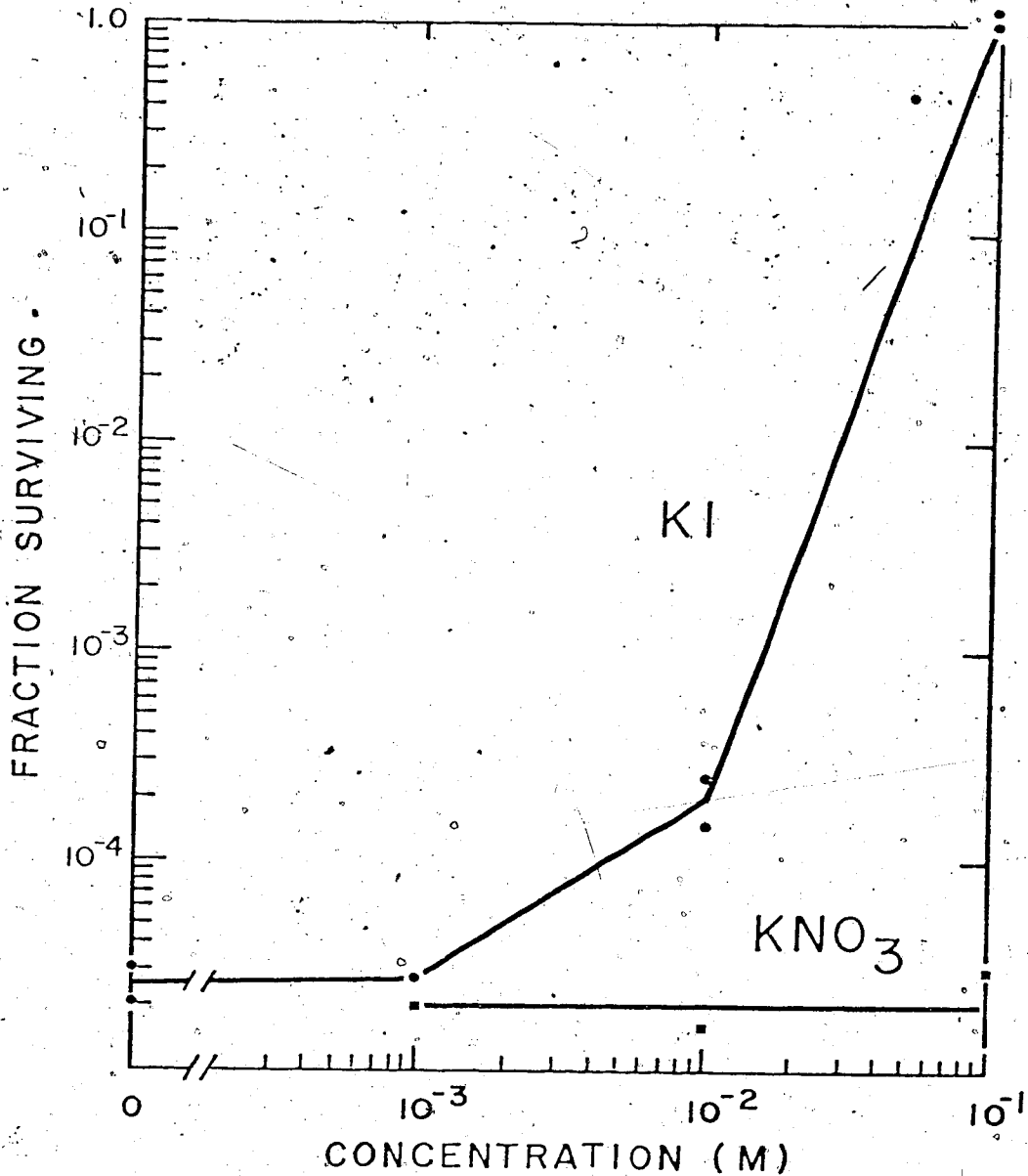


Figure 4.3 The effect of the presence of free radical scavengers in ascorbate- $Cu^{2+}$ -phage incubation mixtures.

Individual incubation mixtures (0.5 ml) containing  $10^{-3}M$  ascorbic acid,  $10^{-5}M$   $Cu^{2+}$ ,  $1.2 \times 10^{13}$  R17 particles/ml (PFU/particle of phage = 1/9) and appropriate concentrations of KI or  $KNO_3$  were set up. Each mixture was incubated for 1 min at  $37^\circ$  and quenched with  $50 \mu l$ ,  $10^{-2}M$  EDTA. Each sample was serially diluted and assayed for plaques as described in Materials and Methods.

et al., 1975).

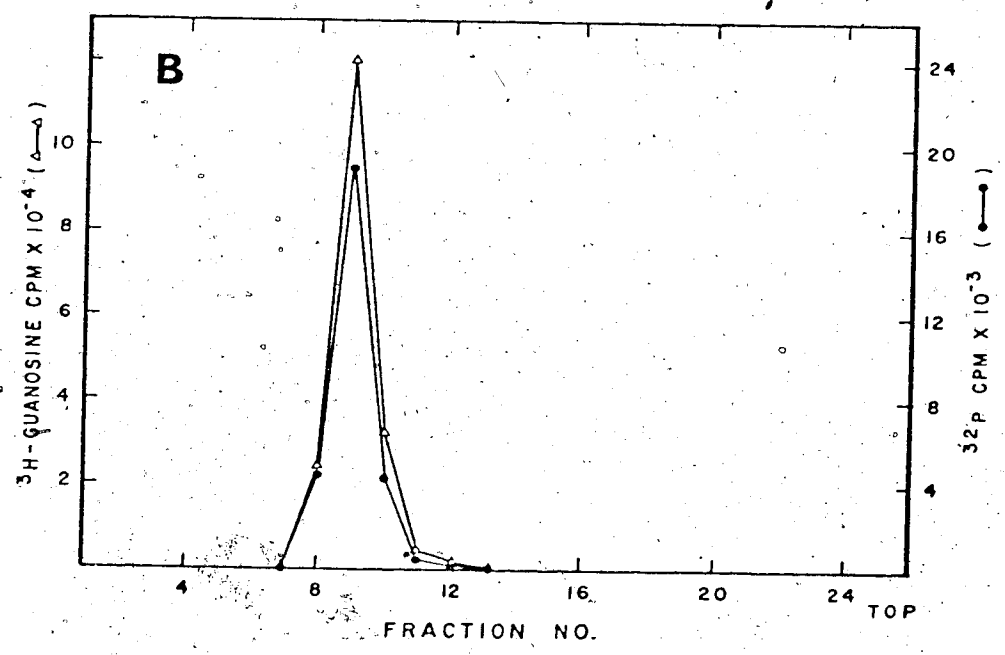
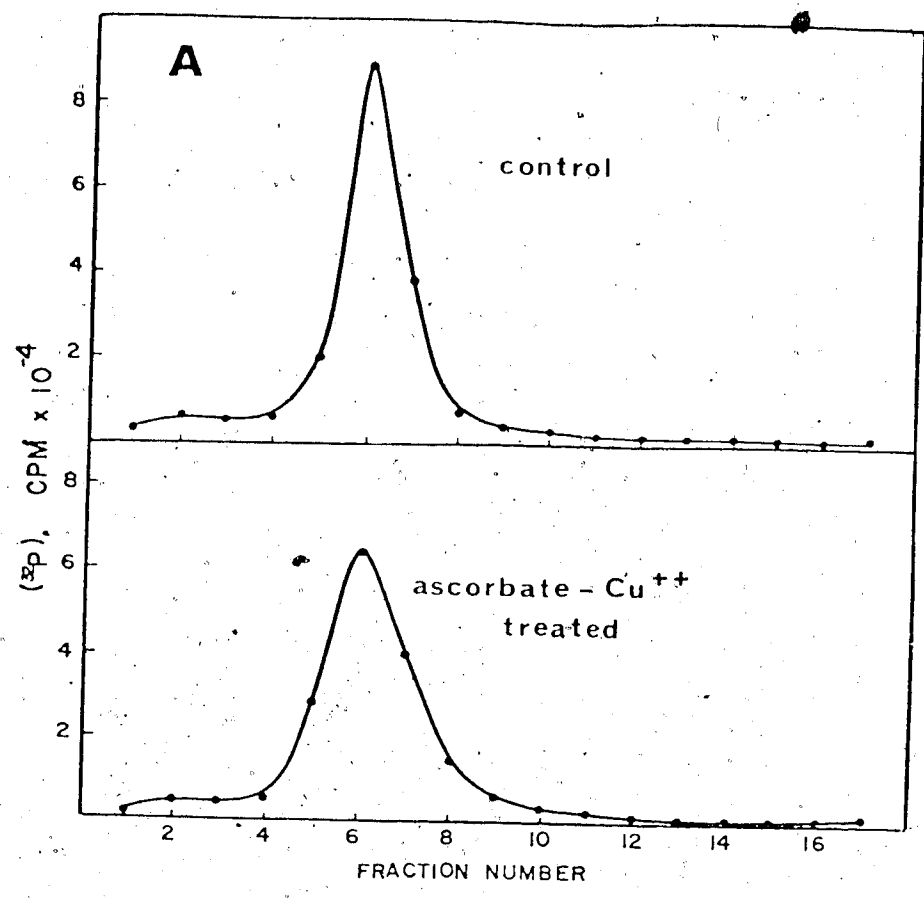
2. Physical and Biological Properties of Ascorbate-Cu<sup>2+</sup>-Treated R17 Phage.

R17 phage infectivity can be destroyed by perturbation of the phage at two sites. (a) The A protein can be removed or its function nullified so that phage attachment to the F-pilus and subsequent RNA ejection fail to occur. (b) The chemical or physical integrity of the RNA genome can be altered by various means to render the RNA noninfectious. A series of studies were carried out to determine the site and the nature of the injury.

Phage samples with various PFU/particle ratios were prepared on a large scale as described in Materials and Methods by treating a single <sup>32</sup>P-labeled phage suspension with ascorbate and Cu<sup>2+</sup>, and then removing aliquots at various times. Sucrose density gradient sedimentation and CsCl isopycnic analysis of the phage samples were carried out to ascertain whether the treatment had caused any gross structural damage to the particles. Figure 4.4A compares the sedimentation profiles of the untreated phage control (PFU/particle =  $5 \times 10^{-2}$ ) and the most highly inactivated phage sample (PFU/particle =  $5.0 \times 10^{-8}$ ). It may be seen that a  $10^6$ -fold reduction of phage infectivity caused no apparent change in the sedimentation properties of the phage. Although not shown, phage suspensions of intermediate PFU/particle values all sedimented as a single band having a mean sedimentation coefficient of 78S. Figure 4.4B shows the CsCl gradient analysis of an untreated <sup>3</sup>H-guanosine labeled phage control and ascorbate-Cu<sup>2+</sup>-inactivated, <sup>32</sup>P-labeled particles in the same gradient.

Figure 4.4 A comparison of the sedimentation property and buoyant density of R17 phage extensively inactivated with ascorbate-Cu<sup>2+</sup> with that of untreated phage.

After being extensively inactivated under standard conditions of ascorbate-Cu<sup>2+</sup> incubation, <sup>32</sup>P-labeled R17 phage was separated from EDTA, ascorbic acid and Cu<sup>2+</sup> as described in Materials and Methods. (A) 0.2 ml aliquots of different preparations were layered onto linear (5-20%) sucrose gradients and centrifugation carried out at 45,000 rpm, for 80 min at 4° (SW50.1 rotor). Fifteen-drop fractions were collected directly into liquid scintillation vials containing 1.0 ml distilled water; radioassay was carried out after each sample was shaken to homogeneity with 10 ml Scinti Verse. (B) <sup>32</sup>P-labeled phage (PFU/particle =  $5 \times 10^{-8}$ ) and <sup>3</sup>H-guanosine labeled phage (untreated with ascorbate-Cu<sup>2+</sup>, PFU/particle = 1/10) were mixed together in 4.0 ml SSC and 2.4 g CsCl added. Equilibrium centrifugation was carried out at 35,000 rpm, 4°, for 18 hrs (SW 50.1 rotor). Fractions (12 drop) were collected into vials with 1.0 ml distilled water and assayed with 10 ml Scinti Verse.



Clearly, the buoyant density of the highly inactivated <sup>32</sup>P-phage (PFU/particle = 1.0 x 10<sup>-8</sup>) was unaltered.

The next parameter examined was that of the A protein activity in treated particles. The primary function of the A protein moiety of R17 phage appears to be that of promoting phage attachment to filamentous receptors (F-pili) on the host cell and the subsequent penetration of phage RNA (Krahn et al., 1972). The biological integrity of the A protein can be partially determined by measuring the capacity of a given phage preparation to attach to F-piliated host bacteria. To this end, the <sup>32</sup>P-labeled phage preparations described in the previous section were subjected to the phage attachment procedure outlined in Materials and Methods. It was found that the attachment capacity of the phage suspensions (having PFU/particle ratios ranging from 10<sup>-2</sup> to 10<sup>-8</sup>) decreased by no more than 5% throughout the range of infectivities. Previous studies by Krahn and co-workers (1972) have shown that the A protein is cleaved into two polypeptide fragments, and penetrates along with the RNA into the cell in a 1:1 mole ratio. As will be shown elsewhere (Chapter V, Figure 5.4), the penetration of A protein was unimpaired under conditions where the phage particles were extensively inactivated by ascorbate-Cu<sup>2+</sup> treatment. From these results then, it was concluded that the ascorbate-Cu<sup>2+</sup>-induced loss of infectivity in R17 phage arises mainly from some perturbation of the RNA moiety of the virion rather than from an inactivation of A protein.

In vitro studies on the reaction of ·OH radicals (produced

by  $\gamma$ -radiation of H<sub>2</sub>O) with polynucleotides in the random coil and double stranded form (Ward and Urist, 1967) have shown that damage is sustained, to varying degrees, by bases, the sugar phosphate backbone and the macromolecular structure (as measured by hyperpolarizability). Boedtker (1967) has reported that approximately 80% of the bases of the R17 RNA strand are involved in intramolecular base pairing. In situ, the single-stranded RNA probably exists as a highly ordered, tightly packed structure within the protein capsid. In order to determine whether the ascorbate-Cu<sup>2+</sup> treatment causes any appreciable reduction in the ordered state of the RNA, the level of secondary structure in treated phage was quantitated. A fluorescence assay involving the binding of the dye ethidium bromide was used as a probe for measuring the extent of base pairing in phage particles. This assay is based on the fact that ethidium bromide will intercalate or bind only to duplex DNA or RNA at high ionic strengths and that the fluorescence of the bound ethidium bromide is enhanced approximately 25-fold relative to the fluorescence of the unbound dye (Le Pecq and Paoletti, 1966). Preliminary studies had indicated that the dye molecule passes through the phage capsid readily to bind to the phage RNA in situ. This observation was not unexpected since the phage capsid is believed to have a porous structure (O'Callaghan et al. 1973; Dunker and Paranchych, 1975). The amount of dye bound by phage particles with PFU/particle ratios ranging from 10<sup>-2</sup> to 10<sup>-8</sup> was assayed as described in Materials and Methods. It was found that the uptake of dye was essentially identical in all cases suggesting that extensive inactivation of phage by ascorbate-Cu<sup>2+</sup> does not cause any detectable change in the level of secondary structure of the RNA in situ.



### 3. Characterization of The RNA Isolated From Ascorbate-Cu<sup>2+</sup>

#### Treated Phage

Since the ascorbate-Cu<sup>2+</sup> treatment had been shown to create single strand breaks in DNA, it was anticipated that the same would occur to the RNA in the phage particles; i.e., the ·OH radicals generated would diffuse through the capsid and cause single-strand breaks in the RNA in situ. That this was the case was easily shown by polyacrylamide gel electrophoresis of the RNA isolated from ascorbate-Cu<sup>2+</sup> treated phage (Chapter V, Figure 5.1A<sub>1</sub>-D<sub>1</sub>). It was observed that the greater the extent of phage inactivation, the greater the extent of RNA fragmentation as displayed by the RNA profiles in the gels.

In a series of experiments conducted to deduce the polarity of RNA penetration into cells, the alkaline hydrolysates of <sup>3</sup>H-adenosine-labeled RNA from ascorbate-Cu<sup>2+</sup>-treated phage were analyzed by paper electrophoresis (Chapter VI). These analyses allowed the determination of the ratio of adenosine to adenosine-2',3'-phosphates A<sub>OH</sub>/Ap in a series of phage preparations. The A<sub>OH</sub>/Ap ratios relative to the infectivity (PFU/particle) of the various phage preparations tested are shown in Figure 4.5. As can be seen, the A<sub>OH</sub>/Ap ratio begins to deviate from the expected value of 0.0013 as the particles from which the RNA was isolated were increasingly inactivated with ascorbate-Cu<sup>2+</sup>. This trend indicates that extraneous 3'-A<sub>OH</sub> residues were produced as the result of strand scissions giving rise to 3'-OH and 5'-phosphate ends. The relative proportion of breaks that resulted in the formation of 3'-phosphate and 5'-OH ends, if any, is an unknown factor at the present time.

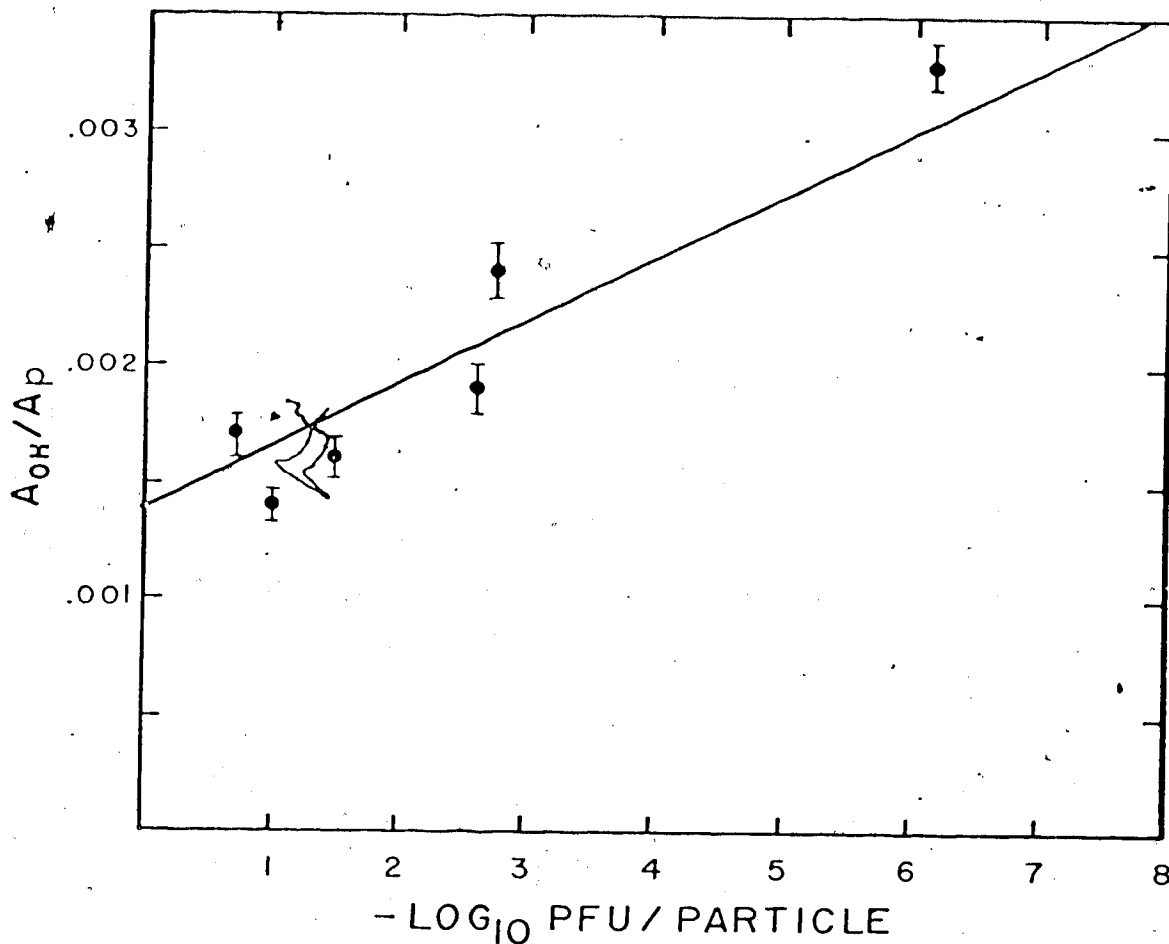


Figure 4.5 The formation of extraneous 3'-A<sub>OH</sub> ends in R17 RNA cleaved *in situ* as a result of ascorbate-Cu<sup>2+</sup> treatment.

Preparations of <sup>3</sup>H-adenosine labeled R17 phage with different PFU/particle ratios were obtained on a preparative scale by ascorbate-Cu<sup>2+</sup> treatment as described in Materials and Methods. Labeled phage suspensions (containing about 10<sup>7</sup> <sup>3</sup>H-cpm) were combined with 1 x 10<sup>14</sup> unlabeled phage particles and the RNA from the mixture was extracted by SDS-phenol. The RNA was then subjected to alkaline hydrolysis and the resultant hydrolysate was analyzed by high voltage paper electrophoresis at pH 3.5 (see Materials and Methods for details of methodology). The A<sub>OH</sub>-cpm/A<sub>p</sub>-cpm ratio was obtained by determining the total radioactivity in the appropriate peaks in an electropherogram. A straight line of best fit was obtained by the least square method.

Nevertheless, a reasonable estimation of the proportion of strand breaks to lethal "hits" can be made from the data given in Figure 4.5.

Studies characterising ascorbate-Cu<sup>2+</sup> treated R17 phage described earlier indicate that the primary site of inactivation appears to be the viral RNA. Therefore, fatal lesions sustained by phage can be regarded in terms of strand scissions or base degradations (Singh and Nicolau, 1971). Since R17 phage is probably inactivated randomly by reactive .OH species, the distribution of fatal lesions sustained by the phage population can be described by the Poisson function:

$$F(y) = \frac{x^y e^{-x}}{y!}$$

where F(y) represents the fraction of the phage particles receiving y number of lesions under conditions in which an average of x "hits"/particle has been introduced into the system. From the Poisson equation, the fraction of survivors (y=0) is given by  $F_s = e^{-x}$  and  $x = -\ln F_s$ . It can be observed in Figure 4.5 that at an  $A_{OH}/Ap$  ratio of twice the expected value (0.0026 versus 0.0013),

$$\begin{aligned} -\log_{10} F_s &= -\log_{10} \text{PFU/particle of ascorbate-Cu}^{2+} \text{ inactivated} \\ &\quad \text{R17} \\ &\quad + \log_{10} \text{PFU/particle of untreated phage} = 3.5 \end{aligned}$$

given that the PFU/particle ratio of untreated phage is equal to 1/10.

From the above, it is calculated that  $x = -\ln F_s = -2.303 \log_{10} F_s$  and  $x = 8$ . This means that approximately one extraneous 3'-A<sub>OH</sub> end is produced when an average of 8 lethal "hits" are introduced per RNA target.

If one assumes reasonably that breaks involving the creation of new ends terminating in 3'-OH and 5' phosphate are formed independently of base composition, then about 4 strand breaks have occurred when  $x = 8$  (since the mole fraction of A in RNA is 0.23). If one makes the less likely assumption that breaks involving the creation of new 3' phosphate and 5'-OH ends are formed with equal probability and independently of base composition, then a strand scission would be produced for every fatal lesion. Note in the foregoing that no attempt has been made to equate every strand scission with a lethal "hit" since Lupker et al. (1973) have shown that not every phosphodiester break introduced into an RNA phage necessarily inactivates it. This point will be discussed in greater detail in Chapter V.

Another approach taken to ascertain the proportion of strand breaks to fatal lesions produced by incubation in ascorbate-Cu<sup>2+</sup> was the estimation of the number of intact RNA molecules left in a phage population after such treatment. The rationale was that if strand breaks constitute a constant fraction (a) of x, the average number of fatal "hits" absorbed per phage particle, then the fraction of the phage RNA population which escapes degradation would be given by:

$$F'_S = e^{-ax}$$

An approximation of (a) was obtained as follows: <sup>3</sup>H-quanosine-labeled R17 phage inactivated to known infectivities by ascorbate-Cu<sup>2+</sup> were combined with freshly prepared <sup>32</sup>P-labeled phage and the mixture subjected to RNA extraction by SDS-phenol. The isolated RNA was then separated in 8M urea polyacrylamide gels at 60° as described in Materials and Methods. F'\_S was obtained by calculating relative amount of <sup>3</sup>H-labeled RNA migrating with the 28S, intact <sup>32</sup>P-marker in the electro-

photograms. From  $F_0^1$ , (a) was calculated.  $F_0^2$  was given by the ratio of the infectivity of the ascorbate- $\text{Cu}^{2+}$  treated phage to that of the untreated phage and from this figure, the value of  $x$ , then (a) was determined. The fraction (a) for several inactivated phage preparations is tabulated in Table 4.2. The average (a) value indicated that a little less than 1 strand break is produced for every 2 fatal lesions. This estimation correlates with the lower value of (a) suggested by the  $N_{OH}/A_p$  results discussed in the preceding section.

## C. Discussion

### 1. The Mode of Action of Ascorbate- $\text{Cu}^{2+}$

The inactivation of R17 phage by ascorbate- $\text{Cu}^{2+}$  has been investigated mainly as a consequence of our interest in using this reagent as a tool in the elucidation of the mechanism of R17 phage RNA penetration in the *E. coli* host. We have characterized a procedure that allows the controlled degradation of the phage genome without affecting in any gross way the properties of the capsid proteins. The resistance of the A protein to destruction by the putative  $\cdot\text{OH}$  radical is not overly surprising. It is known that the ability of DNA bacteriophage to adsorb is not appreciably reduced by direct effects of ionizing radiation (Sharp and Freifelder, 1971a; Coquerelle and Hagen, 1972). Previously De Flora and Badolati (1970) had shown that  $\gamma$ -rays exerted a selective action on some functions of  $A_2/\text{Hong Kong}$ , influenza virus. The dose required to achieve complete removal of infectious particles does not affect its haemagglutinin (HA) titer nor alter its ultrastructural appearance. Seven to eight times the normal dose is

Table 3

Estimation of the Proportion of RNA Strands of a Total RNA Population Produced in R17 Phages Inactivated by Ascorbate

$F_{10}^{100}$ (10 <sup>-6</sup> )	$F_{10}^{100}$ (10 <sup>-6</sup> )	$F_{10}^{100}$ (10 <sup>-6</sup> )	$F_{10}^{100}$ (10 <sup>-6</sup> )	$F_{10}^{100}$ (10 <sup>-6</sup> )
0.33	1.1	0.56	0.6	0.5
0.10	2.3	0.40	1.0	0.5
0.033	3.7	0.20	2.0	0.4
0.01	4.6	0.10	3.1	0.3

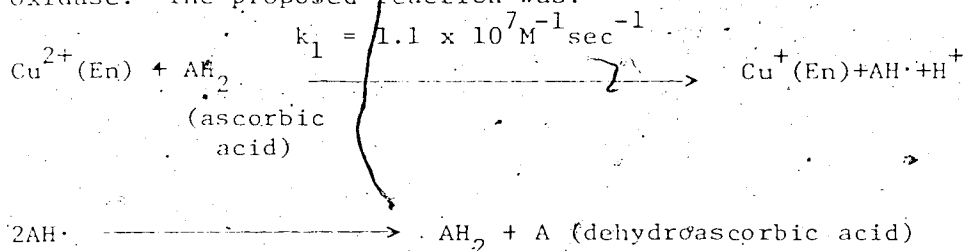
(1)  $\frac{\text{RFU particle of Vit. C treated R17}}{\text{RFU particle of untreated R17}}$

(2) estimate of proportion of RNA migrating as intact molecules in 5M urea gels at 60°C

required to abolish HA ability and alter the viral morphology. Along the same lines, *E. coli* ribosomal function was found to be impaired only after the unit had sustained eight or more hits from  $\gamma$ -radiation (Petranovic *et al.*, 1971). Similarly, the inactivation of A protein may conceivably be a multi-hit phenomenon; under standard conditions of ascorbate-Cu<sup>2+</sup> incubation, the A protein was probably not altered sufficiently to bring about any significant loss of activity.

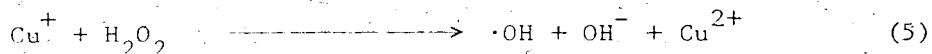
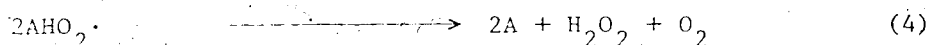
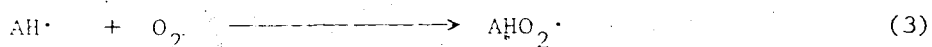
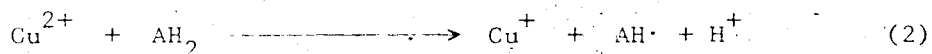
The mechanism by which the RNA is degraded has yet to be completely elucidated. By analogy with studies on DNA strand cleavage by ascorbate (the requirement for O<sub>2</sub>, the enormous enhancement in rate by Cu<sup>2+</sup>, and inhibition by catalase), it would appear that the mode of cleavage is probably identical (Morgan *et al.*, 1975). Initially it seemed that superoxide (O<sub>2</sub><sup>-</sup>) was a likely candidate for the reactive species leading to strand cleavage. Superoxide generated by the oxidation of xanthine by xanthine oxidase did cleave DNA efficiently and cleavage was completely suppressed by less than nanomolar levels of superoxide dismutase. However, superoxide dismutase had no effect on ascorbate-generated strand cleavage of DNA or RNA (Morgan, *et al.*, 1975). Finally, the protection afforded by catalase and  $\cdot$ OH scavengers strongly points to the  $\cdot$ OH radical generated from H<sub>2</sub>O<sub>2</sub> as the most likely candidate responsible for strand cleavage. Hydrogen peroxide itself has no effect on DNA or R17 phage infectivity. However, in the presence of transition metal ions such as Fe<sup>3+</sup> and Cu<sup>2+</sup>, H<sub>2</sub>O<sub>2</sub> is rapidly broken down into products that include  $\cdot$ OH (Pryor, 1966). Other clues to the mechanism of action of ascorbate-Cu<sup>2+</sup> are supplied by past *in vitro* studies on the

ascorbate molecule. Yamazaki and Piette (1961), with the aid of electron paramagnetic resonance techniques, were able to generate ascorbate free radicals ( $AH\cdot$ ) with the copper-containing enzyme ascorbate oxidase. The proposed reaction was:



Furthermore, Barr and King (1956) had previously indicated that ascorbate free radicals ( $AH\cdot$ ) can undergo oxidation to yield dehydroascorbate and  $H_2O_2$ .

Given these considerations and the observed nature of the ascorbate- $Cu^{2+}$  system, the course of events leading to the formation of  $\cdot OH$  radicals probably involves a series of redox reactions with  $O_2$  and  $Cu^{2+}$  acting as catalysts:



An interesting experiment worth doing would be to compare the phage inactivation rates in incubation mixtures where an equimolar quantity of ascorbate oxidase was substituted for free  $Cu^{2+}$  ions. Since the oxidation of ascorbate to its free radical is more efficient with the enzyme, a drastic increase in the rate of phage inactivation would be expected. By the same token, the initial step (equation 2) in the pro-



posed reaction should be rate limiting as the oxidation of ascorbate by  $\text{Cu}^{2+}$  is probably far less efficient. Furthermore, the considerable dependence of the rate of phage inactivation on temperature indicates that a significant activation energy is involved in the formation of  $\cdot\text{OH}$ . It is to be noted that the rate constants for reaction of  $\cdot\text{OH}$  with compounds such as pentoses, purines and pyrimidines are greater than  $10^9 \text{M}^{-1} \text{sec}^{-1}$ . Such values are close to the limit imposed by the rate of diffusion and the actual reaction rates of  $\cdot\text{OH}$  with a substrate should be only slightly temperature dependent.

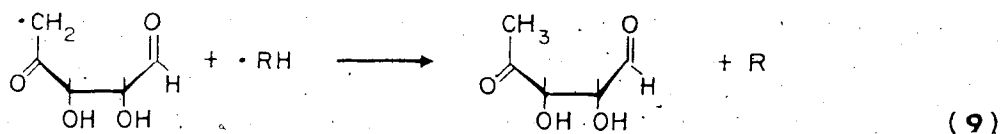
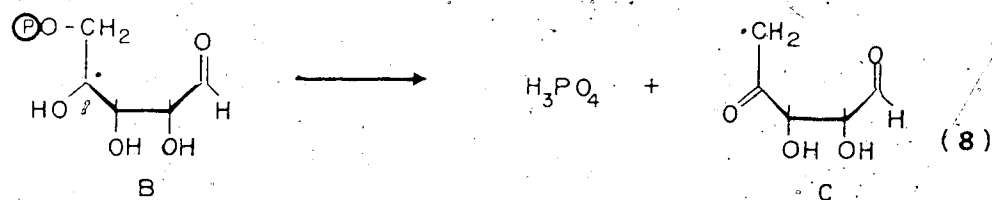
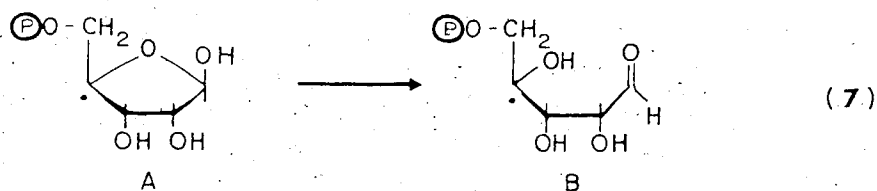
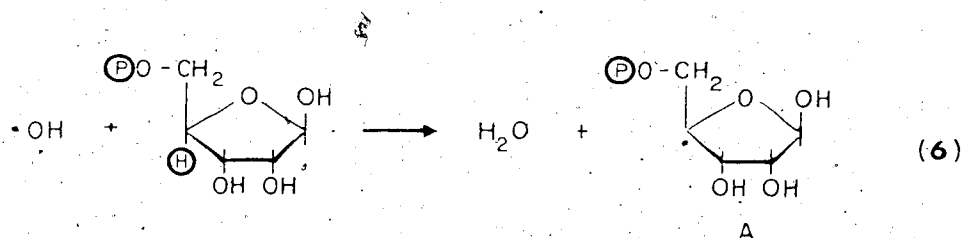
Of interest to the present discussion is the earlier report of Yamamoto and co-workers (1964) on the inactivation of bacteriophage by metals. They found that the sensitive RNA bacteriophages MS2 and f2 and; to a lesser extent the single stranded DNA phage S13, are inactivated when their dilute suspensions come into contact with an aluminum alloy surface or when diluted with fluids which have been in contact with aluminum, zinc, or magnesium. The inactivation is believed to result from the simultaneous action of traces of  $\text{Cu}^{2+}$  and electrolytically formed  $\text{H}_2\text{O}_2$  and may be stimulated by addition of both of these agents, although neither alone was fully active when present in trace amounts. The finding that the phages were protected by adding either catalase or EDTA further supports the suggested mechanism. In retrospect, the simultaneous action of  $\text{Cu}^{2+}$  and  $\text{H}_2\text{O}_2$  described by this group probably represented the schism of  $\text{H}_2\text{O}_2$  by  $\text{Cu}^{2+}$  into  $\cdot\text{OH}$  and  $\text{H}_2\text{O}$  (Pryor, 1966). What this group observed, then, was a system inactivating phage through the ultimate generation of damaging  $\cdot\text{OH}$  species.

## 2. Free Radical Attack on Nucleic Acids

Two main types of lesions are produced in nucleic acids by  $\cdot\text{OH}$  radicals (also by the direct effects of ionizing radiations).

These are base degradations and phosphodiester bond scissions.

Recently Stelter and co-workers (1974) have examined the effect of  $\cdot\text{OH}$  attack on ribose-5-phosphate by the analysis of products by gas liquid chromatography and mass spectrometry. One mechanism they proposed which may serve as a model for the formation of phosphodiester bond scissions in RNA is as follows:



C

5-Deoxy-D-erythro-pentos-4-ulose

Essentially, the reaction scheme involves H abstraction at the C-4 position by  $\cdot\text{OH}$  followed by ring opening. Radicals with an  $\alpha$ -OH group in an  $\alpha$  and a phosphate group in a  $\beta$  position are known to undergo rapid elimination of phosphate. Following the same mechanism, a phosphate group at the C-3 position can also be eliminated. Thus, strand breaks leading to 3'-phosphate or 5'-phosphate end groups could theoretically arise in RNA challenged by  $\cdot\text{OH}$ . A similar reaction mechanism may give rise to 5'-OH, 5'- $\text{PO}_4$  and 3'-OH termini which have been associated with single stranded breaks in DNA isolated from  $\gamma$ -irradiated *E. coli* (Gaziev et al., 1974). The findings of extraneous  $\alpha$ -OH residues in alkaline hydrolysates of ascorbate- $\text{Cu}^{2+}$ -treated R17 RNA strongly indicates that strand breaks resulting in the formation of new 3'-OH and 5'- $\text{PO}_4$  ends are produced by  $\cdot\text{OH}$  attack. However, more extensive chemical analyses of viral RNA degraded in situ by  $\cdot\text{OH}$  must be carried out in order to answer the question of whether any breaks involving the formation of 3'- $\text{PO}_4$  and 5'-OH ends are also produced by ascorbate- $\text{Cu}^{2+}$  incubation. Furthermore, such analyses should indicate whether strand breaks are distributed randomly or nonrandomly amongst the four basic nucleotides in the chain.

Several in vitro studies have been carried out to determine the comparative susceptibility of base and glycosidic phosphate linkages in nucleotides subjected to  $\cdot\text{OH}$  attack. At present there is some disagreement in the literature concerning the results. In some quarters, the suggestion was made that  $\cdot\text{OH}$  attacks bases and phosphate bonds equally (Stelter et al., 1974), while other workers claimed that the phosphate group in free nucleotides is affected 20 to 25% of the time

(Scholes et al., 1960). The analysis of the amount of intact viral RNA migrating in 8M urea polyacrylamide gels (at 60°) presented earlier tend to support a scheme whereby the phosphodiester bonds and bases of the viral RNA in situ are affected equally by free radicals. There is also evidence to indicate that bases in double stranded polynucleotides are protected to varying extents (25-50% protection as compared to free nucleotides or single stranded polynucleotides) from ·OH radical degradation (Ward and Urist, 1967). Since about 80% of the bases in R17 RNA are involved in base-pairing, it is expected that some protection of bases from ·OH attack occurs here as well.

## CHAPTER V

### PENETRATION STUDIES WITH ASCORBATE-Cu<sup>2+</sup> INACTIVATED R17 PHAGE

#### A. Introduction.

As shown in Chapter IV, incubation of R17 phage with ascorbate and Cu<sup>2+</sup> ions results in the fragmentation of the phage RNA in situ without causing any detectable change in the functional properties of the capsid proteins. The rapidity and simplicity of the ascorbate-Cu<sup>2+</sup> procedure was exploited in the present study to produce phage preparations with a wide spectrum of infectivity. These preparations were then utilized in a series of penetration experiments in which the kinetics of the amount of RNA injected, the physical state of the penetrated RNA, and the hydrodynamic properties of the extracellular phage particles remaining after exposure to sensitive E. coli were examined. It will be demonstrated that particles inject only part of their RNA into host cells if strand breaks are introduced into the RNA prior to cell infection. Apparently not all breaks give rise to strand separation since some potential fragments are probably held together by intrastrand hydrogen bonding. In other words, the phage RNA appears to retain part of its secondary structure during the penetration process. Also found in this series of experiments was evidence which suggests that the eclipse or the RNA ejection step of phage infection may also involve the detachment of some coat protein monomers from the capsid. The implications of these findings in relationship to phage infection are discussed.

Finally, it was confirmed in a separate experiment that divalent metal ions are required for the complete ejection of RNA from capsids. Infections carried out in the absence of such ions result in the breaking off and release of variable portions of the viral RNA and the formation of partially empty capsids.

## B. Results

### 1. RNA Penetration of R17 Phage Inactivated by Ascorbate-Cu<sup>2+</sup>

#### (a) Polyacrylamide Gel Electrophoresis of Penetrated RNA

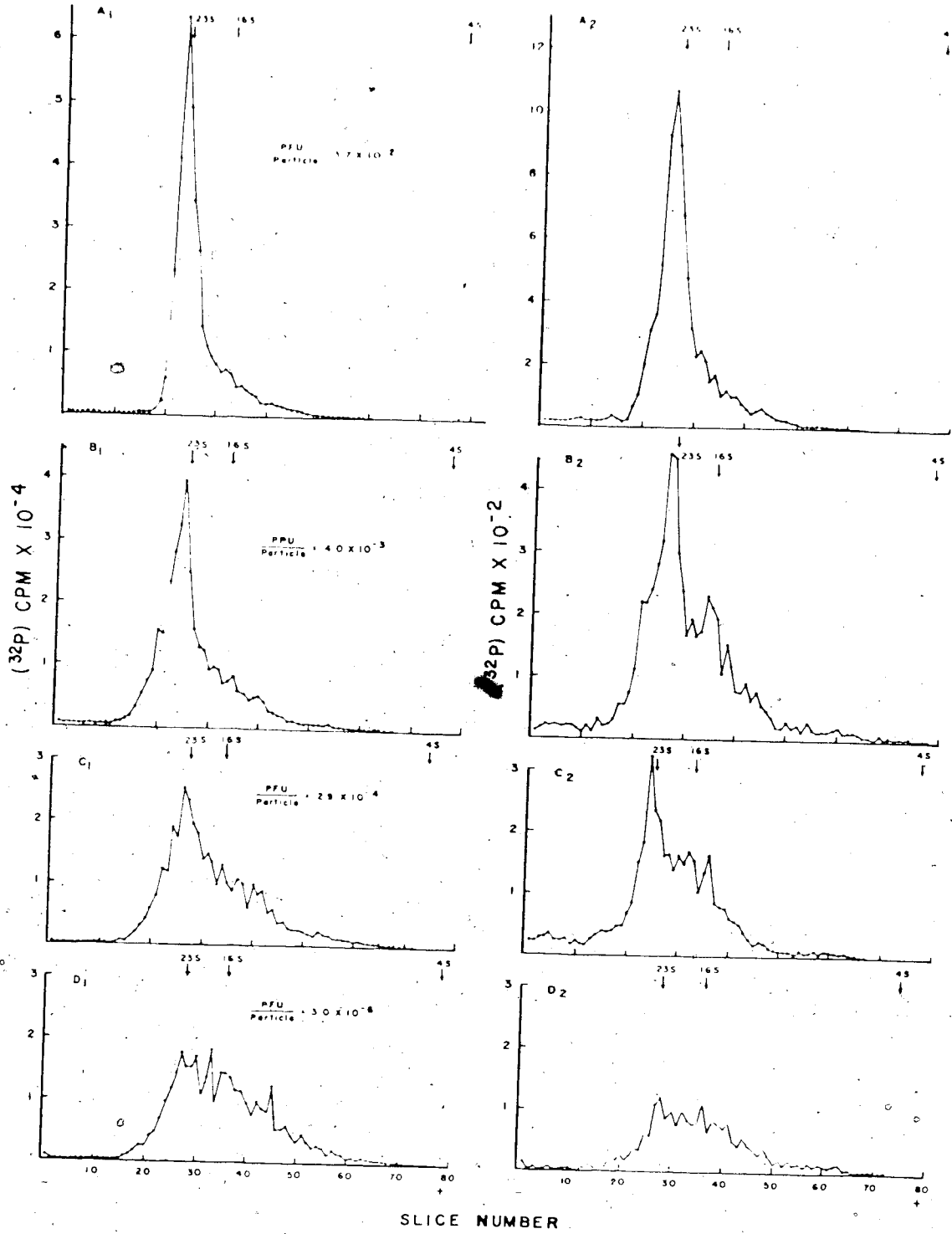
The results in Chapter III have shown that fragments of RNA originating from highly degraded <sup>32</sup>P-labeled R17 phage are able to penetrate sensitive cells. It was expected that R17 RNA degraded in situ by treatment with ascorbate-Cu<sup>2+</sup> would yield similar findings.

To confirm this, an experiment was carried out as follows:

A purified <sup>32</sup>P-labeled R17 phage preparation was treated with ascorbate and Cu<sup>2+</sup> as described in Materials and Methods to prepare a series of phage preparations having PFU/particle ratios ranging from  $3.7 \times 10^{-2}$  (untreated control) to  $3.0 \times 10^{-6}$ . An aliquot of each preparation was subjected to phenol extraction, after which the extracted RNA was examined by polyacrylamide gel electrophoresis. A second aliquot of each phage preparation was allowed to interact with host bacteria for 5 min at 37°. The cells were then chilled and washed to remove extracellular phage, after which the intracellular RNA was isolated by phenol extraction and subjected to polyacrylamide gel electrophoresis. The results of the experiment are shown in Figure 5.1. Panels A<sub>1</sub>-D<sub>1</sub> show the electropherograms of RNA extracted directly from the four phage preparations employed. Panels A<sub>2</sub>-D<sub>2</sub> show the results of poly-

Figure 5.1 Polyacrylamide gel electrophoresis of  $^{32}\text{P}$ -RNA isolated from ascorbate- $\text{Cu}^{2+}$ -inactivated R17 phage and from E. coli (Hfr) cells infected with the same preparation.

Derivative  $^{32}\text{P}$ -labeled phage stocks of different PFU/particle ratios were obtained on a preparative scale by ascorbate- $\text{Cu}^{2+}$  treatment as described in Materials and Methods. E. coli WP156 cells in 25 ml CTMM+aa (prelabeled for 30 min in the presence of 1 uCi/ml  $^3\text{H}$ -5,6-uridine) were infected at a density of  $4 \times 10^8$  cells/ml with each of 4 phage preparations at a MOI of  $10^3$  particles/cell. After 5 min the cultures were quickly chilled and washed 6X to remove extracellular phage. The RNA from washed, infected cells and from a mixture of intact phage ( $10^7$  cpm) and  $10^{10}$   $^3\text{H}$ -uridine labeled cells (combined at  $4^\circ$ ) were isolated by SDS-phenol extraction. About 500  $\mu\text{g}$  of radioactively labeled RNA from each sample was then separated in exponential gradient (2.5-15%) polyacrylamide gels at  $4^\circ$  and 10 volts/cm. (See Materials and Methods for details of methodology).  $A_1$ - $D_1$ : electropherograms of the RNA isolated from intact phage of 4 different infectivities.  $A_2$ - $D_2$ : electropherograms of the RNA isolated from host bacteria infected with corresponding phage preparations shown in  $A_1$ - $D_1$ .





acrylamide gel analysis of the  $^{32}\text{P}$ -RNA found in host bacteria following the 5 min exposure to each of the corresponding phage preparations shown in panels A<sub>1</sub>-D<sub>1</sub>. It is to be noted that  $^3\text{H}$ -labeled 23S, 16S and 4S cellular RNAs served as internal markers in each of the gels.

It is evident from Figure 5.1 that the fragmentation of the RNA recovered from whole particles becomes more extensive as the level of infectivity diminishes. On comparing the RNA profile of the material isolated from intact particles with that isolated from cells infected with the same batch of phage, it is seen that the extent of fragmentation of the penetrated RNA is comparable to that found in the particles. The more degraded the RNA in the particles, the more degraded was the RNA recovered from the infected cells. This finding therefore supports the previous conclusion that RNA penetration is not confined to intact infectious RNA, but that fragments are able to penetrate as well.

One plausible explanation for these observations is that the leading or proximal end of the penetrating RNA becomes separated from the remainder of the molecule at the first phosphodiester scission in the RNA chain. Given the assumption that the position of single-strand breaks is random in any given phage population, the size of the penetrating RNA fragments would be expected to be highly heterogeneous. Moreover, one would predict that the amount of penetrated phage RNA should decrease with increasing levels of fragmentation, since an increase in the average number of breaks per genome would increase the probability of breaks occurring near the leading end of the genome. In fact, Panels A<sub>2</sub> to D<sub>2</sub> in Figure 5.1 do show a decline in the amount of re-

covered parental phage RNA in infected cells as the infectivity of the phage decreases.

Alternatively, it could be argued that phage RNA penetration is an all-or-none process; either the total content of a capsid is injected or none of it is injected. When a particle is challenged by  $\cdot\text{OH}$  radicals, there may exist a threshold level of lesions beyond which that particle will not undergo the processes of RNA ejection and penetration. Although this conjecture may explain the decrease in the amount of RNA injected by phage of decreasing infectivities, it also implies that highly fragmented genomes would not penetrate into the host cell. Consequently, the distribution of the penetrated RNA - although mirroring that of the material isolated from whole particles with relatively high infectivities - should be dominated by large fragments regardless of the infectivity of the parental phage. This prediction appears not to be borne out by the data shown in Figure 5.1

To provide a further basis for assessing the mass distributions shown in Figure 5.1, an attempt was made to generate a computer simulation of the first-piece-only model of RNA penetration. The approach used involved a system of vectors of a defined magnitude and orientation which simulated a population of RNA strands each with 5'- and 3'-ends. In actual runs, parameters such as the number of units or target sites per strand, the number of strands in the system and the average number of nicks,  $x$ , to be introduced per strand could be independently specified. Given these parameters, the program distributed the scissions randomly into the population and then "counted" the number of fragments

of a particular length produced.

In Figure 5.2, the mass distribution of the fragments produced in the whole system and that of the first piece injected (arbitrarily designated as the fragment on the extreme right hand side of each strand) are given for  $x$  values of 0.5, 2 and 3. It must be stressed that the distributions illustrated in the Figure are far from statistically ideal as the parameters of strand number (500) and RNA size (33 units) specified in the runs were relatively small. However, it was decided that the potential information to be gained with much higher numbers did not justify the prohibitive costs that a "true simulation" would entail.

What Figure 5.2 does show - and this is the purpose of the exercise - is that the mass distribution of the fragments in the whole system approximates that of the first piece injected (right hand fragment). Since this is also what was found experimentally, it can be said that the data in Figure 5.1 are at least consistent with the first-piece-only injection model. However, since it had become apparent by this time that this approach would not permit an unequivocal distinction to be made between the two theoretical modes of injection (because of unknown amounts of intracellular degradation of phage RNA, and because of the inability of the gel electrophoresis system to resolve the RNA fragments completely), this avenue of investigation was not pursued further. As described in what follows, other approaches were found to resolve this problem more satisfactorily.

(b) The Relationship Between Phage Infectivity and the Amount of Penetrated RNA.

Figure 3.2. A comparison of the mass distributions of the total fragments produced in a system simulating a first-order injected process.

The system used to simulate the distribution of fragments produced when 500 RNA strands each with a length of 33 nucleotides are subjected to an average of  $x$  breaks is as follows.

(i) A matrix of 500 vectors, each with a length of 33 units of target sites is set up to simulate the RNA population. Each vector is oriented with the right side representing the 3' end of the RNA.

(ii) A computer random number generator is used to obtain a random integer  $n$  ( $1 \leq n \leq 500$ ). This number represents the particular strand receiving a "hit".

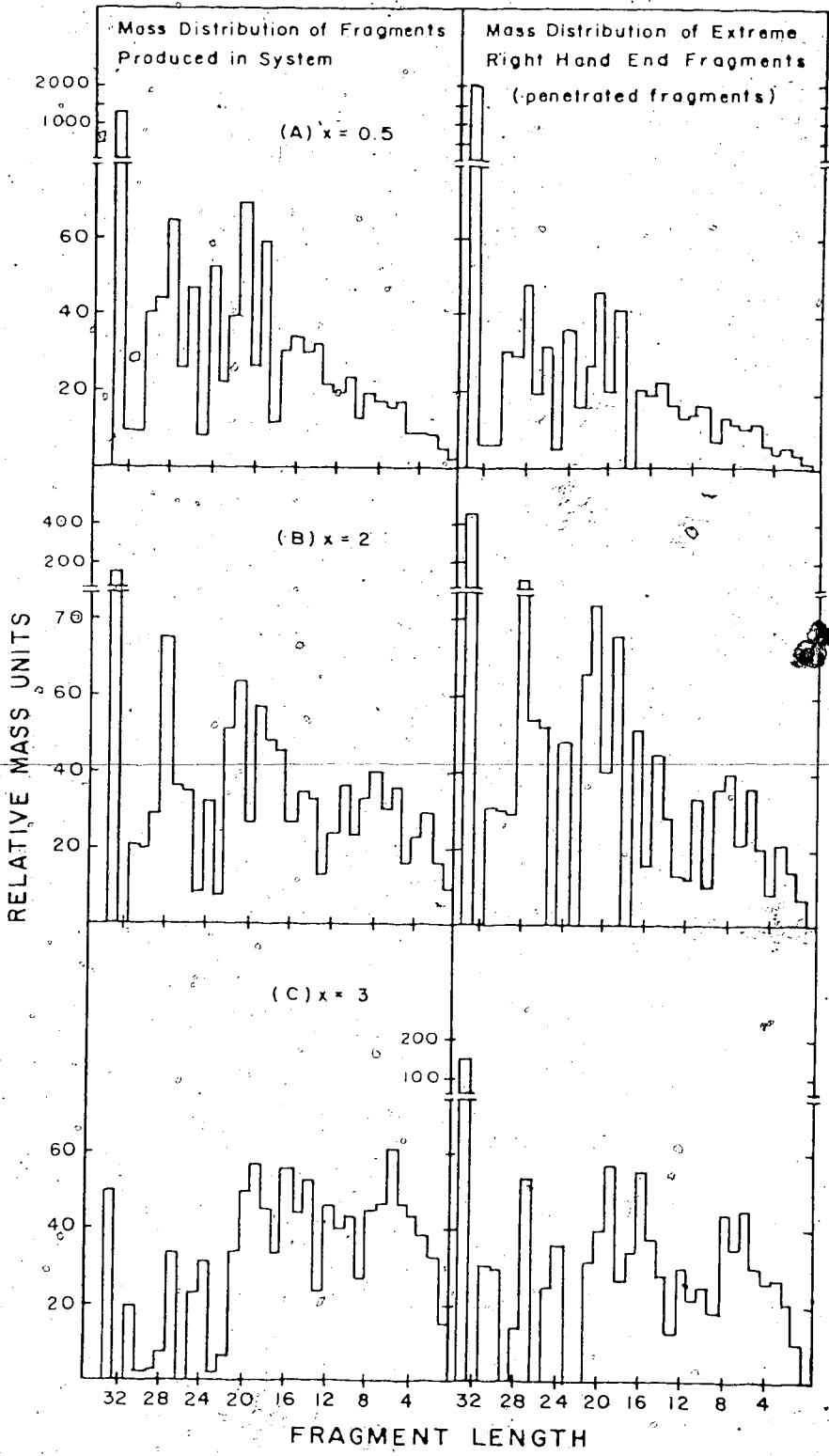
(iii) A new random number  $m$  ( $1 \leq m \leq 32$ ) is generated to represent the site on the strand that is cleaved. The program is set up so that once a position is "hit" it cannot be "hit" again.

(iv) The procedure is independently repeated 500 times.

(v) The 500 ( $x \cdot 1$ ) fragments produced in the system are "measured" and tabulated by the computer. The number of fragments of a particular length formed (33 types of fragments are possible) are expressed as a percent of the total number of fragments generated in the system.

(vi) A separate tabulation of the extreme right hand fragments containing the original 3' end is made. There are always 500 such fragments and this subset of fragments includes all intact or uncut strands.

(vii) In the figure the mass distributions are obtained by plotting the relative mass units ( $C$  composition times length) against the unit length of each type of fragment. (a)  $x=0.5$ , (b)  $x=2$ , (c)  $x=3$ .



As Figure 5.1 qualitatively shows, the amount of parental phage RNA recovered from infected cells declines as the infectivity of the phage decreases. This is shown in a more quantitative manner in Figure 5.3, which illustrates the kinetics of RNA penetration with time of incubation; as anticipated, the amount of penetrated RNA decreases with decreasing infectivity. Furthermore, the relative difference in the amount of RNA injected into cells by the three phage preparations examined was maintained throughout the experimental time period employed.

Subsequently, the relative amount of RNA penetration as a function of the infectivity of the infecting phage preparations was investigated in more detail. In addition, analogous studies were carried out with freshly purified,  $^3\text{H}$ -histidine-labeled phage which had also been treated with ascorbate- $\text{Cu}^{2+}$ . A series of phage stocks thus generated were used to determine the effect of ascorbate- $\text{Cu}^{2+}$  treatment on A protein penetration. The results of these experiments are shown in Figure 5.4. Note that the amount of RNA injected into cells by phage samples has been expressed as a percentage of the amount injected by the untreated preparation (PFU/particle = 1/8), which was assumed to have no breaks in its RNA. Additionally, the ratio of the infectivity (PFU/particle) of a particular phage sample to that of the untreated control was used to obtain the value  $F_s$ , the surviving fraction after ascorbate- $\text{Cu}^{2+}$  treatment. For ease of later analysis, the percent penetration of A protein or RNA has been plotted against the negative log value of  $F_s$  in Figure 5.4.

Clearly, the results show that the relative amount of A protein transported into cells remained constant over a  $10^6$ -fold range of phage

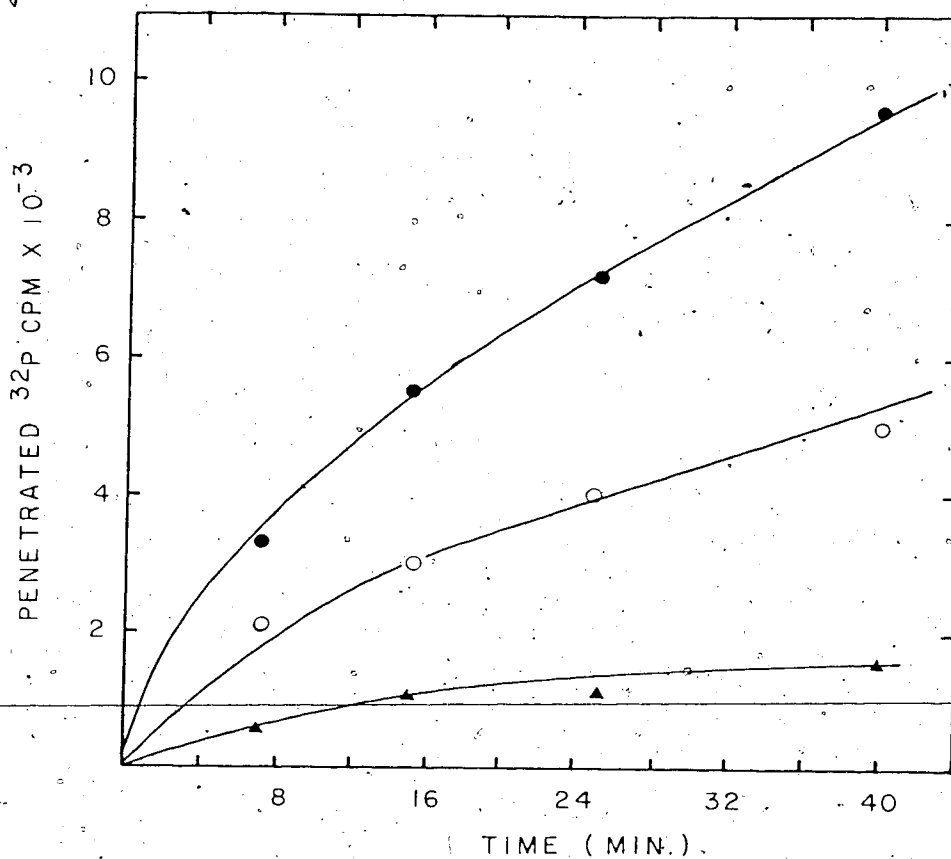


Figure 5.3 The kinetics of RNA penetration of ascorbate-Cu<sup>2+</sup> inactivated R17 phage.

WP156 bacteria at  $4 \times 10^8$  cells/ml (100 ml, CTMM+aa) were infected at a MOI of 1000 particles/cell with <sup>32</sup>P-labeled R17 phage. At different time intervals post infection, 25 ml aliquots were poured onto 12 ml frozen TMM-Mg for quick chilling. The infected cells were washed 6X with cold TMM-Mg<sup>2+</sup> and the volume of all suspensions adjusted to give the same A<sub>650</sub> reading. Three, 1.0 ml aliquots from each sample (about  $4 \times 10^8$  cells) were assayed for radioactivity with 10 ml Scinti Verse. PFU/particle of infecting phage: (●-●) 1/10, (○-○) 1/1200, (▲-▲) 1/1x10<sup>6</sup>.

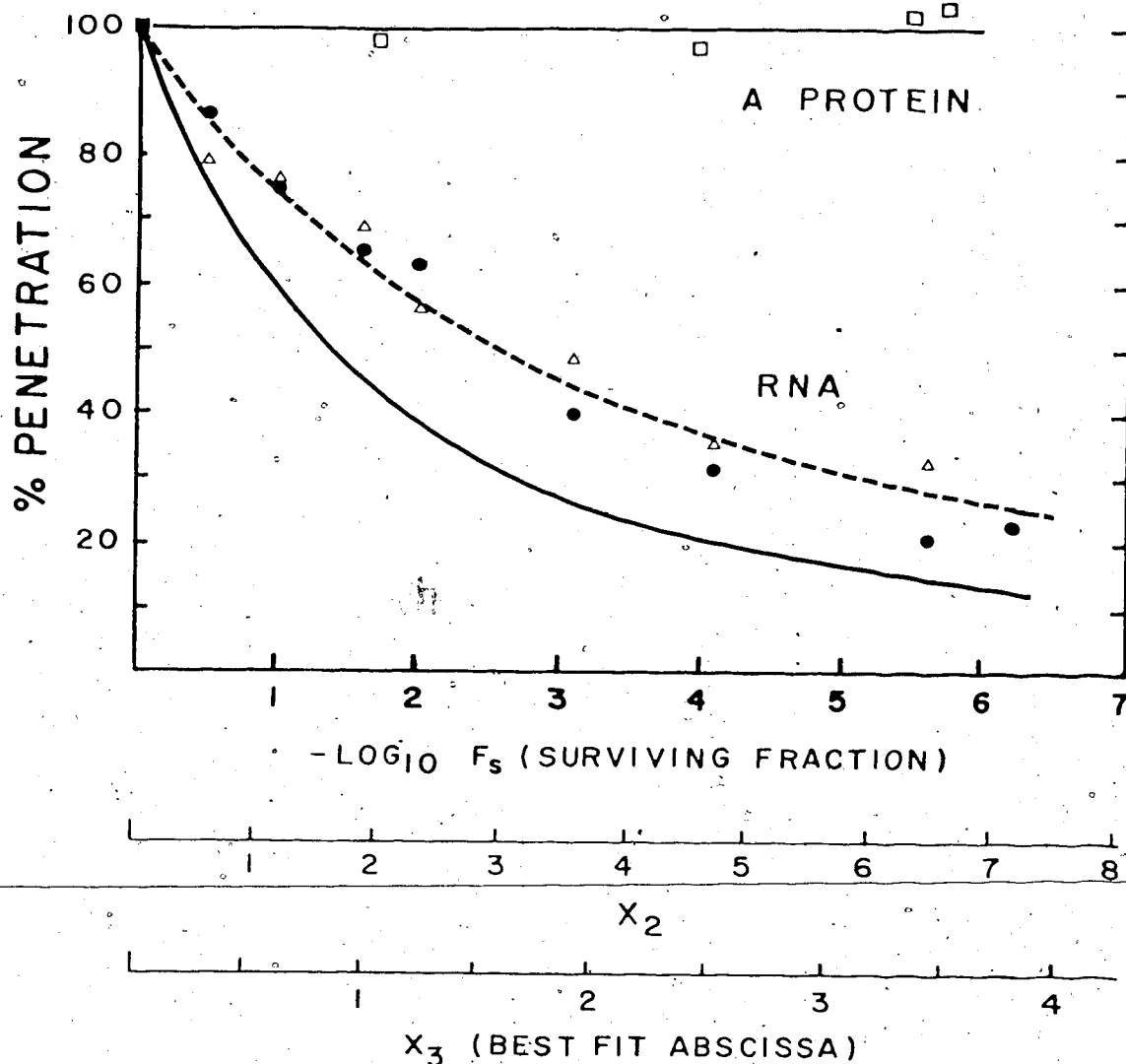


Figure 5.4 The relationship between the amount of RNA or A protein penetration and the infectivity of ascorbate-Cu<sup>2+</sup> treated R17 phage.

A culture of *E. coli* WP156 at  $4 \times 10^8$  cell/ml (in CTMM+aa) was partitioned into 25 ml aliquots and each in turn was infected with <sup>3</sup>H-guanosine-labeled or <sup>3</sup>H-histidine-labeled R17 phage inactivated to a particular PFU/particle value by ascorbate-Cu<sup>2+</sup> treatment. At 10 min post-infection, cells were chilled and washed 6X with TMM-Mg<sup>2+</sup> as described in Figure 5.3. The amount of RNA penetrated was determined by assaying, in triplicate,  $4 \times 10^8$  cells infected with <sup>3</sup>H-guanosine-labeled phage with Scinti Verse. The amount of penetrated A protein was determined by applying  $10^9$  cells infected with <sup>3</sup>H-histidine-labeled phage onto paper discs and treating the discs with hot TCA before radioassay was carried out. The amount of A protein or RNA penetration was expressed as a percentage of the value obtained with the ascorbate-Cu<sup>2+</sup> untreated phage control (PFU/particle ratio = 1/5). (□-□) A protein penetration, MOI = 10<sup>2</sup> part/cell; RNA penetration: (●) MOI = 100 particles/cell, (Δ) MOI = 800 particles/cell; (—) theoretical curve obtained on the premise that one strand break is introduced per 2 lethal hits; (---) best fit theoretical curve (see text for details).



infectivities, while the amount of penetrated RNA decreased in a non-linear manner. In this and other experiments, the percent reduction in RNA penetration was found not to vary with MOI's between 10 to 1000 particles/cell. These observations are consistent with a model that suggests that the A protein penetrates independently of the RNA, or with the "tail model" which envisages the A protein to be physically linked to phage RNA and to be responsible for "pulling" intact RNA or fragments of RNA into the host cell. Since the latter model predicts that the A protein precedes the RNA in cell entry, the amount of penetrated A protein would be independent of the state of fragmentation of the RNA. In this respect, the results given in Figure 5.4 are consistent with the earlier finding (discussed in Chapter III) that A protein penetration is unaffected by the degradation of exposed viral RNA by ribonuclease in the medium.

---

## 2. Evidence for the Preservation of Secondary Structure in Penetrating RNA

In a system such as the R17 phage where physical breaks have been introduced into a linear, single-stranded RNA molecule, a mathematical equation can be derived to relate the amount of penetrated RNA to the average number of breaks introduced per strand if RNA penetration follows the first-piece-only model. Assuming that (a) the breaks are distributed randomly along the length of the RNA molecule and (b) that they are also distributed randomly among the molecule population, the fraction,  $P$ , of RNA injected by a phage population possessing an average of  $x$  breaks per genome as compared to the amount injected where  $x = 0$ .

is given by equation (10) (Sharp and Freifelder, 1971):

$$P = (1 - e^{-x})/x \quad (10)$$

The trend followed by the reduction in RNA penetration versus infectivity was compared to this mathematical model as follows. Firstly, a correct relationship between the surviving fraction,  $F_s$ , and  $x$ , the average number of breaks per RNA that could result in strand separation, must be determined. From the Poisson distribution function, the surviving fraction  $F_s$  is given by  $F_s = e^{-x_1}$ . Here  $x_1$  is defined as the average number of fatal lesions received by each potentially infectious phage. In the case of  $\cdot\text{OH}$  radical attack on phage, these lesions are confined mainly to the RNA and are manifested in the form of strand scissions or base alterations. Furthermore, results presented in Chapter IV indicate that at least one strand scission is produced for every 2 lethal "hits" (lethal hits may also arise from base alterations).

If it is assumed that the phage RNA unravels and issues linearly from the capsid during the RNA ejection step, then every break, regardless of location, should lead to the separation of the resultant fragments. Given these conditions, the average number of breaks,  $x_2$ , per RNA would be given by:

$$x_2 = -(0.5) (2.3) \log F_s \quad (11)$$

By substitution in equation (10), a theoretical function of the form:

$$P = (1 - e^{-x_2})/x_2 \quad (12)$$

was plotted in Figure 5.4. It is evident from a comparison of this theoretical curve with the experimental points that the two are not superimposable. However, it was found that the experimental points best fit a theoretical curve specified by:

$$P = (1 - e^{-x_3})/x_3 \quad (13)$$

where  $x_3 = -(0.26) (2.3) \log F_s$ ; i.e., the experimentally obtained relationship between the amount of penetrated RNA versus phage infectivity reflects a situation where one out of 3.8 fatal lesions (or approximately 1 out of 2 strand breaks) constitutes a lethal break that gives rise to strand separation.

It becomes evident, from a comparison of the theoretical predictions and the experimental results, that not every break necessarily gives rise to strand separation. This is inconsistent with the premise that the phage RNA is ejected or pulled out of the capsid in a linear fashion, but suggests a new hypothesis in which phage RNA would uncoil only partially during ejection and penetration, and retain some of its secondary structure in the form of intra-chain base pairing. Scissions located in single-stranded regions or regions that become single-stranded during RNA penetration would cause separation of fragments, while

---

scissions located within base-paired regions would not, since the potential fragments would be held together by intra-chain hydrogen bonding. Such breaks would be expected to enter cells as "hidden" breaks.

Since equation (10) is based on the assumption that every unit in a linear strand has an equal chance of being cleaved and since the experimental results in Figure 5.4 are consistent with this function, it can further be concluded that the regions in R17 RNA which can give rise to breaks that lead to strand separation are probably spaced approximately equidistant from each other and are equally accessible to  $\cdot OH$  radical attack. In contrast to the foregoing, a biphasic mode of penetration would have been obtained in the plot of percent RNA penetration versus phage infectivity, if susceptible target sites were clustered

in one half of the RNA molecule, or in certain "hot spots". Under this hypothetical situation an initial rapid rate of decrease in RNA penetration would correspond to strand separation occurring primarily at the "hot spots", while a second slower rate of decrease would be seen at other points along the proximal end of the RNA cleaved.

The results of the foregoing experiment were therefore interpreted as being consistent with the first-piece-only injection model, providing the qualification is made that only about 50% of the breaks introduced into the phage RNA give rise to the separation of resultant fragments during the enjection process.

### 3. Characterization of the Structural Integrity of Penetrated RNA

The preceding analysis of the relative amounts of RNA injected by phage preparations of differing infectivities predicts that hidden

breaks will be found in the heterogeneous population of phage RNA fragments recovered at early times from infected cells. This prediction can be verified by analyzing the recovered fragments under denaturing and normal conditions of gel electrophoresis. The rationale is that, under denaturing conditions, fragments formerly held together by base-pairing will be separated and a shift toward lower weight-average molecular weight values should be seen for a given set of fragments.

Such an experiment was carried out as described below.

A  $^{32}\text{P}$ -labeled phage preparation was subjected to the ascorbate- $\text{Cu}^{2+}$  treatment (PFU/particle  $\times 10^6$ ), then used to infect host bacteria for 5 min at a multiplicity of 1000 physical particles/cell.

Following the removal of extracellular phage as described in Materials and Methods, the penetrated RNA was isolated by phenol-SDS extraction, then analysed by polyacrylamide gel electrophoresis under benign and denaturing (8M urea, 60°) conditions as described in Materials and Methods. In both instances, undegraded, <sup>3</sup>H-labeled 28S phage RNA was included as an internal marker. The results are shown in Figure 5.5.

Panel A in Figure 5.5 shows the size distribution of the penetrated RNA under non-denaturing conditions. It may be seen that a significant fraction of the RNA behaves as intact 28S RNA, and that the smallest RNA fragments migrated about 3/4 of the distance along the acrylamide gel column. As seen in panel B, on the other hand, electrophoresis of the penetrated RNA under denaturing conditions resulted in a marked decrease in the amount of 28S RNA, and a marked increase in the amount of small RNA fragments migrating towards the very end of the gel. It is to be noted that similar results were obtained with other phage preparations having higher and lower PFU/particle ratios. From these observations it was concluded that "hidden" breaks do exist in the penetrated RNA and that they are probably stabilized by intra-chain base-pairing. It follows from this that phage RNA probably retains some of its secondary structure during its ejection from the virion and subsequent transfer into the host bacterium.

#### 4. Characterization of Partially Empty Capsids

Although the foregoing observations are all consistent with the concept that partial RNA injection occurs when phage preparations

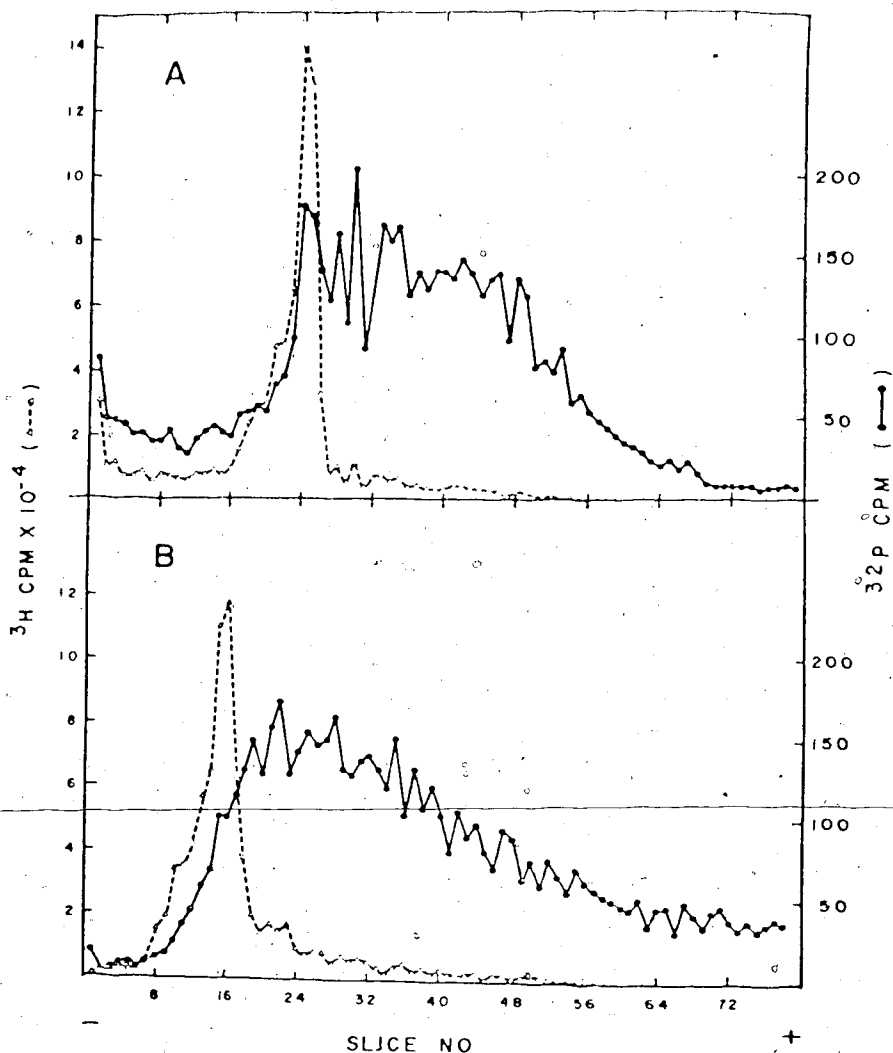


Figure 5.5 Analysis of penetrated phage RNA by polyacrylamide gel electrophoresis under non-denaturing and denaturing conditions.

A  $^{32}\text{P}$ -labeled phage preparation was subjected to ascorbate  $\text{Cu}^{2+}$ -treatment (PFU/particle ratio =  $1.7 \times 10^{-6}$ ), then used to infect a log-phase culture of *E. coli* WP156 ( $4 \times 10^8$  cells/ml) for 5 min at a multiplicity of  $10^3$  particles/cell. Following the removal of extracellular phage as described in Materials and Methods,  $^3\text{H}$ -guanosine labeled R17 (PFU/particles = 1/10) was added to the washed cells and total RNA extraction carried out by SDS phenol. The isolated RNA was analyzed in (A) uniform phosphate-buffer gels at  $4^\circ$  and in (B) 8M urea gels at  $60^\circ$  as described in Materials and Methods.

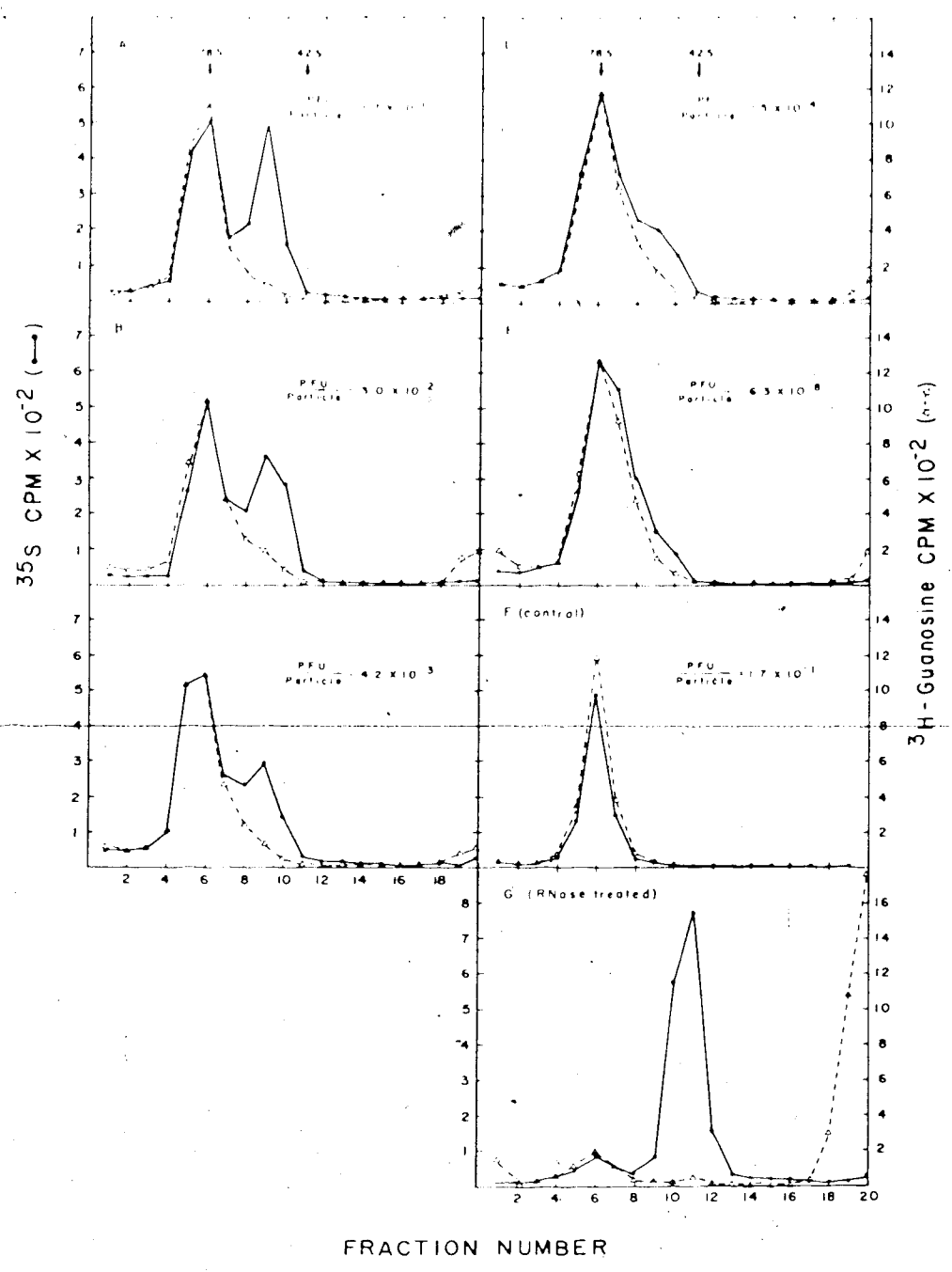
containing fragmented genomes are used to infect cells, a further experiment was designed to provide additional evidence supporting this mode of RNA penetration. The experiment was based on the expectation that partial injection of RNA would result in the formation of partially empty capsids which should be separable from intact or completely empty virions by sucrose density gradient centrifugation techniques. A purified phage preparation labeled in the capsid proteins with  $^{35}\text{S}$  and in the RNA with  $^3\text{H}$ -guanosine was subjected to ascorbate- $\text{Cu}^{2+}$  treatment to produce phage preparations having PFU/particle ratios ranging from  $1.7 \times 10^{-1}$  (untreated control) to  $6.3 \times 10^{-8}$ . Each phage preparation was exposed to sensitive bacteria for 40 min at  $37^\circ$  at a multiplicity of 100 physical particles/cell (these conditions were chosen to maximize the formation of partially empty capsids). After removal of cells from the medium by centrifugation, the supernatant solution was concentrated by Amicon ultrafiltration and subjected to sucrose density gradient centrifugation. The collected fractions were counted for  $^{35}\text{S}$  and  $^{32}\text{P}$  radioactivity, and the results were plotted as shown in Figure 5.6.

Panel F in Figure 5.6 shows the radioactive profile obtained with intact phage particles (at all PFU/particle ratios used) which had not been exposed to host bacteria. Panel G shows the profile obtained when each of the phage preparations exposed to host bacteria were subsequently treated with pancreatic ribonuclease. This treatment resulted in the complete degradation of phage RNA in about 90% of the particles to give rise to completely empty 42S capsids and highly degraded phage RNA. The small fraction of RNase-resistant particles remaining in the 78S position represents the class III particles which have been shown

Figure 5.6 Sucrose gradient analysis of ascorbate-Cu<sup>2+</sup>-treated R17 phage particles following incubation with host bacteria.

Freshly purified <sup>3</sup>H-guanosine labeled phage (PFU/particle = 1/5) and <sup>35</sup>S-labeled phage (PFU/particle = 1/6) were combined together to give <sup>35</sup>S-cpm/<sup>3</sup>H-cpm ratio of about 0.5; the mixture was treated with ascorbic acid and Cu<sup>2+</sup> as described in Materials and Methods to prepare phage populations possessing the PFU/particle ratios given in the figure. The phage preparations were then used to infect 100 ml log-phase cultures of *E. coli* WP156 (4 x 10<sup>8</sup> cells/ml) in CTMM (+0.05% casamino acids) at a MOI of 100 particles/cell. After incubating the cultures for 40 min at 37°, the cells were chilled and pelleted by centrifugation. The remaining supernatant solutions were concentrated by Amicon ultra-filtration, after which 0.2 ml of each concentrate was subjected to sucrose gradient sedimentation analysis. Centrifugation was carried out at 45,000 rpm (SW50.1 rotor) for 80 min at 4°, and 15 drop fractions collected and assayed with Scinti Verse. Panels A-E show the radioactive profiles of phage particles remaining in the culture medium following exposure of each of the phage preparations to host bacteria. Panel F shows the radioactive profile obtained with intact particles which had not been exposed to host bacteria. Panel G shows a typical profile obtained when each of the phage preparations exposed to host bacteria was in turn incubated with pRNase (100 µg/ml) for 30 min at 37°.





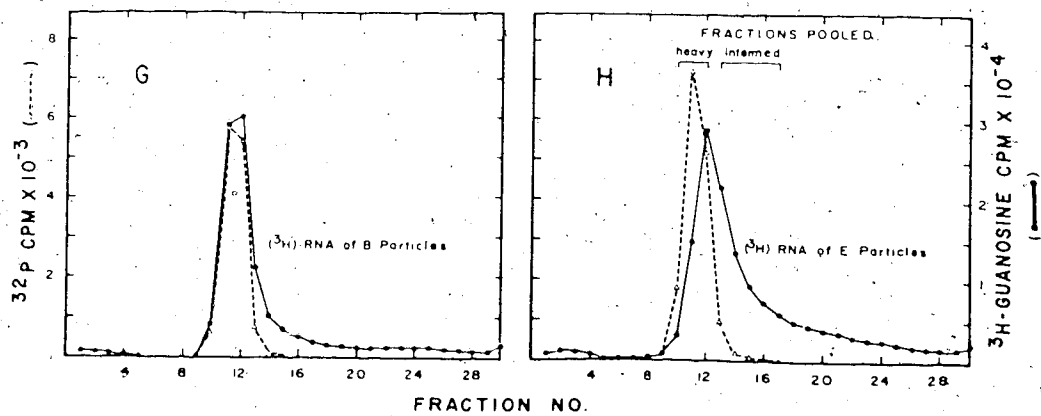
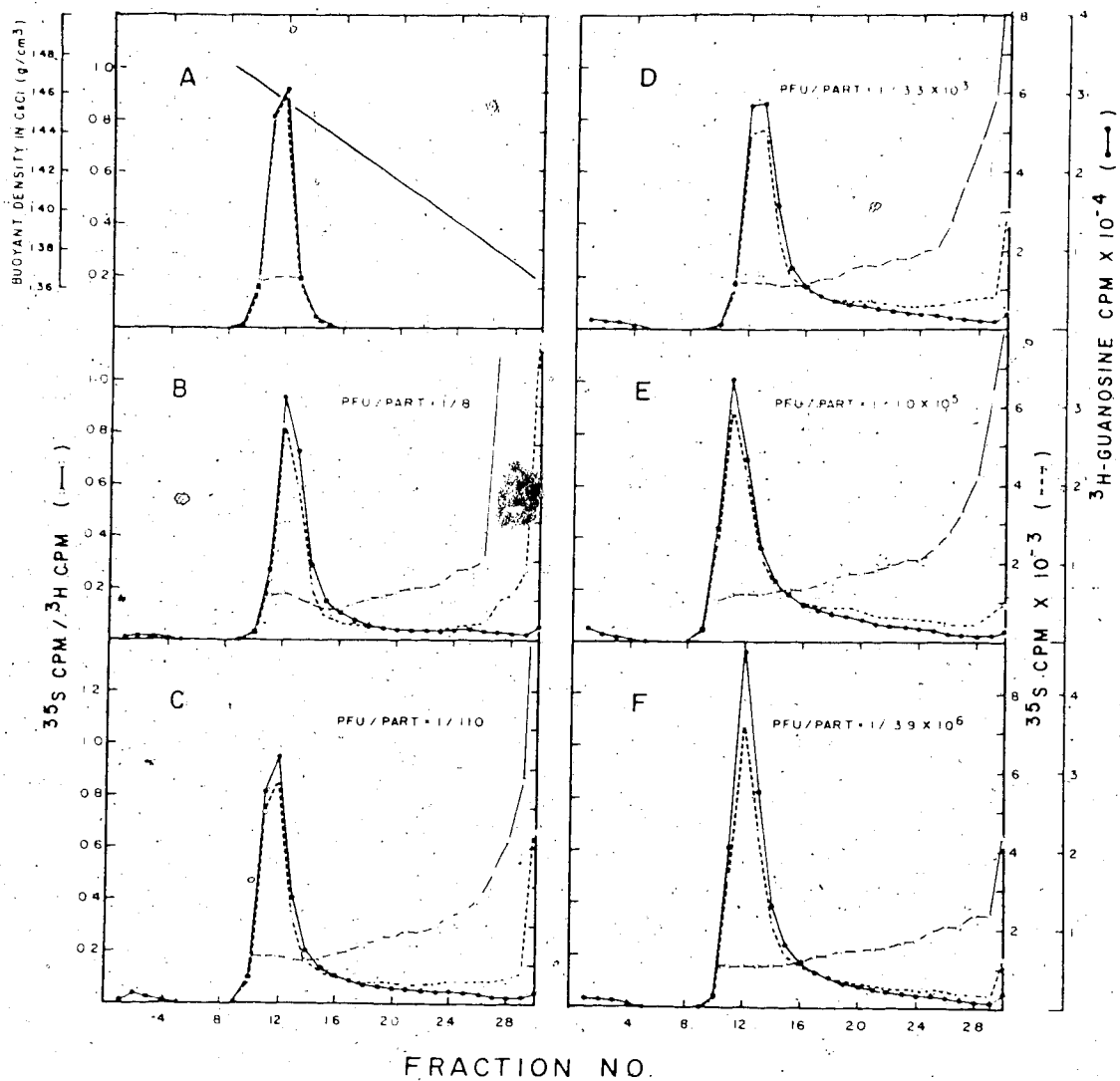
FRACTION NUMBER

to lack the A protein (Friedberg, Parmschick, 1971). It must be noted that phage particles become sensitive to ribonuclease treatment only after having been exposed to heat-labile proteinase (Friedberg et al., 1970). Panel A-F in Figure 5.6 shows the radioactivity profiles of the phage particles remaining in the culture media after exposure of each of the phage preparations to heat-labile proteinase (RNase). On visual inspection of the  $^{35}\text{S}/^3\text{H}$  ratio of each fraction, it may be seen that partially empty capsids were produced under these conditions, and that the amount of RNA remaining in the partially empty capsids increased with decreasing levels of infectivity. In other words, as the PFU/particle ratio decreased from  $1.7 \times 10^{-1}$  to  $0.3 \times 10^{-8}$ , the average sedimentation coefficient of the slower-sedimenting capsids gradually shifted towards the 78S value, while the ratio of  $^{35}\text{S}/^3\text{H}$  counts gradually decreased. Moreover, it is evident from the differing ratios of  $^{35}\text{S}/^3\text{H}$  radioactivity within each region of slower-sedimenting particles that the partially empty virions display considerable heterogeneity with respect to their RNA content. The preceding observations are, therefore, consistent with the partial injection model of RNA penetration, and provide further evidence that the average size of the penetrating RNA fragments decreases as the number of breaks per RNA genome increases.

The foregoing experiment was also carried out using CsCl density gradients to analyze the partially empty capsids. The rationale for examining the isolated phage particles in CsCl gradients was based on the fact that a different physical parameter is measured by this technique. Sucrose gradients separate particles

Figure 5.7 CsCl isopycnic analysis of ascorbate-Cu<sup>2+</sup> treated R17 phage particles following incubation with host bacteria.

An experimental protocol identical to that described in Figure 5.6 was followed except that CsCl gradient equilibrium centrifugation was carried out after 2.4 g of CsCl was dissolved in 4.0 ml of concentrated supernatant. Equilibrium centrifugation was carried out at 5° and 35,000 rpm using the SW50.1 rotor. At the end of 18 hours, the cellulose nitrate tubes were pierced at the bottom with a hollow needle and 12 drop fractions were collected into scintillation vials containing 1.0 ml H<sub>2</sub>O. Radioassay for <sup>35</sup>S and <sup>3</sup>H radioactivity was determined after the addition of 10ml Scinti Verse to each fraction. (A) phage particles before being exposed to sensitive bacteria, (B-F) phage particles in supernatants recovered from infected cultures. (G-H) particles from B and E respectively analyzed with intact <sup>32</sup>P-labeled R17 phage which had not been exposed to cells. Buoyant density in (A) was determined refractometrically.



on the basis of size (MW) and shape (frictional coefficient) while CsCl gradients separate species on the basis of buoyant density. Since the density of the gradients used in this work normally varied from 1.54 g/ml at the bottom to 1.37 g/ml at the top, free RNA which possesses densities usually greater than 1.6 g/ml would band at the bottom of the gradient, while proteins, which as a group possesses densities less than 1.37 g/ml, would be found at the top of the gradient. For R17 phage with a normal buoyant density of 1.46 g/ml, a loss of some protein components may cause a shift toward greater densities while a loss of part of its RNA may result in a shift toward lower densities. It is pertinent to note that altered phage particles may undergo a change in sedimentation velocity but not necessarily in buoyant density (O'Callaghan *et al.*, 1973a; Verbraeken and Fiers, 1972).

The protocol for preparing supernatants for CsCl gradient analysis was identical to that described previously except that a different  $^{35}\text{S}$  and  $^3\text{H}$ -guanosine labeled R17 phage series were used. Equilibrium centrifugation was carried out after CsCl was dissolved in 4.0 ml of concentrated supernatant to give a final solution with a uniform density of 1.42 g/ml.

The results of the radioactive assay of the gradient fractions are illustrated in Figure 5.7. In each gradient, the  $^{35}\text{S}$ -cpm/ $^3\text{H}$ -cpm ratio of each fraction was also plotted. Panel A shows a typical profile of radioactivity for particles of any infectivity before exposure to sensitive cells. Panels B to F display the profiles of the particles recovered from the supernatants of cells infected with phage stocks.

with PFU/particle ratios ranging from  $1/8$  to  $1/4 \times 10^6$ . In situation (B) where cells were infected with phage of optimum infectivity (PFU/particle =  $1/8$ ), about 40% of the phage population had injected all or most of their RNA. These empty capsids are located in the top fractions of gradient B. It may be seen that the remainder of the particles retained all or most of their RNA and banded at a density of 1.46 g/ml. This latter conclusion is more clearly discerned in gradient G where the same particles from B were analyzed with an internal normal phage marker. This large peak is composed mainly of inert Class III particles and Class II particles which had undergone the RNA ejection step, lost their A protein component but which had retained the bulk of their RNA. If panels B to F are scrutinized carefully, it is seen that the data are again consistent with that expected of a partial injection mode of RNA penetration; i.e., as the average number of breaks introduced per genome increases, the fraction of the RNA left in the capsid also increases. Concomitantly the average buoyant density of partially empty capsids underwent a shift from 1.29 g/ml (density of empty capsids) (Hohn and Hohn, 1970) to values near that of intact phage. The presence of partially empty capsids in cell-exposed phage preparations are more easily seen in gradient H where particles from E have been analysed with an intact phage marker. The greater skewing of the RNA peak towards lower densities in H as compared to G is due to the presence of more partially empty capsids in E than in B.

Due to the heterogeneity of the size of the RNA fragments injected, partially empty capsids of all intermediate densities should be found in every gradient except perhaps B where the majority of particles injected only intact 28S RNA. The mass distribution of partially empty capsids would thus depend on the infectivity of the parental phage. The above statement is also supported by the pattern of the  $^{35}\text{S}/^3\text{H}$  ratios plotted for each sample. These show that the asymptotic nature of the curves is precisely the type expected from an in vivo system in which scissions and strand separations may occur in any number of locations on the single-stranded RNA; i.e., as the size of the RNA fragment retained by the capsid approaches zero, the  $^{35}\text{S}/^3\text{H}$  ratio tends to infinity.

Finally, the low level of  $^3\text{H}$ -radioactivity found at the bottom of the gradients indicates that insignificant amounts of free RNA were released into the medium during cellular infection. This further supports the interpretation that RNA fragments were injected into cells and not released haphazardly from fragmented genomes. It could also be stated with confidence that the RNA banding between the top of the gradient and the position of normal phage must be associated with intact phage capsids and not with capsid subunits because the sucrose gradient results had indicated that the coat protein label sedimented as a homogeneous 42S peak after RNase digestion of any cell-exposed phage sample (Figure 5.6 G).

##### 5. Polyacrylamide Gel Electrophoretic Analysis of RNA Isolated from Partially Empty Capsids.

To further demonstrate that RNA fragments were encapsidated in

particles of intermediate buoyant densities, the fractions from a CsCl gradient such as those delineated in Figure 5.6 H were combined into 2 aliquots and labeled as heavy and intermediate particles. These two fractions were dialyzed and the RNA isolated and analyzed by polyacrylamide gel electrophoresis. The distribution of the RNA isolated from the parental phage (PFU/particle =  $1 \times 10^{-4}$ ) and for the heavy and intermediate particles in a corresponding CsCl gradient are plotted in panels A, B and C in Figure 5.8 respectively. Since the heavy particles possessed a density similar to that of the parental phage, they were each expected to encapsidate a full complement of RNA and yield the same set of fragments upon separation of the isolated RNA by gel electrophoresis. This is shown by the profiles of radioactivity illustrated in A and B. The intermediate particles on the other hand were of lower densities and should contain a preponderance of RNA fragments. In panel C, the amount of intact 28S phage RNA is much reduced as compared to that observed in A and B, and a definite bias toward smaller RNA fragments is displayed by the distribution shown. This finding, therefore, strengthens the concept that many of the phage particles of intermediate densities had undergone partial ejection of their genomes.

#### 6. Evidence for the Loss of Coat Protein Subunits from Eclipsed Particles

The ratio of  $^{35}\text{S}/^3\text{H}$  radioactivity in intact phage preparations (prior to interaction with host cells) employed in the experiments described in Figure 5.7 was found to be 0.19. Upon interaction with cells,



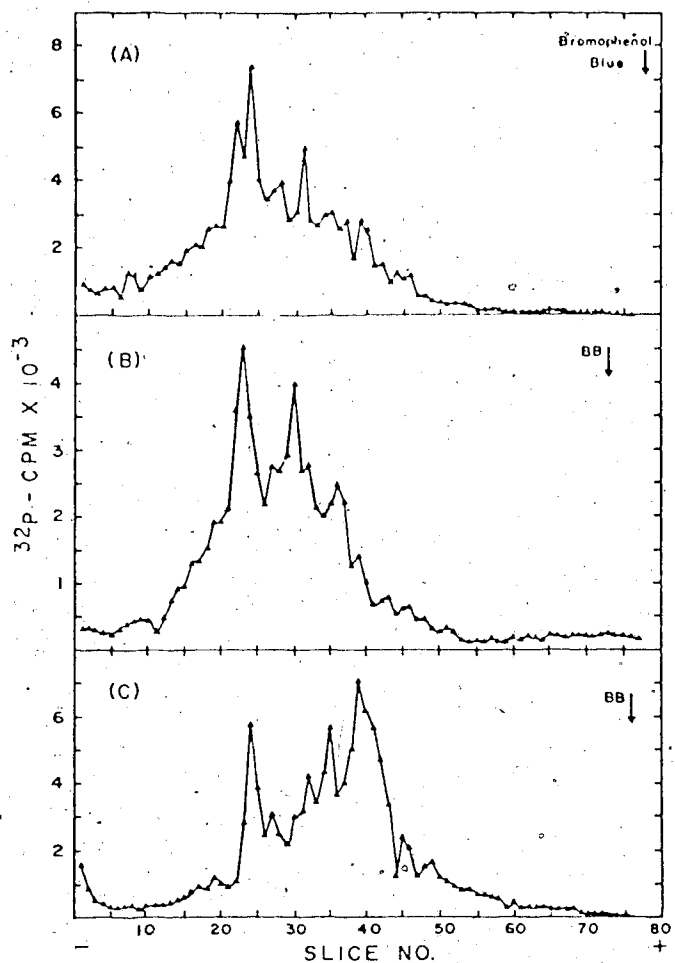


Figure 5.8 Polyacrylamide gel electrophoresis of RNA isolated from particles banding in heavy and intermediate regions of a CsCl gradient.

*E. coli* WP156 cells ( $4 \times 10^8$  cells/ml) in CTMM + 0.05% casamino acids (total volume = 1.2 l) were infected with  $^{32}\text{P}$ -labeled phage (PFU/particle =  $1 \times 10^{-5}$ ) at a MOI of  $10^2$  particles/cell for 40 min. After bacteria were removed by centrifugation, the supernatant was concentrated to about 10 ml and 4.0 ml were subjected to CsCl gradient equilibrium centrifugation as before. The fractions corresponding to the heavy and intermediate regions of the gradient (similar to the positions delineated in Figure 5.7 H) were pooled and dialyzed against 0.01 Tris (pH 7.3), 0.01 M KCl, and 0.005 M  $\text{MgCl}_2$ . About  $10^{14}$  unlabeled phage particles were added to each dialyzed sample as carrier and RNA extraction was carried out. The isolated phage RNA was analyzed in exponential gradient gels as described in Materials and Methods. (A) Profile of RNA fragments isolated from the phage preparation prior to cell exposure. (B) Profile of RNA isolated from cell-exposed particles banding in the "heavy" region of the CsCl gradient. (C) RNA profile of cell-exposure particles banding in the "intermediate" region of the CsCl gradient.

as much as 40% (in the case of untreated phage) of the RNA is injected and this leads to an increase of the overall ratio of  $^{35}\text{S}$ -cpm/ $^3\text{H}$ -cpm in the phage population recovered in the supernatant to approximately 0.28. The increase in the case of ascorbate- $\text{Cu}^{2+}$ -treated phage is somewhat less depending on the amount of RNA injected. Since it was generally believed that no coat protein is lost from virions during the injection process (Edgell and Ginoza, 1965), it was anticipated that the ratio of  $^{35}\text{S}/^3\text{H}$  radioactivities would never fall below the value of 0.19 found with intact phage. However, as may be seen in Figure 5.7B through 5.7F, the  $^{35}\text{S}/^3\text{H}$  ratio of the cell-exposed phage particles banding at or near a density of  $1.46 \text{ g/cm}^3$  was consistently lower than the anticipated value of 0.19 (values ranged from 0.16 to 0.18). This implied that part of the phage capsid had disappeared from the virion, and suggested that some coat subunits may dissociate from the virion during the RNA ejection step of the infectious process. It is to be noted that some  $^{35}\text{S}$ -radioactivity is removed from the phage particles as a result of the ejection of  $^{35}\text{S}$ -labeled A protein. However, this represents approximately 0.5% of the  $^{35}\text{S}$ -radioactivity and is therefore of minor importance in the foregoing considerations.

Since the possibility of coat protein loss during RNA injection represented a significant departure from the accepted point of view, additional experiments were carried out to examine this apparent new phenomenon in a more quantitative manner. The experiment described in Figure 5.7 was expanded to include an analysis of the  $^{35}\text{S}/^3\text{H}$  ratios in the overall phage population remaining in the culture medium after re-

removal of infected cells, but prior to fractionation of the phage by CsCl density gradient centrifugation. The results of this portion of the experiment are shown in Table 5.1

The  $^{35}\text{S}/^3\text{H}$  ratios of each of the phage suspensions B to F can be calculated from the equation:

$$(^{35}\text{S}/^3\text{H})_{\text{B-F}} = \frac{a}{1 - bP_{\text{B-F}}} \quad (14)$$

Here "a" represents the  $^{35}\text{S}/^3\text{H}$  ratio which would be obtained if phage particles having interacted with sensitive bacteria did not inject any RNA. Thus, in the case where no coat protein is lost "a" would be equal to 0.19. On the other hand, in the case where 10% of the coat protein is lost, "a" would be equal to 0.17. "b" is the fraction of the overall RNA injected into cells by phage with undegraded genomes (supernatant B). For example, the value "b" was determined by calculating the fraction of the total  $^{35}\text{S}$  radioactivity that had banded in the top 5 fractions of gradient B in Figure 5.7. It was found that 0.40 of the total coat label can be considered to exist in the form of empty capsids indicating that 40% of the total RNA in the particles recovered in supernatant B had been injected into cells. P represents the amount of RNA injected by a phage sample (derived from ascorbate- $\text{Cu}^{2+}$  treatment) and expressed as a fraction of the amount injected by the control (undegraded phage). The fraction, P, for each of the phage stocks used in experiments B to F (Figure 5.7) was obtained for any given  $F_s$  value from the "best fit" theoretical curve shown in Figure 5.4. Column 5 in Table 5.1 lists the theoretical ratios predicted by equation (14). These values were calculated on the assumption that the integrity of the

TABLE 5.1

A Comparison of the  $^{35}\text{S}$ -CPM/ $^3\text{H}$ -CPM Ratios of Cell-Exposed R17 Particles to Their Calculated Values

supernatant (a)	$-\log F_s$ (b)	P- Fraction of RNA injected (c)	$^{35}\text{S}$ -CPM/ $^3\text{H}$ -CPM		
			Observed	Expected if capsids re- main intact	Expected if an av. 10% of each capsid were lost to cell pellet
B	0	1.00	0.28	0.32	0.28
C	1.50	0.66	0.23	0.26	0.23
D	1.93	0.58	0.22	0.25	0.22
E	4.10	0.37	0.20	0.22	0.20
F	5.69	0.28	0.18	0.21	0.19

(a) The letters refer to the supernants obtained under experimental conditions described in Figure 5.7. The  $^{35}\text{S}$  and  $^3\text{H}$ -guanosine radioactivities in R17 phage populations were assayed following interaction with host bacteria and subsequent removal of infected cells from the culture medium by centrifugation.

(b)  $F_s = \frac{\text{PFU/particle ratio of ascorbate-Cu}^{2+} \text{ treated phage}}{\text{PFU/particle ratio of untreated phage}}$

(c) derived from best-fit curve of data presented in Figure 5.4.

phage capsid was maintained throughout the process of RNA penetration ( $a = 0.19$ ). In column 6, the  $^{35}\text{S}/^3\text{H}$  ratios have been calculated on the assumption that 10% of the capsid proteins from each particle had become associated with the cell pellet. A comparison of the calculated ratios with those obtained experimentally indicated that the approximation of a 10% loss of coat protein from the virion was in close agreement with the actual values found. It was concluded, therefore, that the RNA ejection process is probably accompanied by a loss of about 10% of the viral capsid.

#### 7. Polyacrylamide Gel Electrophoresis of Total Proteins Isolated from Cells Infected with $^{35}\text{S}$ -labeled R17

If coat protein subunits were separated from the main capsid structure during RNA ejection and penetration, then they must either be released into the medium or become cell-associated by way of penetration into cells or adsorption to F-pili. Since the sucrose gradients illustrated in Figure 5.5 revealed insignificant amounts of  $^{35}\text{S}$ -label at the tops of the gradients, it was concluded that few coat protein subunits appear to be released into the medium. In an experiment where cells were infected at a MOI of 100 particles/cell with  $^{35}\text{S}$ -labeled phage, then exhaustively washed afterwards,  $^{35}\text{S}$  counts equivalent to 2-3 particles were found to be associated with each cell. In order to distinguish between  $^{35}\text{S}$ -labeled A protein and  $^{35}\text{S}$ -labeled coat subunits, the total proteins of the washed cells were analyzed in SDS polyacrylamide gels. In Figure 5.9, panel A, the  $^{35}\text{S}$ -labeled A and coat proteins from whole particles have been electrophoresed with an

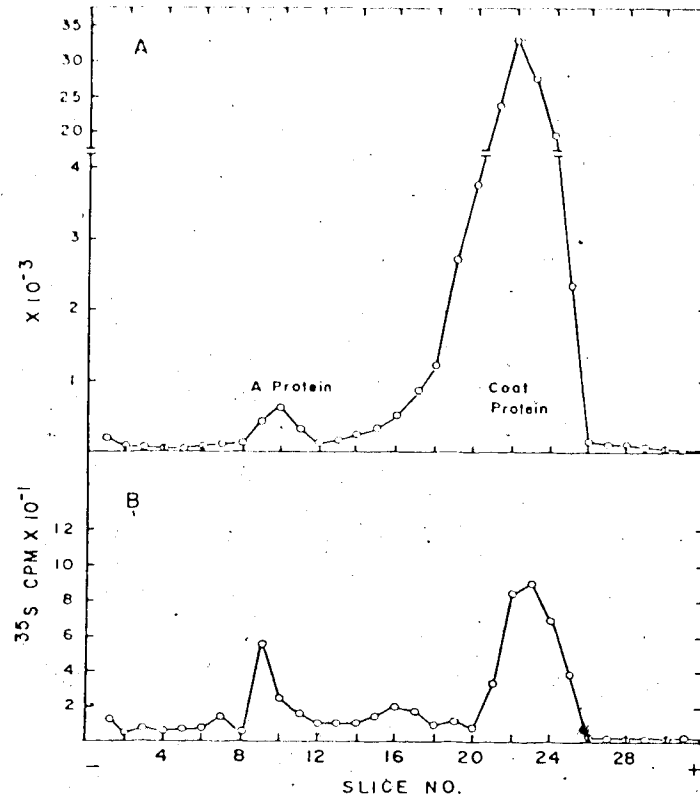


Figure 5.9 Polyacrylamide gel electrophoresis of total proteins extracted from *E. coli* WP156 infected with  $^{35}\text{S}$ -labeled R17 phage.

*E. coli* WP156 cells (in 25 ml CTMM + 0.05% casamino acids) were infected at  $4 \times 10^8$  cells/ml with freshly purified,  $^{35}\text{S}$ -labeled R17 phage at a MOI of 100 particles/cell for 40 min ( $37^\circ$ ). The cells were then chilled and washed 6X with TMM(- $\text{Mg}^{2+}$ ) to remove extracellular  $^{35}\text{S}$ -label as described in Materials and Methods. The final cell pellet was resuspended to a density of  $1 \times 10^9$  cells/ml in a solution containing 0.0625 M Tris-HCl (pH 6.8), 2% SDS, 10% glycerol, 5% 2-mercaptoethanol and 0.001% bromophenol blue. For a control, uninfected WP156 cells were suspended to the same density in the preceding solution and  $^{35}\text{S}$ -labeled R17 phage added to a final concentration of  $4 \times 10^{11}$  particles/ml. The two cells suspensions in pyrex test tubes were then immersed in boiling water for 7 min, cooled and 0.5 ml from each subjected to electrophoretic analysis in the Laemmli gel system. In this application, gels were sliced into fifty, 1.67 mm wide discs and two slices were treated and counted per scintillation vial. The details of the methodology are given in Materials and Methods. (A) Control; (B)  $^{35}\text{S}$ -labeled material from washed, infected cells.

amount of *E. coli* protein equivalent to that included in B. Although some trailing of the coat protein occurred, the A protein peak was adequately resolved from that of the coat. A summation of the counts in the gel showed that the A protein  $^{35}\text{S}$ -radioactivity constituted only about 1% of the total radioactivity in the gel. In panel B, the total proteins from six times washed infected cells were analyzed. It may be seen that about 3/4 of the  $^{35}\text{S}$  radioactivity migrated with the mobility of coat protein molecules; the rest of the  $^{35}\text{S}$ -labeled material found in the gel probably correspond to  $^{35}\text{S}$ -labeled A protein and A protein fragments that were reported by Krahn *et al.*, (1972) to penetrate cells. The implication of this finding is that coat protein subunits appear either to have penetrated into cells infected with phage or to become tightly associated with them. This finding thus provides additional support for the concept that a small amount of coat protein accompanies the RNA and A protein during the ejection step of the infectious process.

#### 8. The Formation of Partially Empty Capsids in Infections Carried Out in the Absence of $\text{Mg}^{2+}$

It is well known that divalent metal ions are required for phage RNA penetration but not for the adsorption and ejection (phage eclipse) steps (Paranchych, 1966). Silverman and Valentine (1969) in turn had shown that in most cases RNA is unable to be ejected from its capsid in cellular infections carried out in the presence of EDTA, although the RNA is rendered RNase sensitive as a result of the interaction of phage with host bacteria. These workers also reported that a small fraction of the input RNA remains bound to the cell, is sensitive to RNase, and is removed from the cell by treatments which remove F-pili. Due to the low levels of radioactivity present in their samples (200-300 cpm's),

they were unable to characterize the desorbed phage particles or cell bound RNA in any great detail. The possibilities were raised, however, that in the absence of divalent metal ions some intact RNA molecules are able to dissociate from capsids or that fragments remain attached to F pili after the desorption of phage. It was decided that further information might be gained by reexamining the phenomenon using the protocol and techniques described earlier for the characterization of partially empty capsids.

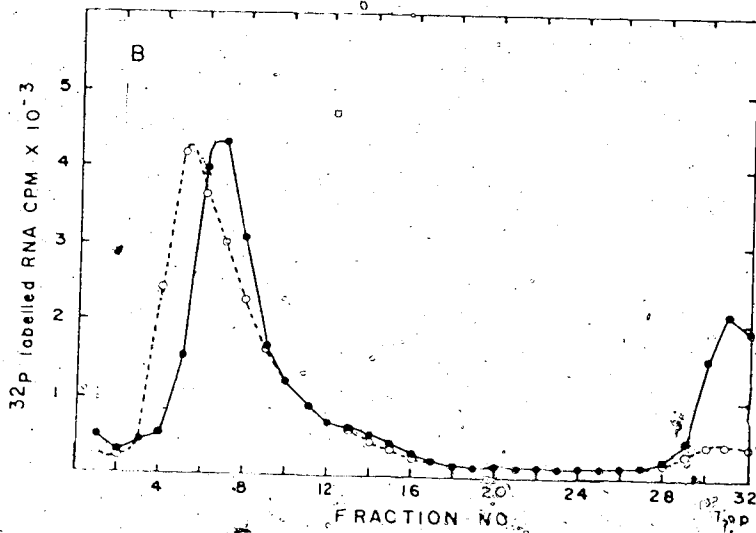
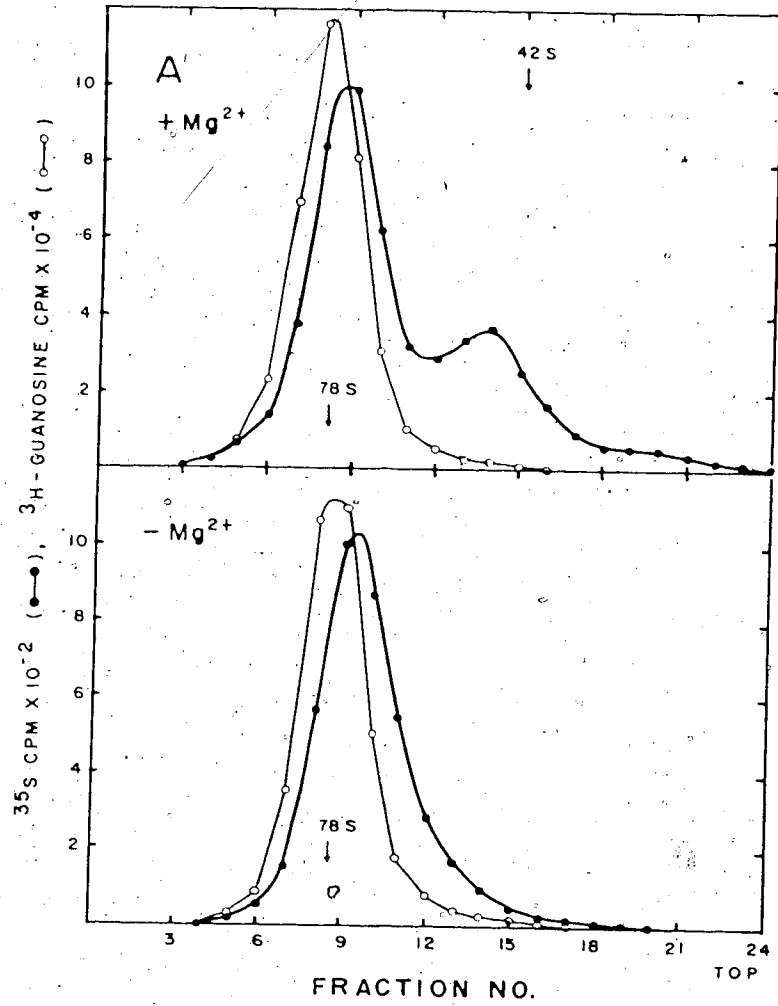
Host bacteria were first incubated for 40 min at 37° with <sup>35</sup>S-labeled R17 phage at MOI of 100 particles/cell in the presence and in the absence of Mg<sup>2+</sup>. After cells were removed by centrifugation, the desorbed particles in the supernatant medium were concentrated by Amicon ultrafiltration and suitable aliquots were analyzed by sucrose and CsCl gradient centrifugation as described in Materials and Methods.

The results of the sucrose gradient analysis are shown in Figure 5.10. Under control conditions in which Mg<sup>2+</sup> ions were present in the medium, the sedimentation pattern of the eclipsed <sup>35</sup>S-labeled particles was similar to the profile given in Figure 5.6 A and to that reported by Paranchych et al. (1970). Not present in the previous examples but included in this control was an internal 78S phage marker which clearly brought out the shift to a lower S value of the main peak. This shift was quite expected since eclipsed Class II particles (the main component in the large peak) are considered to have lost their A protein, some coat monomers and perhaps a fragment of RNA as a result of the RNA ejection process. In the lower panel of Figure 5.10 A, the same infection carried out in the absence of Mg<sup>2+</sup> resulted in the abolition of material sedimenting in the 42S-60S region of the gradient.



Figure 5.10 Sucrose gradient analysis of phage R17 particles exposed to sensitive host bacteria in the absence of free  $Mg^{2+}$

(A) *E. coli* WP156 cells (in 100 ml CTMM-aa) were grown up to  $4 \times 10^8$  cells/ml and EDTA added to a final concentration of 10 mM, five min before phage infection. The cells were infected at a MOI of 100 particles/cell with  $^{35}S$ -labeled phage for 40 min. The + $Mg^{2+}$  control infection was carried out under similar conditions except that EDTA was not included. After cells were removed by centrifugation, and the supernatant concentrated to 10 ml by Amicon ultrafiltration 0.2 ml of the concentrate (containing  $^3H$ -guanosine-labeled phage as a marker) were layered onto a 5-20% sucrose gradient (made up with SSC). Centrifugation was performed at 45,000 rpm (SW 50.1 rotor) at  $4^\circ$  for 1 hr. Collection and radioassay of fractions were carried out as described in Materials and Methods. (B) the experiment was repeated using  $^{32}P$ -labeled R17 phage (●-●). The Amicon concentration step was omitted. (○-○) control: A similar concentration of  $^{32}P$  phage in CTMM-aa was incubated at  $37^\circ$  for 40 min in the presence of 10 mM EDTA but in the absence of cells. Sucrose gradient centrifugation was carried out at 45,000 rpm for 80 min. The figure represents a superpositioning of the results from two gradients.



indicating that little, if any, RNA ejection had occurred. This latter experiment was repeated using R17 phage labeled in the RNA with  $^{32}\text{P}$ . The concentration step involving Amicon filters was omitted to avoid losing any small molecular material. The sucrose gradient results shown in Figure 5.10 B indicates that the exposure of cells to phage in the absence of  $\text{Mg}^{2+}$  results in the release of some RNA fragments which remain at the top of the gradient.

$\text{CsCl}$  density gradient analysis of the above  $^{35}\text{S}$ -labeled supernatants yielded similar and more detailed results as shown in Figure 5.11. As can be discerned in the figure, the number of empty capsids banding in the top 2 to 3 fractions of the gradient is drastically reduced in the infection carried out in the absence of free  $\text{Mg}^{2+}$ . Interestingly, the recovered  $^{35}\text{S}$ -labeled capsids appear to band at densities between 1.46 and 1.40  $\text{g}/\text{cm}^3$ .

The near absence of empty capsids in the minus  $\text{Mg}^{2+}$  supernatants as seen in both types of gradients confirms Silverthorn and Valentine's earlier finding that  $\text{Mg}^{2+}$  or other divalent metal ions are required for the complete uncoating of phage RNA during the ejection process. If the RNA was only partially extruded from phage capsids,  $\text{CsCl}$  results would have shown a single peak banding at the same density as the marker phage. The appearance of particles at intermediate densities (between 1.46 and 1.40  $\text{g}/\text{cm}^3$ ) further indicates that a limited ejection of a varying portion of the viral genome might have occurred in  $-\text{Mg}^{2+}$  infections and that such protruding segments of the RNA were removed either by mechanical shear or by enzymatic activity. It is of interest to note that the distribution of partially empty capsids illustrated in the lower panel of Figure 5.11 very much resembles the distribu-

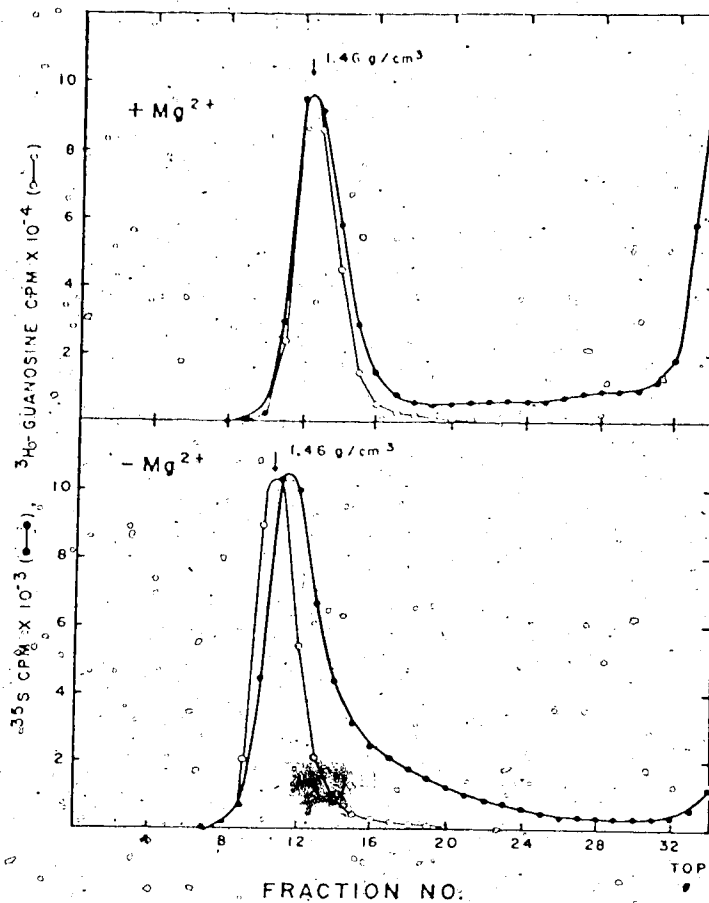


Figure 5.11 CsCl gradient analysis of R17 phage exposed to host cells in the absence of  $Mg^{2+}$ .

Isopycnic analysis of the  $^{35}S$ -labeled phage particles obtained as described in Figure 5.10 A was carried out by dissolving 2.4 g CsCl in 4.0 ml concentrated supernatant (with added  $^3H$ -labeled intact phage) and centrifuging at 35,000 rpm (SW50.1 rotor) at  $4^\circ$  for 18 hrs. The radioassay of collected fractions was performed according to procedures described in Materials and Methods.

tion given in Figure 5.7 H. In the latter experiment, the partially empty capsids were produced as a result of fractional RNA injection; for the ascorbate-Cu<sup>2+</sup>-treated phage in question, the amount of injected RNA is equal to 37% of that injected into cells by an untreated control phage. In contrast, penetration studies showed that the amount of RNA injected in the presence of 10 mM EDTA (MOI = 100 particles/cell) is less than 3% of the amount injected by phage in +Mg<sup>2+</sup> infections. Therefore most of the RNA fragments that are produced in minus-Mg<sup>2+</sup> infections must have remained outside the cell. As shown in Figure 5.10 B some of the fragments were released into the medium while the remainder may have adsorbed to F-pili as reported earlier by Silverman and Valentine, (1969).

### C. Discussion

#### 1. Implications of the Possible Loss of Coat Protein Subunits from the Capsid During RNA Penetration

Although the evidence supporting the hypothesis that some of the coat protein subunits detach from the phage capsid just before or during RNA ejection may not yet be entirely convincing, it does offer certain insights into the behavior of phage RNA under various conditions of infection. Before exposure to sensitive cells, all 3 types of particle in a phage preparation are resistant to RNase. Class III particles remain so even after exposure to cells (Paranchych et al., 1970; Krahn and Paranchych, 1971). If nonpermissive RNase I<sup>-</sup> bacteria are infected with RNA phage containing an amber mutation in the A cistron, defective particles are assembled which lack the A protein component and carry a full size strand of RNA, part of which is protruding from the capsid

(Heisenberg, 1966, 1967; Argetsinger and Gussin, 1966). Incubation with RNase will remove only the protruding piece of RNA while the RNA within the particle remains resistant (Argetsinger and Gussin, 1966; Lodish, 1968a, b). The simplest explanation that can be advanced to account for these phenomena is that RNase molecules cannot pass through an intact phage capsid to degrade the RNA. If the RNA ejection step were to involve the concomitant detachment of a coat protein aggregate such as an IIS unit containing 18 copies of coat protein (O'Callaghan *et al.*, 1973b), then an opening would be created through which RNase molecules could pass. In this way RNA remaining within Class II particles as a result of an abortive RNA ejection event or within Class I particles following partial injection, would be rendered vulnerable to RNase degradation.

One of the early concepts of RNA ejection predicted that the viral RNA unravels and issues forth through a hole in the hexagonal net in a linear manner. However, the results presented here, and those of Lupker and co-workers (1973) have indicated that the RNA retains part of its secondary structure during the ejection process. The presence of folded regions in the RNA would confer a greater cross-sectional area to the emerging RNA which would be incapable of passing directly through the coat protein net. On the other hand, the creation of a large hole in the net as the result of the detachment of an aggregate of coat protein would allow the folded RNA to pass easily through the capsid wall.

## 2. The Implication of Secondary Structure in RNA Penetration

As was pointed out in the introductory chapter, several working models have been advanced to explain the mechanism of transport of both phage RNA and A protein along the F-pilus and into the host cell. The two most obvious possibilities are (a) that the RNA and A protein are in some way transported through a hollow core of the F-pilus, or (b) that the RNA and A protein remain anchored to the exterior surface of the pilus and are transported to the cell surface either by pilus retraction (Novotny & Fives-Taylor, 1974) or sliding filament (Brinton, 1971) mechanisms.

The preceding two possibilities can be distinguished on the basis of a retention or nonretention of secondary structure by the phage RNA during its ejection from the capsid and penetration into the host cell. For instance, the RNA would presumably have to become unravelled into a linear single-stranded structure if it were to pass through a hollow core in the F-pilus, since negatively stained pili appear to have an axial hole or groove about 2.5 nm in diameter (Brinton, 1965; Lawn, 1966). According to this model, a break located in any position in the RNA chain would be expected to result in the separation of RNA fragments during the penetration process. On the other hand, if a significant portion of the RNA molecule retained its secondary structure during the penetration process, this RNA would be expected to remain on the exterior surface of the F-pilus rather than passing through its interior. According to this model, single-strand breaks within base-paired regions of the RNA would be expected to enter the pilus as "hidden" breaks, and to be detectable only after denaturation

of the penetrated RNA.

In view of the results described earlier concerning the presence of secondary structure in penetrating RNA, the model involving the threading of the phage RNA into the lumen of the F-pilus now seems highly unlikely. Initially, the presence of secondary structure in penetrating RNA was indicated indirectly by the mathematical analysis of the kinetics of RNA penetration. Calculations showed that not all breaks necessarily result in strand separation but that about one in two breaks are probably "hidden" or masked by hairpin loops which hold potential fragments together. Subsequent denaturation studies of the penetrated parental phage RNA by polyacrylamide gel electrophoresis in 8 M urea revealed that some hidden breaks do exist in the penetrated RNA and that some fragments are probably stabilized by intra-chain base-pairing.

It is to be noted that these findings are in complete agreement with those of Lupker *et al.* (1973), who showed that the efficiency of killing,  $\alpha$ , of strand breaks arising from the decay of  $^{32}\text{P}$  in highly  $^{32}\text{P}$ -labeled MS2 RNA phage is  $0.60 \pm 0.08$ ; i.e. about 6 out of 10 breaks are lethal. This value of  $\alpha$  is significantly lower than the value of 1.0 (where every break is lethal) expected for a single-stranded bacteriophage, and suggests both that "hidden" breaks are injected into the host cell and that they do not interfere with the replication process. Although our data provide no information as to whether "hidden" breaks are subjected to repair processes in the cell, they do indicate that a significant portion of the RNA genome remains in a folded state during its transfer to the cell. It follows from



this that the RNA and A protein probably remain on the exterior surface of the pilus during the injection process, and it is tempting to speculate that some form of pilus retraction mechanism may be involved in bringing the RNA and A protein to the surface of the cell. Whether or not the F-pilus also promotes the penetration of phage components through the cell membrane remains to be determined in future experiments.

The overall results discussed in this chapter strongly support a first-piece-only or partial injection model of RNA penetration for phage containing breaks in its RNA. The model in a modified form predicts that an RNA fragment, during the process of RNA ejection, separates from the rest of the genome at the first break, proximal to the leading end, that is not protected by intra-strand hydrogen bonding. The kinetics of RNA and A protein penetration as observed for particles with varying average number of breaks per genome, the absence of a substantial amount of free RNA fragments in the supernatant of cell infections, and the increase in the average molecular weight and buoyant density of partially empty capsids as the average number of breaks per genome increased in the infecting phage are all observations which can be rationalized on the basis of a partial injection model. In contrast, it is difficult to explain the foregoing results in terms of an all-or-none model. What the data do not show, however, is whether or not there is a polarity to RNA injection. The question raised is: "does the injected RNA fragment originate from the 3'-end or 5'-end of the phage RNA, or does each end serve equally in the role of pilot end?" This problem is discussed further in Chapter VI.

## CHAPTER VI

### DIRECTION OF PENETRATION OF R17 RNA

#### A. Introduction

The genomes of various DNA bacteriophages such as SP82G (McAllister, 1970) and T7 (Pao and Speyer, 1973) have been shown to be injected into host cells linearly and with a definite polarity. In the case of the  $\lambda$  phage, the penetration of DNA was demonstrated to be nonpolar (Sharp et al., 1971b). The experimental design used by the foregoing investigators involved a study of the penetration of DNA fragments into the host. This was accomplished by means of chilling and blending techniques (McAllister, 1970), or by the prior breakage of DNA in situ by X-irradiation (Sharp et al., 1971a; Pao and Speyer, 1973) or  $^{32}\text{P}$  decay (McAllister et al., 1973). The genes carried on the penetrated fragments and the order of DNA injection were usually identified through the use of marker rescue techniques.

It was shown in Chapter IV that R17 phage incubated in the presence of ascorbic acid and  $\text{Cu}^{2+}$  is inactivated as a consequence of the cleavage of the RNA in situ as well as by some as yet uncharacterized base alterations. It was demonstrated that such particles retain the ability to attach to F-pili and to inject A protein and RNA. Furthermore, evidence obtained by several experimental approaches (Chapter V) strongly indicates that such particles on interacting with sensitive cells, inject only a fraction of their RNA. If a unique orientation of the RNA strand occurs during penetration, then the penetrated fragments should contain the nucleotide sequence of the 3'-end only if the

3'-end were the leading end in RNA penetration, or the 5'-end sequence if the 5'-end were the pilot end.

Although it is not presently feasible to use marker rescue techniques to identify RNA fragments, it is theoretically possible to deduce the direction of penetration of the RNA by quantifying the end groups of such penetrated fragments. It is already established that the R17 phage RNA terminates in a guanosine 5'-triphosphate at the 5'-end (Roblin, 1968) and an adenosine 3'-OH residue at the 3'-end (Thirion *et al.*, 1968). Alkaline hydrolysis of the RNA thus generates guanosine 5'-tri, 2', 3'-monophosphate (pppGp) and adenosine ( $A_{OH}$ ) as the natural terminal residues as well as a mixture of 2' and 3'-nucleoside monophosphates (Np) from the internal residues. If the injection of phage RNA is unidirectional, then fractional RNA injection should result in the transportation of one of the end terminal residues into the cell while its opposite end remains in the partially empty capsid released to the medium. For example, if the 3'-end of the viral RNA were the leading end, then fractional injection would result in the formation of partially empty capsids whose RNA fragments were missing the adenosine residue from the 3'-end of the original RNA. Concurrently, the number of pppGp's relative to the total Gp residues produced in the alkaline hydrolysate of the RNA isolated from the partially empty capsids would increase when compared to the normal ratio of 0.0012 calculated for 28S R17 RNA. The opposite findings would be obtained if the 5'-end of the RNA were the leading end; namely, the proportion of the original 3'-end terminus to total RNA would increase in the partially empty capsids. The following series of experi-

ments were carried out with the aim of distinguishing between the foregoing possibilities.

## B. Results

### 1. Isolation of Partially Empty Capsids on a Preparative Scale

Partially empty capsids and phage particles which have interacted with host cells were obtained on a large scale by infecting 1.0 to 1.2 liters of *E. coli* WP156 cells (in CTMM + 0.05% casamino acids) with either  $^3\text{H}$ -guanosine- or  $^3\text{H}$ -adenosine-labeled R17 phage at a MOI = 100 particles/cell for 40 min at 37°. These conditions of infection were designed to maximize the number of particles entering into the RNA ejection step, and the formation of partially empty capsids in intact cells where the parental phage was pretreated with ascorbate. At the end of 40 min, the culture was chilled and the cells removed by centrifugation (10,000 g, 10 min); the supernatant was then filtered through a GA-6 Gelman membrane to remove any remaining cells and F-pili. Subsequently, the cell-free supernatant was concentrated to about 10 ml by ultrafiltration through Amicon membranes with an exclusion limit of MW = 100,000 (see Methods and Materials). The phage particles in the concentrated supernatant were then separated on the basis of buoyant density by equilibrium CsCl gradient centrifugation at 4°. The gradients were dripped out into about 30 fractions, and a small aliquot from each was assayed by liquid scintillation methods for  $^3\text{H}$ -labeled RNA. Appropriate fractions delineated in the profile of radioactivity were combined into 2 populations labeled "heavy" and "intermediate" as described previously (Figure 5.7H).

Chapter V). The CsCl was removed from the fractions (volume about 1 to 1.5 ml) by 24 hr dialysis against 0.01 M Tris buffer, after which about 3 to 6  $A_{260}$  units of unlabeled phage were added to the dialyzed samples to serve as a carrier during the SDS-phenol extraction procedure for RNA which followed. The isolated RNA was then hydrolyzed in 0.3 N KOH for 24 hr at 37°, neutralized, and the hydrolysate analysed by high voltage paper electrophoresis. The details of methods are described in Materials and Methods.

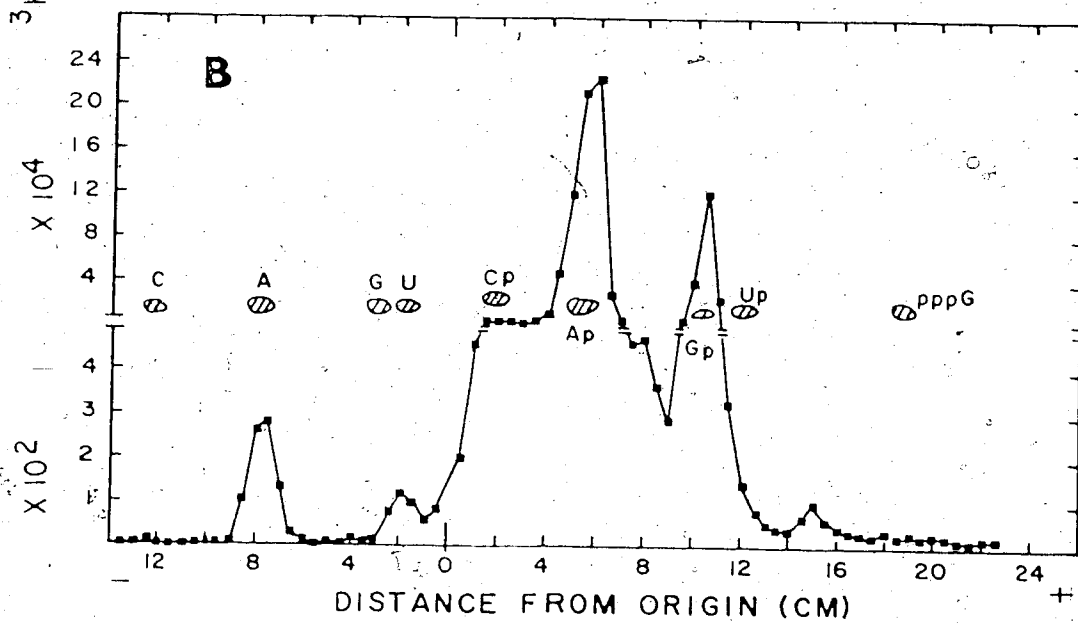
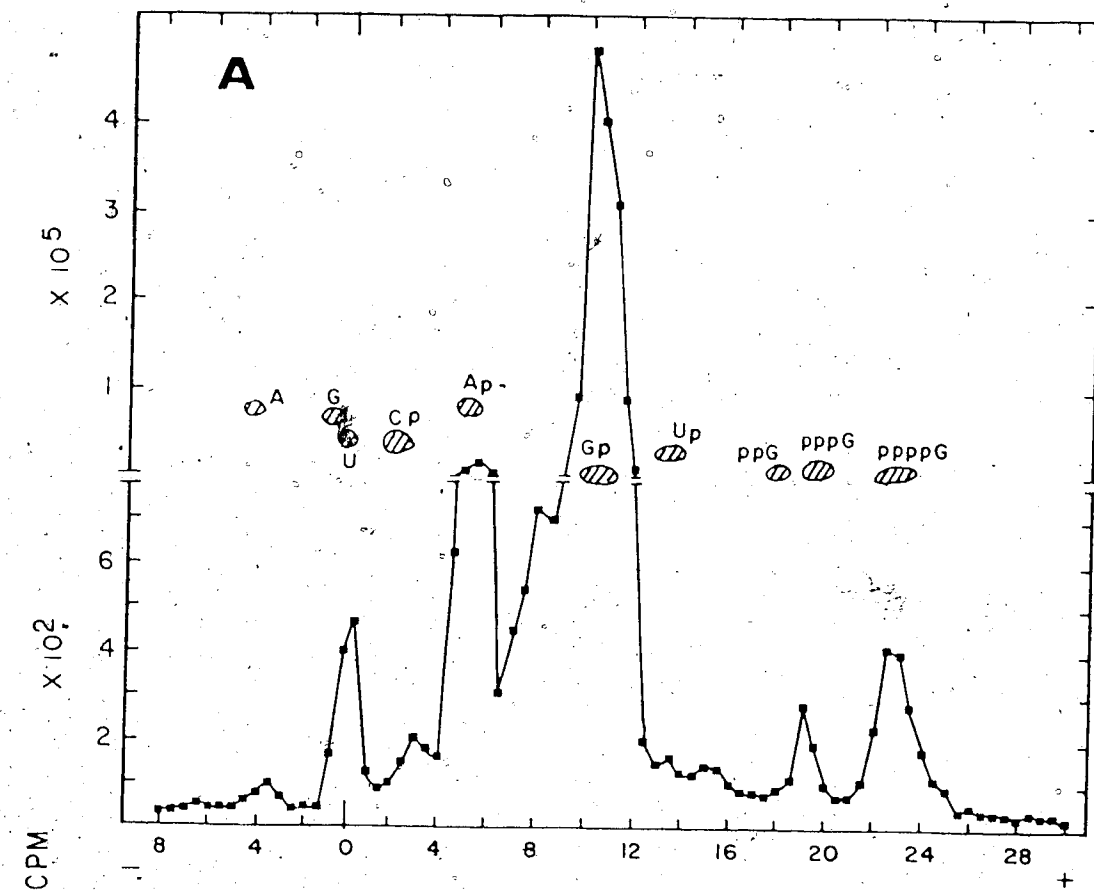
## 2. Paper Electrophoresis of Alkaline Hydrolysates of $^3\text{H}$ -Adenosine and $^3\text{H}$ -Guanosine-Labeled R17 RNA

Typical electropherograms of  $^3\text{H}$ -adenosine and  $^3\text{H}$ -guanosine - labeled R17 RNA alkaline hydrolysates obtained by high voltage paper electrophoresis at pH 3.5 are illustrated in Figure 6.1 A and B respectively. It is seen from each profile that radioactivity was recovered in both the 2', 3'-guanosine monophosphate (Gp) and 2', 3'-adenosine monophosphate (Ap) regions of the paper when  $^3\text{H}$ -adenosine or  $^3\text{H}$ -guanosine, respectively, were used as the labeled precursors. Under the labeling conditions described in Methods and Materials, approximately 2% of the  $^3\text{H}$ -radioactivity appears in Ap by metabolic interconversion if  $^3\text{H}$ -guanosine was the precursor. With  $^3\text{H}$ -adenosine as precursor, about 20% of the radioactivity was incorporated into Gp.

As may be seen in Figure 6.1 B,  $^3\text{H}$ -adenosine was easily identified in electropherograms of alkaline digests of  $^3\text{H}$ -adenosine-labeled R17 RNA. If the RNA was isolated from phage particles with PFU/particle ratios of 1/10 or greater, the ratio of radioactive counts found in this peak to Ap counts varied from 0.0013 to 0.0015.

Figure 6.1 High voltage paper electrophoresis of alkaline hydrolysates of R17 RNA.

Conditions of electrophoresis: 0.04M sodium citrate buffer, pH 3.5, 30 volts/cm for 10<sup>5</sup> min. The details of the hydrolysis and electrophoretic procedures are given in Materials and Methods. (A) electropherogram of alkaline hydrolysate of R17 RNA labeled with <sup>3</sup>H-8-guanosine precursor. Fractions counted for Gp radioactivity: 9-12 cm; for pppGp radioactivity: 21.5-25 cm. (B) electropherogram of alkaline hydrolysate of R17 RNA labeled with <sup>3</sup>H-2, 8-adenosine precursor. Fractions counted for A<sub>OH</sub> radioactivity: 6-9 cm (on cathode side of origin); for Ap radioactivity: 4-7 cm.



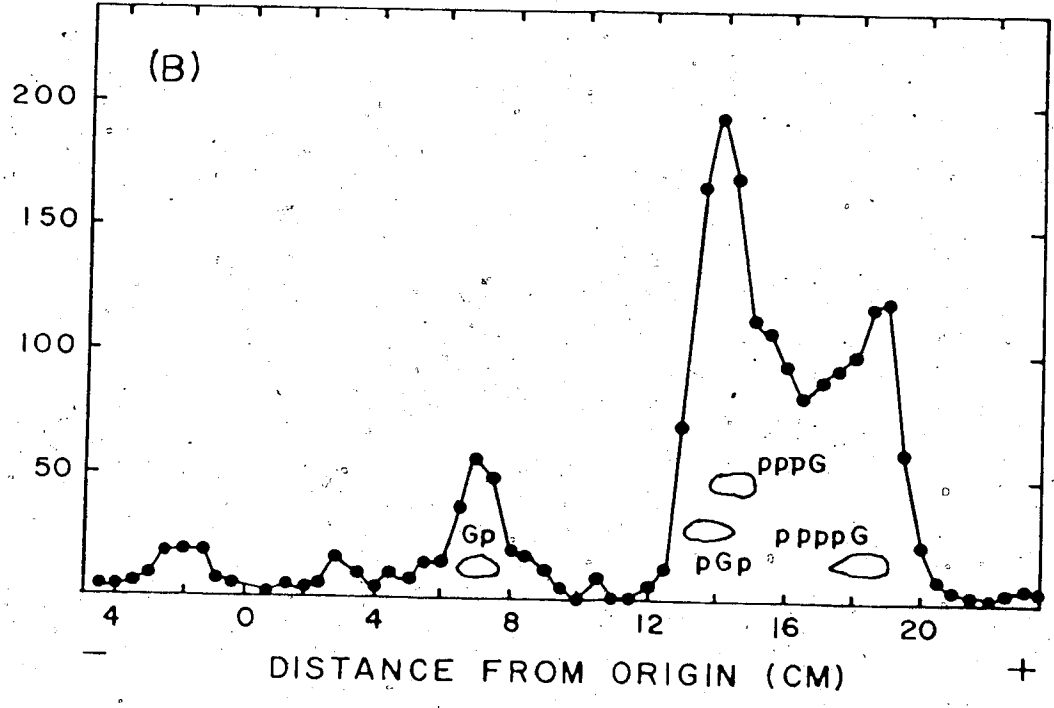
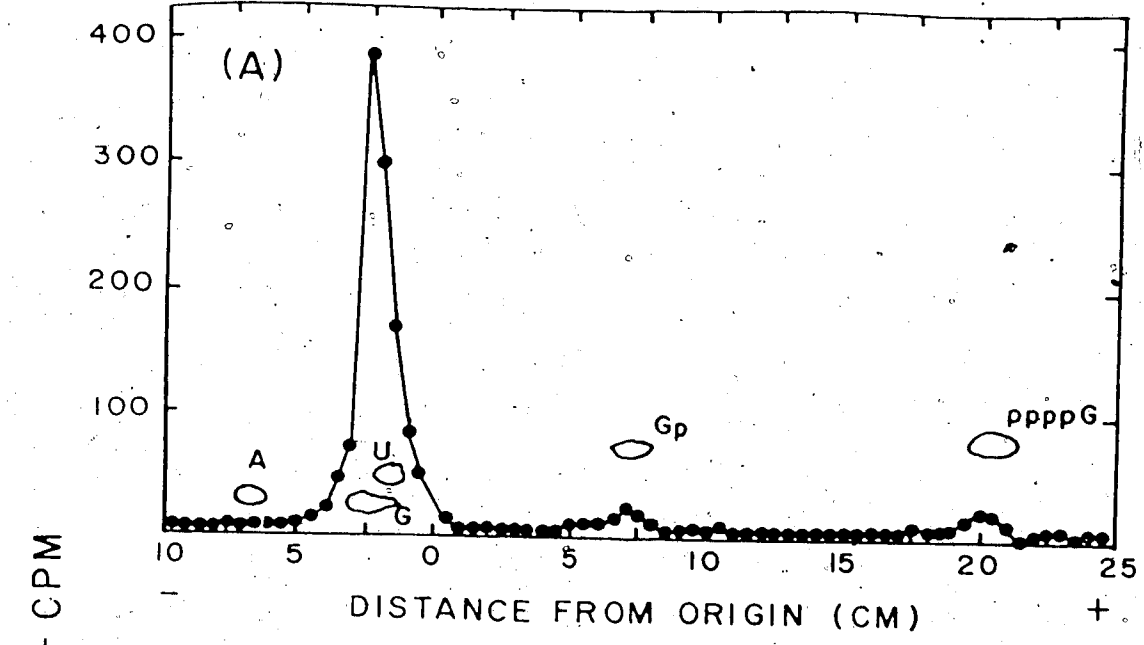
This is in good agreement with the theoretical value of 0.0013 calculated on the basis of an estimated R17 RNA length of 3300 nucleotides (Sinha *et al.*, 1965), and a base composition of 23% A, 26% U and 25% C (Mitra *et al.* 1963). If the RNA was isolated from phage particles inactivated by ascorbate-Cu<sup>2+</sup> treatment, it was found that the  $A_{OH}/A_p$  ratio, as determined from radioactive counts in electropherograms, increased linearly with the  $-\log$  (PFU/particle) value of the phage (Figure 4.5, Chapter IV). As discussed earlier, this increase is attributable to the formation of additional 3'-A<sub>OH</sub> termini arising from free radical-mediated cleavage of the RNA. The peak migrating beyond pppG in the electropherogram of material labeled with <sup>3</sup>H-guanosine precursor (Figure 6.1 A), was identified as pppGp by Watanabe and August (1968), Shimura *et al.* (1968), and Dahlberg (1968), who analyzed phage RNA hydrolysates under similar conditions of paper electrophoresis. Additionally this peak co-migrated with added ppppG, an isomer of pppGp which had been shown by Dahlberg (1968) to possess an identical mobility in paper electrophoretic conditions of pH 3.5.

Further confirmation of the identity of this peak was provided by enzymatic digestion of the material eluted from this position. Alkaline phosphatase digestion was carried out according to the procedure published by Roblin (1968) and the products were again characterized by paper electrophoresis. The result of the experiment is illustrated in Figure 6.2 A. Clearly, phosphatase incubation caused all the <sup>3</sup>H-radioactivity to migrate with unlabeled guanosine markers. No radioactivity was observed in the position of adenosine. It was thus concluded that the substrate does not possess any internucleotide



Figure 6.2 Enzymatic digestion of pppGp.

The  $^3\text{H}$ -labeled material migrating beyond pppG in the electropherogram illustrated in Figure 6.2 A was eluted and desalted as described in Materials and Methods. (A) The lyophilized material ( $\sim 2500$  cpm) was redissolved in 0.1 ml of a solution consisting of 5 mM Tris buffer (pH 7.6) and 1 unit of alkaline phosphatase (capable of hydrolyzing 1  $\mu\text{mole}$  of p-nitrophenol/min at 25 $^\circ$ ) and incubated for 45 min at 37 $^\circ$ . Part of the mixture (50  $\mu\text{l}$ ) was applied as a 4 cm band on 3MM paper and separated by paper electrophoresis at 30 volts/cm at pH 3.5 for 104 min. (B) SVP digestion. Another portion of the  $^3\text{H}$ -labeled pppGp material ( $\sim 3300$  cpm) was dissolved in 0.1 ml of a solution with the following composition: 4.5  $\mu\text{g/ml}$  SVP, 0.7 M Tris-HCl (pH 7.6), 1.3 mM  $\text{MgCl}_2$ . The mixture was incubated at 37 $^\circ$  for 2 hrs, then 50  $\mu\text{l}$  was applied as a 4 cm band on 3 mm paper and separated by paper electrophoresis as in (A). In both (A) and (B) unlabeled standard compounds (conc = 1 mg/ml) were dissolved in a solution with the same composition as the reaction mixtures and 5  $\mu\text{l}$  spotted on the origin for separation. The radioassay of paper electropherograms is described in Materials and Methods.



linkage which is resistant to the phosphatase.

Incubation of the same  $^3\text{H}$ -labeled material with snake venom phosphodiesterase (SVP) in the system described by Roblin (1968) gave the result illustrated in Figure 6.2 B. As can be discerned from this figure, part of the original material (about 60%) was hydrolyzed to a product migrating at the position of pGp. This result is consistent with Roblin's original findings that SVP hydrolyses pppGp to pGp and pyrophosphate (Roblin, 1968).\*

### 3. 5'-end Group Analysis

The relative proportion of the 5'-end terminus to total RNA was determined by summing up the radioactive counts in the pppGp and Gp peaks in the electropherograms and calculating the resulting ratio. As the results in Table 6.1 A indicate, the pppGp/Gp ratios of the RNA isolated from intact particles before exposure to cells varied from 0.0010 to 0.0011. These ratios are consistently lower than the expected value of 0.0012 and may reflect the fact that a small portion of the residues was degraded during the course of the experiment.

In the experiment where the infecting phage was not ascorbate- $\text{Cu}^{2+}$  inactivated (PFU/particle = 1/30), the pppGp/Gp ratios found for the RNA isolated from particles in the heavy and intermediate fractions of a  $\text{CsCl}$  gradient differed only slightly from that of the control (intact phage). This is not surprising since Class I particles in this preparation probably carried out complete RNA injection and very few partially empty capsids were formed. Previously,  $\text{CsCl}$  and sucrose gradient analyses had shown that the RNA content of the Class II and III particles after exposure to cells was insignificantly altered; there-

fore the RNA isolated from these particles was expected to yield pppGp/Gp ratios similar to the theoretical value.

In order to maximize the number of partially empty capsids formed and thus the number of partial genomes with significantly altered end terminal ratios, sensitive *E. coli* were exposed to phage preparations inactivated by ascorbate-Cu<sup>2+</sup> treatment to give PEU/particle ratios less than 10<sup>-5</sup>. Previous studies (Chapter V, this thesis) have shown that the majority of partially empty capsids produced from such parental phage retained a major fraction of their original genome and banded at buoyant densities in CsCl near that of intact particles. The results of experiments carried out with highly inactivated phage were consistent and always yielded the same pattern shown in Table 6.1A; namely a moderate increase in the pppGp/Gp ratio in the heavy fraction, and a fairly significant additional increase in the intermediate fraction. The observed overall increase in the relative proportion of pppGp residues found in the RNA of cell exposed phage is precisely the result expected for a partial RNA injection mode where fragments containing the original 3'-end termini had been injected into the host. The lesser enrichment of pppGp residues in the RNA isolated from the heavy particle fraction can be attributed to the fact that the partially empty capsids in this fraction are comparatively denser and possess relatively longer fragments of RNA.

#### 4. 3'-end Group Analysis

The procedure followed for the large scale preparation of cells exposed to <sup>3</sup>H-adenosine-labeled particles was identical to that employed in the 5'-end group experiment. However, phage preparations were not

TABLE 6.1

End Group Analysis of the RNA Isolated from Partially Empty Capsids of R17

(A)

PFU/Particle Ratio of $^3\text{H}$ -Guanosine- R17 Phage Following Vit.C-Cu $^{++}$ Treatment	pppGp/Gp Ratio ( $\times 10^4$ )		
	Intact Phage Before Expo- sure to Cells	CsCl Gradient-Fractionated Phage After Exposure to Cells	
		Heavy	Intermediate
1/30	10.0	12.0	12.0
1/240,000	10.0	13.0	17.0
1/250,000	11.0	22.0	37.0

(B)

PFU/Particle Ratio of $^3\text{H}$ -Guanosine- R17 Phage Following Vit.C-Cu $^{++}$ Treatment	$A_{\text{OH}}/A_{\text{p}}$ Ratio ( $\times 10^4$ ) (Corrected for extraneous $A_{\text{OH}}$ residues generated by Vit.C-Cu $^{++}$ treatment)		
	Intact Phage Before Expo- sure to Cells	CsCl Gradient-Fractionated Phage After Exposure to Cells	
		Heavy	Intermediate
1/5	13.0	2.4	2.7
1/417	13.0	2.8	3.0
1/556	13.0	5.0	5.0

inactivated too extensively with ascorbate and  $\text{Cu}^{2+}$  in order to minimize the formation of extraneous 3'-termini containing adenosine residues (Figure 4.5, Chapter IV). Where necessary, the  $A_{\text{OH}}/\text{Ap}$  ratios listed in Table 6.1 B have been corrected for the contribution from extraneous  $A_{\text{OH}}$  residues.

If an RNA fragment with the 3'- $A_{\text{OH}}$  terminus is injected as a result of fractional injection, then it follows from this that the  $A_{\text{OH}}/\text{Ap}$  ratios of the RNA isolated from cell-exposed particles will decrease and this decrease will be more acute in the RNA isolated from intermediate particles than in the material extracted from the heavy fraction. A zero  $A_{\text{OH}}/\text{Ap}$  ratio would not be expected as the RNA isolated from particles collected in the two fractions would include overlapping material from Class II and III particles, which apparently retain a full complement of RNA.

In view of the above expectation, it was surprising to find from an infection carried out with control phage (PFU/particle = 1/5), the low  $A_{\text{OH}}/\text{Ap}$  ratios of  $2.4$  to  $2.7 \times 10^{-4}$  obtained for the RNA isolated from the heavy and intermediate fractions, respectively. Under the conditions of the infection, up to 40% of the particles recovered in the supernatant had injected all or almost all of their RNA and banded at the top of the CsCl gradient. Inert Class III particles which normally comprise 10% of the particles before exposure to cells would now make up 17% of the particles suspended at buoyant densities near 1.46 g/ml. If the 3'-ends of the Class III particles are subtracted from the overall  $A_{\text{OH}}/\text{Ap}$  ratios, it can be calculated that up to 95% of the other particles in the main peak (namely Class II particles which had under-

gone the RNA ejection step) had lost the 3'-adenosine residue. A similar pattern was exhibited by the results obtained for experiments carried out with two ascorbate-Cu<sup>2+</sup> inactivated phage preparations. In the infections carried out with these phage preparations (PFU/particle = 1/400-500), some of the original Class I particles would appear as partially empty capsids in the intermediate and heavy fractions. However, they would be indistinguishable from eclipsed Class II particles since the RNA encapsidated in the former would also be missing the original 3'-A<sub>OH</sub> residue as a result of the injection of a fragment from the 3'-end into the host cell. The additional presence of Class I partially empty capsids was, therefore, not expected to alter the trend of the A<sub>OH</sub>/Ap ratios determined for the RNA isolated from the heavy and intermediate fractions of a CsCl gradient.

The collective results of Table 6.1 B clearly indicate that the interaction of Class II particles with host cells gives rise to a loss of a small fragment of RNA at the 3'-end in addition to the A protein component (Parandych *et al.*, 1971). The length of the 3'-end sequence lost is probably quite short since the density of eclipsed Class II particles is almost identical to that of noneclipsed phage. Conceivably, the loss may even be restricted to the terminal 3'-adenosine residue. It is not known at present whether or not the putative short fragment that detaches from Class II particles upon interaction with sensitive bacteria is transported into the host.

### C. Discussion

The results obtained from the 5'-end and 3'-end group analyses strongly indicate that R17 phage RNA is injected in a polar manner and

that partial injection of RNA from phage particles results in a loss of the 3'-end of the phage RNA. Moreover it is clear that there is a marked loss of 3'-ends even in Class II particles which have not been treated with ascorbate and  $\text{Cu}^{2+}$ . Presumably, Class II particles already have a break in the RNA chain very close to the 3'-end so that interaction of these particles with host bacteria results in the ejection of the A protein plus a very short fragment of RNA from the 3'-terminus. This preexisting nick in the RNA near the 3'-end may have arisen during the assembly or release stages of Class II particles. A precedent for this exists in the report by Argetsinger and Gussin (1966) which showed that the RNA of A protein amber mutants assembled in a nonpermissive ( $\text{RNase I}^+$ ) host is partially degraded by cellular endonucleases. Alternatively, a break near the 3'-end of the RNA may be introduced during or after the onset of the RNA ejection step triggered by the interaction of the particle with cell-associated F-pili. Whatever the chronology of this event, it can be said that the cleavage is restricted to a position close to the 3'-end since the RNA isolated from a freshly prepared RL7 phage suspension (containing both Class I and Class II particles) behaves as a single homogeneous peak under denaturing conditions in sucrose gradients or polyacrylamide gels.

Although inferred by various observations described here and elsewhere, a specific complex between RL7 RNA and A protein has yet to be demonstrated directly. Recently, additional support for such a complex was furnished by Shiba and Miyake's (1975) finding that isolated MS2 RNA mixed with purified A protein was infectious for intact, F-piliated *E. coli* cells while RNA by itself was not. Leipold and Hofschneider (1975), in a similar experiment, found that an A protein-



RNA complex precipitated from M12 particles treated with acetic acid (the coat protein is solubilized) was also infectious for intact cells. It is tempting to interpret these results in terms of a tail model in which the viral RNA is indirectly attached to a F-pilus and pulled into the cell via the A protein. The end group analyses discussed in this chapter suggest that the RNA sequence that might be involved in such a complex would probably encompass all or part of the tightly hydrogen-bonded loop of about 25 nucleotides at the 3'-end which are not translated into protein (Cory et al., 1970). On a more speculative note, the possibility exists that the terminal trinucleotide of  $-CCA_{OH}$  may function as a necessary but not sufficient component of the A protein binding site much in the manner that tRNA's terminating in  $-CCA_{OH}$  are recognized by amino acyl synthetases. Further developments concerning the nature of the putative interaction between the A protein and the viral RNA must await the isolation and *in vitro* characterization of a discrete A protein-RNA complex.

The finding that the 3'-end of the phage RNA probably acts as the leading end during penetration is significant in that it contradicts previously held beliefs, based on circumstantial evidence, that it is the 5'-end of the RNA which penetrates initially into the cell. For instance, during conjugation in *E. coli*, one of the two complementary DNA strands in the donor is transferred to the recipient with the 5'-end acting as the origin of transfer (Ohki and Tomizawa, 1968; Rupp and Ihler, 1968). By inference, phage RNA was thought to penetrate 5'-end first in analogy to bacterial DNA transfer. Often cited in support of this concept was Lodish's investigation on defective

A protein-minus particles assembled in nonpermissive hosts infected by f2 amber mutants in the A protein. He found that treatment of such particles with RNase removed a fragment of RNA containing the 5'-terminus (Lodish, 1968 a,b). The interpretation advanced was that the protruding strand of RNA would normally be complexed with A protein and that this complex would precede the rest of the genome in cell entry.

A weakness of the foregoing interpretation resides in the inherent assumption that the molecular organization of the RNA in the defective particle is identical to that in normal phage. This assumption may not necessarily be valid as the defective particles are assembled in the absence of the A protein, a component which has been postulated to play an important organizational role in the early stages of assembly of infectious phage (Richelson and Nathans, 1967; Kaerner, 1970; Bonner, 1974). In contrast, the results of the end group analyses described in the chapter have been derived from RNA isolated from partially empty capsids whose predecessors were RNase resistant and competent with respect to the attachment and RNA ejection processes. These partially empty particles were formed as a direct consequence of a normal physiological process - phage interaction with sensitive cells followed by RNA injection - and not as the result of some overt chemical or enzymatic perturbation of structurally altered particles. It is felt that the approach taken here to elucidate the polarity of phage RNA penetration is more direct and the results obtained more indicative of the molecular orientation of the RNA within the phage capsid and during its penetration.

\* It is to be noted that the peak of radioactive material migrating more slowly than pppGp shown in Figure 6.1 is probably pGp (although GTP and alkaline resistant dinucleotides have a similar mobility). Some of this material may arise from the degradation of pppGp. However, the contribution from this source is not significant since the pppGp/Gp ratio obtained for phage RNA is close to the theoretical value. More likely, the creation of new 3'-N<sup>OH</sup> and 5'-pG ends in viral RNA as a result of ·OH attack and subsequent alkaline hydrolysis of this RNA may give rise to extra pGp residues. Consistent with this conjecture is the observation that more of the slower moving material appears in ascorbate-Cu<sup>2+</sup> degraded phage RNA than in untreated RNA.

## CHAPTER VII

### SUMMARY

The original findings presented in this thesis may be summarized as follows:

1. At high MOI's of infection (MOI = 100-1000 particles/cell), some phage RNA is able to penetrate host bacteria in the presence of saturating concentrations of RNase. The injected RNA is intact and infectious if the RNA in the infecting phage is not degraded by ascorbate-Cu<sup>2+</sup> treatment or by <sup>32</sup>P-decay prior to cellular infection.

2. If Mg<sup>2+</sup> ions in a culture medium are chelated by EDTA, Class I particles undergo incomplete RNA injection. Some of the partially ejected RNA is degraded with the result that particles carrying partial genomes are produced.

3. Rapid inactivation of R17 phage occurs when particles are incubated in the presence of ascorbic acid and Cu<sup>2+</sup> ions. The combination of the two reagents results in the formation of hydroxyl free radicals ( $\cdot\text{OH}$ ) which bring about phage inactivation primarily through the cleavage of viral RNA and probable base alterations. Under conditions where phage infectivities are reduced 10<sup>6</sup>-10<sup>7</sup> fold, the structural organization of R17 phage remains unaltered and no significant change is observed in the ability of treated particles to undergo the adsorption, RNA ejection and penetration processes.

4. Phage RNA penetration is polar; the 3'-end of the viral RNA acts as the pilot end and, together with the A protein polypeptides, precedes the rest of the genome in cell entry.

5. During the ejection and penetration steps, the phage RNA unfolds only partially; it retains part of its secondary structure in

the form of loops containing complementary base pairs.

6. If strand breaks are introduced into the RNA of potentially infectious phage (Class I particles) by ascorbate-Cu<sup>2+</sup> treatment or by <sup>32</sup>P-decay in labeled particles, then fractional RNA ejection and penetration occurs; strand separation probably occurs at the first break nearest the 3'-end which is not protected by intrastrand base-pairing in the partially unfolded RNA.

7. The interaction of Class II particles (treated or untreated with ascorbate-Cu<sup>2+</sup>) with sensitive host bacteria results in the loss of the adenosine residue from the 3'-end of the RNA. A scission introduced into the RNA near the 3'-end during particle assembly or during the RNA ejection step of Class II particles may have resulted in the ejection of a small fragment to the F-pilus of medium.

8. Both Class I and Class II particles, upon interaction with sensitive bacteria, appear to lose about 10% of their coat protein monomers to the cell. At least some of the coat subunits are transported into the cell.

9. RNA fragments injected into bacteria are rapidly degraded by cellular nucleases soon after entry. It was observed that these messenger fragments appear to be stabilized in the presence of the RNA polymerase inhibitor, rifampicin.

The new insights provided by the preceding observations together with existing information have been incorporated into a revised, working model for RL7 phage infection. Depicted schematically in Figure 7.1 are the fate of Class III, Class II and Class I particles

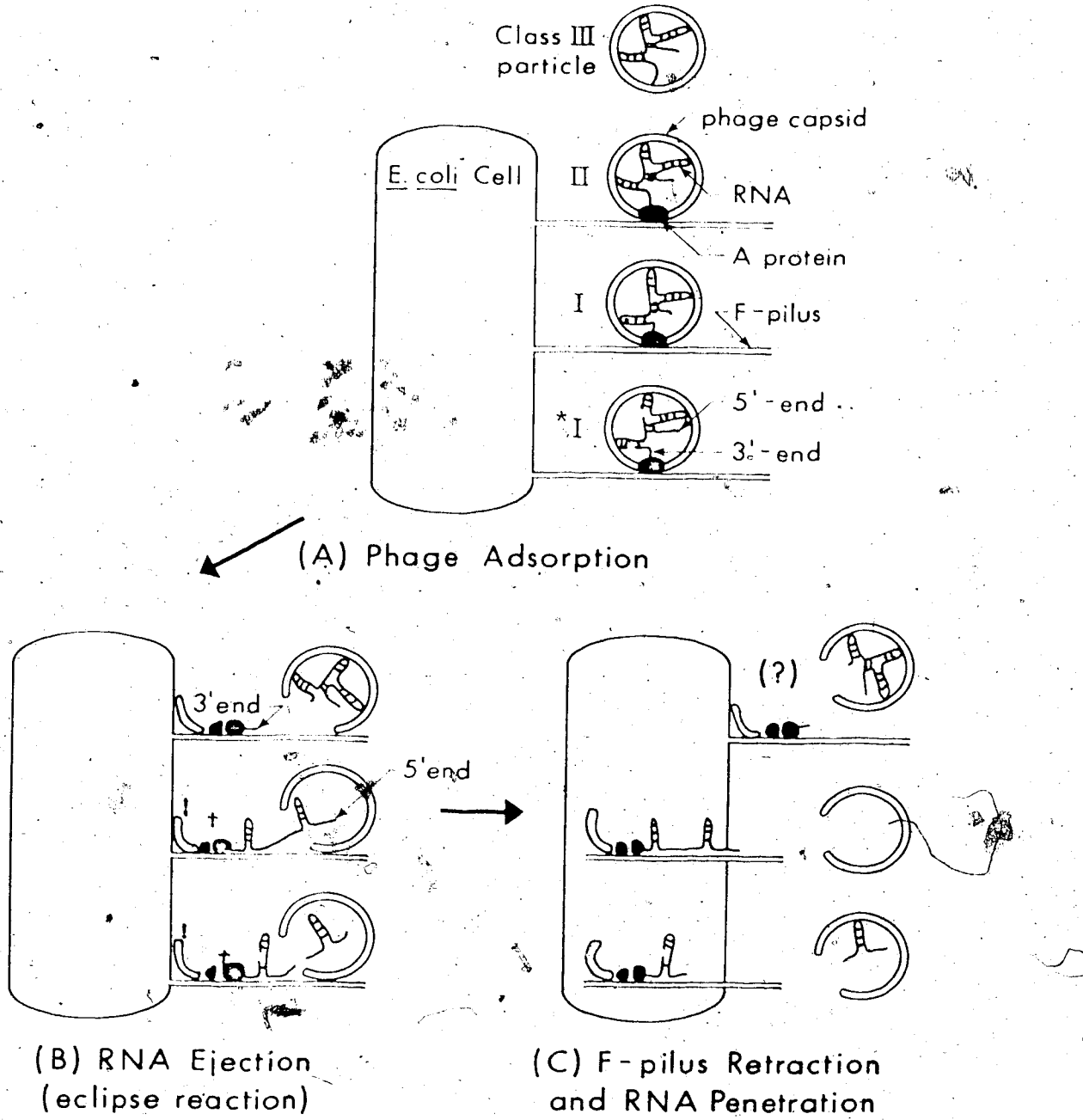


Figure 7.1 Schematic representation of a revised working model depicting the mechanism of R17 phage infection of *E. coli* host cell.  
 \* Class I particle with scissions in the RNA  
 † coat-protein aggregate detached from capsid  
 ‡ cleaved A protein polypeptides

(with or without strand scissions) during the early stages of cellular infection under normal physiological conditions. As demonstrated previously, Class III particles do not interact with F-piliated host cells since they lack the A protein; both Class I and II particles adsorb to F-pili but the latter do so only weakly (Paranchych et al., 1970; Krahn and Paranchych, 1971). The reason for the weaker adsorption of Class II particles is still not clear.

The cumulative data indicate that Class II particles, although attaching comparatively weakly, undergo a similar RNA ejection (or phage eclipse) step as Class I particles. In the illustrated scheme, the RNA ejection step is envisaged to involve the cleavage of the A protein into 2 subunits of  $MW = 24,000$  and  $15,000$ , the detachment of an aggregate of coat monomers from the capsid to the F-pilus, and complete or partial RNA ejection. Not illustrated is a minor A protein fragment of  $MW = 10,000$  which Krahn et al., (1972) had attributed to a further degradation product of one of the larger fragments. The A protein and the 3'-end of the viral RNA is shown in the model to exist as a complex within the phage and also during the RNA ejection and penetration processes. Part of its secondary structure is retained by the RNA as it unfolds and extrudes from the capsid.

As discussed previously, the presence of base-paired loops in the ejected RNA implies that the RNA is likely to

remain on the outer surface of the F-pilus and to be brought to the cell membrane via some movement of the pilus. In light of recent evidence, the transportation of A protein and RNA up to and perhaps through the cellular membrane is shown in the model to be mediated by a F-pilus retraction mechanism. Support for such a mechanism has come from recent observations which indicate that F-pili are in an equilibrium state of outgrowth and retraction. For example, Novotny and Fives-Taylor (1974) have reported that cells exposed to sodium cyanide or to temperatures between 25-30° lose pili from their surface; the level of cell-free pili was demonstrated not to rise as a result of such treatment. The interpretation advanced was that low temperatures or cyanide prevented the outgrowth of pili but not retraction. Furthermore, these workers found that if pili were coated with pili antiserum or with excessive R17 phage before cells were cooled or cyanide added, no pili loss occurred. Presumably the antiserum or phage coating the sides of pili prevented retraction. This explanation was also advanced to account for the accumulation of I-pili on the cell surface of *E. coli* carrying I-like sex factors and growing in the presence of I-pili antibody (Lawn and Meynell, 1972). In this laboratory, it was observed by Moore and Paranchych (unpublished data) that the *E. coli* strain WP102 carrying a mutation in the F plasmid exists in a multipiliated state (7-8 pili/cell) and is only slightly sensitive to R17 and Q8 phages. The defect in this mutant appears to reside in its inability to retract pili since cooling of these cells to 30° does not



result in the loss of pili whereas cooling of the wild type strain (ED2602) does. Finally, the observations that F-pili become shorter and disappear after attachment of filamentous DNA phage to their tips and that eventually phage appears to be attached directly to the cell surface also indicate that pili are able to retract with phage attached to their tips (Jacobson, 1972; Marvin and Hohn, 1969).

It must be stressed that the model postulated in Figure 7.1 represents only one interpretation of phage infection consistent with experimental data. Although Figure 7.1 shows the pilus retracting intact into the cell, the alternate possibility exists that shortening of pili may be brought about by depolymerization of pilin subunits into the cell membrane. Additionally, it is conceivable that shortening of the pilus only transports the A protein and RNA to the cell surface while the actual penetration of phage components may be mediated by a membrane-associated transport system.

Another nebulous area concerns the fate of the A protein during phage infection. It has not been firmly established as to how and where the cleavage of the A protein occurs and whether or not the RNA remains complexed to one or both A protein fragments during penetration. Krahn et al., (1972) have reported that A protein and RNA are injected into cells in approximately equimolar amounts and the suggestion was made that the penetration of phage RNA into the host cell may involve the injection of an A protein-RNA complex rather than free RNA. As described in this thesis, the amount of A protein penetration remains at a steady level while the amount of RNA penetration decreases in infections carried out in the presence of RNase

or with ascorbate-Cu<sup>2+</sup>-treated phage. These observations suggest that either A protein penetrates into cells independently of RNA or that the A protein, with one end of the RNA anchored to it, is able to "pull" an RNA fragment of varying lengths into the cell. The results of these experiments also indicated that the phage equivalents of A protein penetrated per cell are similar to those of RNA. This, however, brings up the question of the fate of A protein molecules which dissociate from eclipsed Class II particles. It was reported that A protein is not released to the medium in infected bacterial cultures and that some of the A protein presumably of Class II origin adsorbed to cell-associated F-pili (Paranchych *et al.*, 1971; Krahl *et al.*, 1972). These observations in conjunction with the pilus retraction hypothesis of transportation of viral components, however, point to a paradoxical situation in phage infection. It appears that, after the onset of the phage eclipse step and the transfer of A protein to the F-pilus, only the A proteins from Class I particles with an intact RNA attached are transported into the cell while A proteins of Class II origin (perhaps with a truncated piece of RNA) are not. On the other hand, the mole equivalents of A protein penetrating cells would certainly exceed that of viral RNA if A protein from Class II particles were also transported into cells. The possibilities, therefore, exist that Class II A proteins are excluded in some manner from penetration at the cell surface or that they may desorb from F-pili (due to their weak interaction with the latter) before they could be moved up to the cell membrane. But if A proteins from Class II particles are excluded at the cell surface, then they should slough off as the F-pilus retracts or shortens and be found in

the medium. Although not detected in sucrose gradients, free A protein from supernatants of infected cultures has been observed to band at the bottom of CsCl gradients (buoyant density =  $1.54 \text{ g/cm}^3$ ) either as a precipitate or as an A protein-RNA complex (data not shown). However, this result was not always reproducible. A possible explanation for the failure to detect free A protein in sucrose gradients and sometimes in CsCl gradients may be due to the strong adherence of free A protein to surfaces such as dialysis membranes (Roberts and Steitz, 1967) and cellulose nitrate tubes (S. Reynolds, private communication). It is possible that all or most of the A protein molecules in solution may be lost as a result of their adsorption to glassware or centrifuge tubes before they could be assayed.

The preceding discourse clearly points to a need for further studies to verify earlier findings, to resolve contradictions, and to bridge the gap existing between results and theory. Similarly, the hypothesis concerning the dissociation of coat monomers from eclipsed phage and the fate of such subunits requires confirmation and expansion through additional quantitative studies. As can be discerned from this brief overview, there is much scope for future investigations.

## BIBLIOGRAPHY

- Achey, P., and Duryea, H. (1974). *Int. J. Radiat. Biol.* 25, 595.
- Achtman, M., Willetts, N., and Clark, A.J. (1972). *J. Bact.* 110, 831.
- Albertsson, P.A. (1967). In "Methods in Virology" (K. Maramorosch and H. Koprowski, eds.), Vol. 2, p. 303. Academic Press, New York.
- Anbar, M., and Neta, P. (1967). *Int. J. Appl. Radiat. Isotopes*, 18, 493.
- Argetsinger, J.E., and Gussin, G.N. (1966). *J. Mol. Biol.* 21, 421.
- Auda, H., and Emborg, C. (1973). *Radiat. Res.* 53, 273.
- Barr, N.F., and King, C.G. (1956). *J. Am. Chem. Soc.* 78, 303.
- Blok, J., Luthjens, L.H., and Roos, A.L.M. (1967). *Radiat. Res.* 30, 468.
- Blok, J., and Verhey, W.S.D., (1968). *Radiat. Res.*, 34, 689.
- Boedtker, H. (1967). *Biochemistry* 6, 2718.
- Boedtker, H. (1968). *J. Mol. Biol.* 35, 61.
- Boedtker, H. (1971). *Biochim. Biophys. Acta* 240, 448.
- Bonner, P.H. (1974). *J. Virol.* 14, 1152.
- Bradley, D.E. (1972a). *Genet. Res.* 19, 39.
- Bradley, D.E. (1972b). *J. Gen. Microbiol.* 72, 303.
- Brinton, C.C., Jr., Genski, P., Jr., and Carnahan, J. (1964). *Proc. Natl. Acad. Sci. U.S.A.* 52, 776.
- Brinton, C.C., Jr. (1965). *Trans. N.Y. Acad. Sci.* 27, 1003.
- Brinton, C.C. Jr., and Beer, H. (1967). In "The Molecular Biology of Viruses" (J.S. Colter and W. Paranchych, eds.), p. 251. Academic Press, New York.
- Brinton, C.C. Jr., (1971). *Critical Rev. Microbiol.* 1, 105.
- Brinton, C.C. Jr., (1975). *Bacteriol. Rev.*, In Press.
- Brock, T.D. (1962). *Biochem. Biophys. Res. Commun.* 9, 184.
- Brock, T.D., and Wooley, S.O. (1963). *Science* 131, 1065.
- Brownlee, G.G., and Sanger, F. (1967). *J. Mol. Biol.* 23, 337.

- Brownlee, G.G., Sanger, F., and Barrell, B.G. (1968). *J. Mol. Biol.* 34, 379.
- Brownlee, G.G., and Sanger, F. (1969). *Eur. J. Biochem.* 11, 395.
- Byrne, R., Levin, J.G., Bladen, H.A., and Nirenberg, M.W. (1964). *Proc. Natl. Acad. Sci. U.S.* 52, 140.
- Caspar, D., and Klug, A. (1962). *Cold Spring Harbor Symp. Quant. Biol.* 27, 1.
- Coquerelle, G., and Haged, U. (1972). *Int. J. Radiat. Biol.* 21, 31.
- Corv, S., Spahr, P.F., and Adams, J.M. (1970). *Cold Spring Harbor Symp. Quant. Biol.* 35, 1.
- Crawford, E. M., and Gesteland, R.F. (1964). *Virology* 22, 165.
- Curtiss, R., III (1969). *Ann. Rev. Microbiol.* 23, 69.
- Curtiss, L.K., and Krueger, R.G. (1974). *J. Virol.* 14, 503.
- Danziger, R.E., and Paranchych, W. (1970a). *Virology* 40, 547.
- Danziger, R. E., and Paranchych, W. (1970b). *Virology* 40, 554.
- De Flora, S., and Radolati, G. (1973). *J. Gen. Virol.* 20, 261.
- Dreyer, W.J., and Bynum, E. (1967). In "Methods in Enzymology" (C.H.W. Hirs, ed.), Vol XI, p. 32. Academic Press, New York.
- Dunker, A.K. (1974). *J. Virol.* 14, 878.
- Dunker, A. K., and Paranchych, W. (1975). *Virology in the press.*
- Edgell, M., and Ginoza, W. (1965). *Virology* 27, 23.
- Engelberg, H., and Artman, M. (1970). *J. Mol. Biol.* 48, 181.
- Eger, M.D., and Kaesberg, P. (1965). *J. Mol. Biol.* 13, 260.
- Fiers, W., Contreras, R., Deerinck, F., Haegmean, G., Merregaert, J., Min Jou, W., Raeymaekers, A., Volckaert, G., and Ysebaert, M., Van de Kerckhove, J., Nolf, F., and Van Montagu, M. (1975). *Nature* 256, 273.
- Fischbach, F. A., Harrison, P.M., and Andereg, J.W. (1965). *J. Mol. Biol.* 13, 638.
- Fomenko, L.A., Leontieva, G.A., Gaziev, A.I., and Kuzin, A.M. (1974). *Radiobiologiya* 14, 579.
- Fukuma, I., and Cohen, S.S. (1975). *J. Virol.* 16, 222.

- Garen, A., and Puck, T.T. (1951). *J. Exptl. Med.* 94, 177.
- Gaziev, A.I., Gergøeva, S.A., and Zakrevskaja, D.T. (1974). *Stud. Biophys.* 42, 203.
- Gesteland, R.F., and Boedtker, H. (1964). *J. Mol. Biol.* 8, 496.
- Gill, G.S., and MacHattie, L.A. (1975). *Virology* 65, 297.
- Ginoza, W. (1963). *Nature* 199, 453.
- Gussin, G.N. (1966). *J. Mol. Biol.* 21, 435.
- Heisenberg, M., and Blessing, J. (1965). *Z. Naturf.* 20b, 859.
- Heisenberg, M. (1966). *J. Mol. Biol.* 17, 136.
- Heisenberg, M. (1967). *Biochem. Biophys. Res. Commun.* 27, 131.
- Hershey, A.D., Kamen, M.D., Kennedy, J.W., and Gest, H. (1951). *J. Gen. Phys.* 34, 305.
- Hindley, J. (1973). *Progress in Biophysics and Molecular Biology* 26, 269.
- Hohn, T. (1969). *Eur. J. Biochem.* 8, 552.
- Hohn, T., and Hohn, B. (1970). *Adv. Virus Res.* 16, 43.
- Horiuchi, K., Lodish, H.F., and Zinder, N.D. (1966). *Virology* 28, 438.
- Ippen-Ibler, K., Achtman, M., and Willetts, N. (1973). *J. Bact.* 110, 857.
- Jacobson, A. (1972). *J. Virol.* 10, 835.
- Jeppesen, P.G.N., Steitz, J.E., Gesteland, R.F., and Spahr, P.F. (1970). *Nature*, 226, 230.
- Kaerner, H.C. (1970). *J. Mol. Biol.* 53, 515.
- Kamen, R. (1969). *Nature* 221, 321.
- Knolle, P., and Kaudewitz, F. (1963). *Biochem. Biophys. Res. Commun.* 11, 383.
- Knolle, P. (1967a). *Biochem. Biophys. Res. Commun.* 27, 81.
- Knolle, P. (1967b). *Zentralbl. Bakteriol. I. Abtlg. Orig.* 202, 417.
- Kozak, M., and Nathans, D. (1971). *Nature New Biology* 234, 209.
- Kozak, M., and Nathans, D. (1972). *Bacteriol. Rev.* 36, 109.

- Krahn, P.M. (1971). Ph.D. Thesis: University of Alberta.
- Krahn, P.M., and Paranchych, W. (1971). *Virology* 43, 533.
- Krahn, P.M., O'Callaghan, R.J., and Paranchych, W. (1972). *Virology*, 47, 628.
- Laemmli, U.K. (1970). *Nature* 227, 680.
- Lavelle, F., Michelson, A.M., and Dimitrijević, L. (1973). *Biochem. Biophys. Res. Commun.* 55, 350.
- Lawn, A.M. (1966). *J. Gen. Microbiol.* 45, 377.
- Leipold, B., and Hofschneider, P.H. (1975). *FEBS Letters* 55, 50.
- Le Pecq, J.B., and Paoletti, C. (1966). *Anal. Biochem.* 17, 100.
- Levinthal, C., Keynan, A., and Higa, A. (1962). *Proc. Natl. Acad. Sci. U.S.A.* 48, 1631.
- Lodish, H.F., Horiuchi, K., and Zinder, N.D. (1965). *Virology* 27, 139.
- Lodish, H.F. (1968a). *Nature (London)* 220, 345.
- Lodish, H.F. (1968b). *J. Mol. Biol.* 32, 681.
- Loeb, T., and Zinder, N.D. (1961). *Proc. Natl. Acad. Sci. U.S.A.* 47, 282.
- Loening, U. (1957). *Biochem. J.* 102, 251.
- Lupker, J.H., Glickman, B.W., Rorsch, A., and Bosch, L. (1973). *Eur. J. Biochem.* 35, 206.
- Mans, J., and Novelli, G.D. (1960). *Biochem. Biophys. Res. Commun.* 3, 540.
- McAllister, W.T., and MacDonald Green, D. (1973). *J. Virol.* 12, 300.
- McAllister, W.T. (1970). *J. Virol.* 5, 194.
- McCord, J.M., and Fridovich, I. (1968). *J. Biol. Chem.*, 243, 5753.
- McCord, J.M., and Fridovich, I. (1969). *J. Biol. Chem.* 244, 6049.
- Marvin, D.A., and Hohn, B. (1969). *Bacteriol. Rev.* 33, 172.
- Matthews, K.S., and Cole, R.D. (1972a). *J. Mol. Biol.* 65, 1.
- Matthews, K.S., and Cole, R.D. (1972b). *J. Mol. Biol.* 65, 17.

- Meynell, E.W., and Datta, N. (1967). *Nature* 214, 855.
- Meynell, G.G., and Aufreiter, E. (1969). *J. Gen. Microbiol.* 59, 429.
- Miller, O.L., Jr., Beatty, B.B., Ankalo, B.A., and Thomas, C.A., Jr. (1970). *Cold Spring Harbor Symp. Quant. Biol.* 35, 505.
- Min Jou, W., Haeghebaert, G., Ysebaert, M., and Fiers, W. (1972). *Nature* 237, 82.
- Mirault, M.E., and Scherrer, K. (1971). *Eur. J. Biochem.* 23, 372.
- Mitra, S., Enger, M.D., and Kaesberg, P. (1963). *Proc. Natl. Acad. Sci. U.S.A.* 50, 68.
- Miyake, T., Shiba, T., Sakurai, T., and Watanabe, I. (1969). *Japanese J. Microbiol.* 13, 375.
- Morgan, A.R., Cone, R.L., and Elgert, T.M. (1975). *Can. J. Biochem.*, in press.
- Neu, H.C., and Heppel, L.A. (1964). *Biochem. Biophys. Res. Commun.* 14, 109.
- Nichols, J. (1970). *Nature* 225, 147.
- Nossal, N.G., and Heppel, L.A. (1966). *J. Biol. Chem.* 241, 3055.
- Novotny, C.P., Taylor, P.F., and Lavin, K. (1972). *J. Bacteriol.* 112, 1083.
- Novotny, C.P., and Fives-Taylor, P. (1974). *J. Bacteriol.* 117, 1306.
- O'Callaghan, R.J., Bradley, R., and Paranchych, W. (1973a). *Virology* 54, 226.
- O'Callaghan, R., Bradley, R., and Paranchych, W. (1973b). *Virology* 54, 476.
- O'Callaghan, R.J., Bundy, L., Bradley, R., and Paranchych, W. (1973c). *J. Bacteriol.* 115, 76.
- Ohki, M., and Tomizawa, J. (1968). *Cold Spring Harbor Symp. Quant. Biol.* 33, 651.
- Oriel, P.J. (1969). *Arch. Biochem. Biophys.* 132, 8.
- Orr, C.W.M. (1967a). *Biochemistry* 6, 2995.
- Orr, C.W.M. (1967b). *Biochemistry* 6, 3000.



- Pao, C., and Speyer, J.F. (1973). *J. Virol.* 11, 1024.
- Paranchych, W., and Graham, A.F. (1962). *J. Cell. Comp. Physiol.* 60, 199.
- Paranchych, W. (1966). *Virology* 30, 90.
- Paranchych, W., Krahn, P.M., and Hev, R.D. (1970). *Virology* 41, 465.
- Paranchych, W., Ainsworth, S., Dick, A.J., and Krahn, P.M. (1971). *Virology* 45, 615.
- Paranchych, W. (1975). In "RNA Phages" (N.D. Zinder, ed.), p. 85. Cold Spring Harbor Laboratory.
- Petranović, D., Pečevsky-Kučan, I., and Kučan, Z. (1971). *Radiat. Res.* 46, 621.
- Powers, E.L., and Campel-Jobbagy, Z. (1972). *Int. J. Radiat. Biol.* 21, 353.
- Pryor, W.A. (1966). *Free Radicals*, p. 138. McGraw Hill Book Co., New York, N.Y.
- Reijnders, L., Sloof, P., Sival, J., and Borst, P. (1973). *Biochim. Biophys. Acta.* 324, 320.
- Richelsen, F., and Nathans, D. (1967). *Biochem. Biophys. Res. Commun.* 29, 842.
- Roberts, J.W., and Steitz, J.E. (1967). *Proc. Natl. Acad. Sci.* 58, 1416.
- Roblin, R. (1968). *J. Mol. Biol.* 31, 51.
- Rothwell, J.D., and Yamazaki, H. (1972). *Biochemistry* 11, 333.
- Rupp, W.D., and Ihler, G. (1968). *Cold Spring Harbor Symp. Quant. Biol.* 33, 647.
- Sagik, B.P., Green, M.H., Hayashi, M., and Spiegelman, S. (1962). *Biophys. J.* 2, 409.
- Sakurai, T., Miyake, T., Shiba, T., and Watanabe, I. (1968). *Japanese J. Microbiol.* 12, 544.
- Sanger, F., Brownlee, G.G., and Barrell, B.G. (1965). *J. Mol. Biol.* 13, 373.
- Schindler, J. (1965). *Biochem. Biophys. Res. Commun.* 18, 119.

- Scholes, G., Ward, J.F., and Weiss, J. (1960). *J. Mol. Biol.* 2, 379.
- Sharp, J.D., and Freifelder, D. (1971a). *Virology* 43, 166.
- Sharp, J.D., Donta, S., and Freifelder, D. (1971b). *Virology* 43, 176.
- Sharp, P.A., Hsu, M.-T., Ohtsubo, E., and Davidson, N. (1972). *J. Mol. Biol.* 71, 471.
- Shiba, T., and Miyake, T. (1975). *Nature* 254, 157.
- Shimura, Y., Faizer, H., and Nathans, D. (1968). *J. Mol. Biol.* 38, 453.
- Silverman, P.M., Rosenthal, S., and Valentine, R. (1967). *Biochem. Biophys. Res. Commun.* 27, 668.
- Silverman, P.M., Rosenthal, S., Mobach, H., Valentine, R.C. (1968). *Virology* 36, 142.
- Silverman, P.M., and Valentine, R.C. (1969). *J. Gen. Virol.* 4, 111.
- Singh, B.B., and Nicolau, C. (1971). *Progress in Biophysics and Molecular Biology* 23, 23.
- Sinha, N.K., Fujimura, R.K., and Kaesberg, P. (1965). *J. Mol. Biol.* 11, 84.
- Spahr, P.F., and Hollingworth, B.R. (1961). *J. Biol. Chem.* 236, 823.
- Spirin, A.S. (1964). *Macromolecular Structure of Ribonucleic Acids*. Rheinhold, New York.
- Steitz, J.E. (1968a). *J. Mol. Biol.* 33, 923.
- Steitz, J.E. (1968b). *J. Mol. Biol.* 33, 937.
- Steitz, J.E. (1968c). *J. Mol. Biol.* 33, 947.
- Steitz, J.E. (1969). *Nature* 224, 957.
- Sugiyama, T., Korant, B.D., and Lonberg-Holm, K.K. (1972). *Ann. Rev. Microbiology* 26, 467.
- Thach, S., and Boedtker, H. (1969). *J. Mol. Biol.* 45, 451.
- Thirion, J. P., and Kaesberg, P. (1968). *J. Mol. Biol.* 33, 379.
- Thirion, J.P., and Kaesberg, P. (1970). *J. Mol. Biol.* 47, 193.
- Valentine, R., and Wedel, H. (1965). *Biochem. Biophys. Res. Commun.* 21, 106.
- Valentine, R.C., and Strand, M. (1965). *Science* 148, 511.

- Valentine, R.C., Ward, R., and Strand, M. (1969). *Adv. Virus Res.* 15, 1.
- Vasquez, C., Granboulan, N., and Franklin, R.M. (1966). *J. Bacteriol.* 92, 1779.
- Verbracken, E., and Fiers, W. (1972). *Virology* 50, 690.
- Ward, J.F., and Urist, M.M. (1967). *Int. J. Radiat. Biol.* 12, 209.
- Watanabe, M., and August, J.T. (1968). *Proc. Natl. Acad. Sci. U.S.* 59, 513.
- Weber, K. (1967). *Biochemistry* 6, 3144.
- Wohrli, W., and Stachelin, M. (1971). *Bact. Rev.* 35, 290.
- Weissmann, C. (1974). *FEBS Letters* 40, S10.
- Willetts, N., and Achtman, M. (1972). *J. Bact.* 110, 843.
- Willetts, N. (1973). *Genet. Res.* 21, 205.
- Wong, K., Morgan, A.R., and Paranchych, W. (1974). *Can. J. Biochem.* 52, 950.
- Yamamoto, N., Hiatt, C.W., and Haller, W. (1964). *Biochim. Biophys. Acta* 91, 257.
- Yamazaki, H. (1969). *Virology* 37, 429.
- Yamazaki, I., and Piette, L.H. (1961). *Biochim. Biophys. Acta* 50, 62.
- Zinder, N.D. (1963). *Persp. Virol.* 3, 58.
- Zipper, P., Kratky, O., Herrmann, R., and Hohn, T. (1971). *Eur. J. Biochem.* 18, 1.

APPENDIX

PHAGE SUICIDE BY  $^{32}\text{P}$ -DECAY

The efficiency of killing RNA phage by  $^{32}\text{P}$  decay can be calculated using the formula of Hershey et al. (1951):

$$\log S_t = \log S_0 - 1.48 \times 10^{-6} \alpha A_0 N (1 - 3^{-\lambda t})$$

$S_0$  and  $S_t$  are the survivors at time zero and time  $t$  (in days), respectively.  $\alpha$  (efficiency of killing) equals the number of lethal hits in the genome.  $N$  equals the number of  $\text{P}$  atoms in the genome (3300 for R17).  $A_0$  is the specific activity of  $^{32}\text{P}$  in the infecting medium (in mCi/mg).  $\lambda$  is the decay constant of the radioactive isotope and equals 0.0486 for  $^{32}\text{P}$  if the time is express in days.

$A_0$  of the  $^{32}\text{P}$  labeled R17 stocks used routinely in the experiments described in this thesis is equal to about 2 mCi/mg. (see Materials and Methods). If secondary effects of  $^{32}\text{P}$  decay are not a factor, then at the end of 30 days, the above equation predicts that  $S_t/S_0$  (fraction surviving) = 0.99. i.e., 1% of the infectious particles would be inactivated over 30 days if only the direct effects of  $^{32}\text{P}$  decay were considered.

The  $^{32}\text{P}$  suicide studies of Lupker et al. (1973) were done with typical  $A_0$ 's = 800 mCi/mg. At the end of 30 days,  $S_t/S_0$  would be 0.016. The crude cell lysates of such radioactive preparation along with free, unassimilated  $^{32}\text{P}$  were frozen immediately at  $-80^\circ$  to minimize phage inactivation by secondary effects of  $^{32}\text{P}$  decay. However, if RNA penetration studies were to be carried out with phage of such high  $A_0$ , the phage must be separated from the free  $^{32}\text{P}$  by using standard purification procedures, otherwise free  $^{32}\text{P}$  would be taken up by infected cells.

During the purification steps, however, secondary effects of  $^{32}\text{P}$  decay would come into play and the purified phage would almost certainly end up with an undesirably low initial PFU/particle ratio. Such starting phage stocks are less than ideal for penetration studies in which the amount of RNA injected by phage with increasing number of strand breaks is to be compared to that injected by an original population with no breaks.